Developing a Platform to Compare Effects of Somatotopic Accuracy of Feedback on Upper-Limb Myoelectric Performance

by

Eric Wells

A thesis submitted in partial fulfillment of the requirements for the degree of

Master of Science

Department of Mechanical Engineering
University of Alberta

Abstract

Despite advancements in myoelectric prostheses, a high percentage of prosthesis users continue to abandon their devices. A commonly cited reason for abandonment is lack of grip force sensory feedback. Researchers have attempted to restore grip force sensory feedback by stimulating the residual limb's skin surface in response to the prosthesis hand's measured grip force. Many techniques for stimulating the residual limb have been explored, such as electrotactile, vibrotactile, and mechanotactile feedback. Different experimenters use different stimulation sites, such as the forearm, upper-arm, or the finger of non-disabled participants. Promising results indicating improved prosthesis performance have been observed using these methods. However, each experiment typically has a unique apparatus with a different feedback stimulation location, making comparisons between studies difficult. The impact of the feedback location on myoelectric prosthesis performance has not been investigated. This thesis focused on developing a platform and experimental protocol to analyze the effects of feedback simulation location on prosthesis performance.

Simulated prostheses are used to study myoelectric control with non-disabled participants while ensuring consistency between participants. In this work, a modular simulated prosthesis with location adjustable mechanotactile feedback devices was developed. The design was focused on comfort, weight reduction, and modularity. Low-cost pressure sensors were encapsulated in a compliant material and fit in the fingertips of the device. These compliant fingertips allowed for a substantial reduction in error for all non-standard loading conditions typical to prosthesis use. The simulated prosthesis will help researchers study feedback and control techniques in myoelectric prostheses by providing a reliable test apparatus that easily allows for manipulating various parameters.

An experimental protocol was developed for comparing the performance differences of mechanotactile feedback delivered to the forearm or the fingertip. This protocol was validated through a pilot study of three participants. All participants showed similar difference values in the comparison between the finger

feedback condition and the arm feedback condition, creating large between-participant effect sizes for all outcome measures. These preliminary results indicate that the feedback location could play a factor in myoelectric prosthesis performance. A power analysis revealed that an estimated participant pool of n=8 would be required to achieve significance for comparing the arm and finger feedback conditions for all proposed metrics. Data analysis techniques were developed that will scale to a more extensive study. Recommendations were made on experimental apparatus improvements and protocol adjustments to reduce potential error sources for future experiments.

Preface

This thesis contains information from one conference paper authored by the writer.

1. Wells, E. D., Carpenter, S., Dawson, M. R., Shehata, A. W., Carey, J. P., & Hebert, J. S. (2020). Development of a Modular Simulated Prosthesis and Evaluation of a Compliant Grip Force Sensor. *Myoelectric Controls and Upper Limb Prosthetics Symposium*, 179–182.

The writer led the writing of the manuscript and the device development; the system's mechanical design was shared between the first two authors. All authors shared the revision of the manuscript. Chapter 3 discusses the system in detail.

A full experimental study, informed from the pilot study results shown in Chapter 4, was planned to be completed in the summer of 2020. However, the COVID-19 pandemic arrived during the pilot study. The proposed experimental protocol requires the researchers to be in physical contact with participants, which was not allowed by the University of Alberta's pandemic restrictions. Further data collection for the pilot study and a full study was postponed to ensure the participants' and researchers' safety. The pilot study data was analyzed in greater detail to ensure the MSc. degree requirements were upheld.

Acknowledgments

I would like to sincerely thank my two supervisors, Jacqueline Hebert and Jason Carey, for all their guidance during my time in the lab. You've both shown me immense support and flexibility, and I truly could not have asked for better supervisors. The lessons I've learned from your leadership will continue to support me throughout my career.

I am incredibly grateful to everyone in the BLINC Lab for all their technical support and friendship. From karaoke to tea-time games, you've all made my time in the lab memorable and worthwhile. I want to thank Ahmed Shehata, who contributed immensely to this thesis. I appreciate our weekly discussions and hope to have many more ping-pong matches in the future. I want to thank Michael R. Dawson for the countless pun-filled hardware and software discussions that always improved my designs and mood. Also, thank you to Shealynn Carpenter for all the mechanical design expertise.

I am very grateful for the funding I received from the Natural Sciences and Engineering Research Council of Canada and the University of Alberta. I would not have been able to dedicate the time and effort towards my research without this support.

Thank you to my family, who has unconditionally supported me for all these years. You are always ready to lend a listening ear and provide invaluable insight, for which I am tremendously be grateful. Finally, thank you to my friends for believing in me and picking me up when I'm down. I'd like to specifically thank Mark Sherstan for the countless hours put into all our projects. Your admirable technical expertise and work ethic are goals I strive to achieve.

Table of Contents

List of Tables

List of Figures

1 Introduction

1.1 Problem Statement

Upper limb amputation results in loss of both motor and sensory function of the hand, negatively impacting an individual's economic, psychological, and social well-being. Prosthetic technology attempts to mitigate these effects by restoring functionality to the lost limb. Recent research in the area focuses on electrically powered prostheses controlled by the residual limb's muscle signals, termed myoelectric control [1]. These myoelectric devices utilize the existing neural pathways responsible for natural movement [2]. Although research in the area has focused mainly on improving myoelectric control, studies continue to report rejection rates for electrically powered prosthetics as high as 35% in children and 23% in adults [3]. Another study showed that two of the most common reasons for rejection were poor functionality (98% of respondents) and a lack of sensory feedback (85% of respondents) [4].

Implementing exteroceptive sensory feedback into prosthetic devices is hypothesized to improve function by providing information about the prosthesis state to the user. The prosthetic hand's grip force is a highly desired sensory signal among prosthesis users [5]. The measured grip force can be transferred to a prosthesis user's residual limb, closing the loop during grasp control. Many different surface-mounted methods to translate the measured grip force back to the user have been investigated, including mechanotactile, vibrotactile, and electrotactile [6], [7]. Different experiments use different stimulation sites, such as the forearm, upper-arm, or finger (with non-disabled participants). Promising results indicating improved prosthesis performance have been observed using these methods. However, each experiment typically has a unique apparatus with a different feedback stimulation location, making comparisons between studies difficult. The impact of the feedback location on myoelectric prosthesis performance has not been investigated. We propose closing this gap in the literature by developing a method to analyze the functional performance of non-disabled individuals using myoelectric devices while controlling the feedback stimulation location of applied grip force feedback.

1.2 Specific Objectives

1. A simulated prosthesis device will be designed and manufactured, allowing multiple feedback locations to be easily accessed on non-disabled participants during myoelectric control.
2. A pilot experiment will be run comparing the myoelectric performance when modality matched grip force feedback is given in a somatotopically accurate location (feedback on fingertips) to a non-somatotopically accurate location (feedback on the forearm). Data will be analyzed to develop an analysis framework and determine sample size for a future study.

1.3 Thesis Outline

Chapter 2 presents a literature review on feedback methods for upper limb prostheses. Topics include an overview of the history of prosthesis use, somatotopically matched methods, feedback techniques available, and feedback locations.

Chapter 3 provides a detailed description of a simulated prosthesis's technical design, including mechanical, electrical, and software subsystems.

Chapter 4 details a pilot study results with three participants, comparing somatotopically matched feedback to non-somatotopically matched feedback.

Chapter 5 contains a thesis summary, drawing of conclusions, an overview of contributions, and future recommendations.

2 Literature Review

2.1 History and Epidemiology

In 2005 the United States had an estimated 1.6 million people living with limb loss. This estimate is expected to increase to 3.6 million by 2050. Around 42% of these are considered major amputations, involving more than only fingers, toes, or partial hands and feet. Only 6% of major amputations are upper limb. Trauma is the leading cause of major upper-limb amputations (83%), typically occurring before age 45 [8]. Since upper limb amputation generally occurs at a younger age than lower limb, those affected live for many years with functional and economic disadvantages. Upper limb amputation is much more difficult to replace than lower limb amputation. Lower limb primary function is mostly limited to locomotion and maintaining balance. In contrast, upper limb primary function requires fine motor control for more complex tasks such as interaction with the environment, self-care, and communication [9]. Figure 2.1 shows a visualization of major amputation by cause based on prevalence estimates in the United States. Figure 2.2 illustrates the amputation level in upper limb amputation based on yearly incidence statistics in Italy and the United Kingdom.

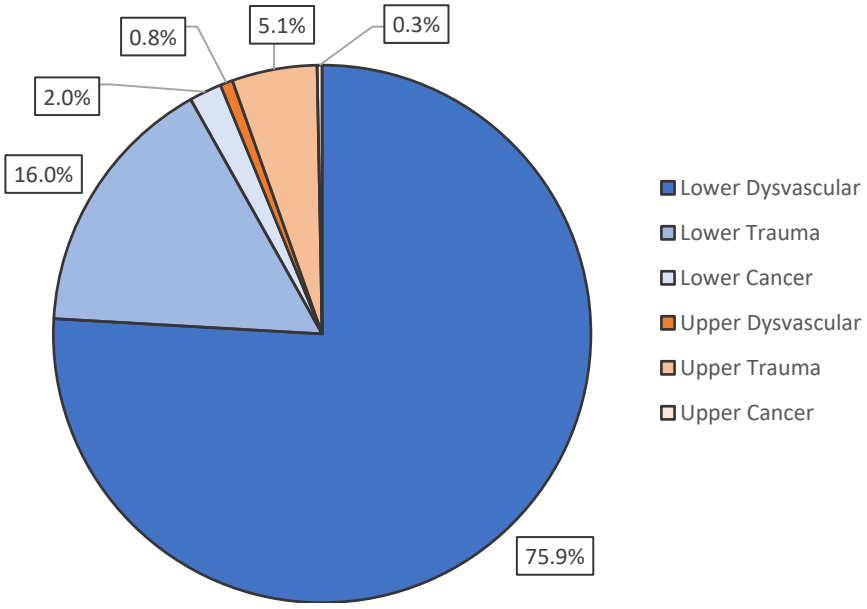

Figure 2.1: Estimated Number of Major Amputation in the United States by Cause in 2005 [8]

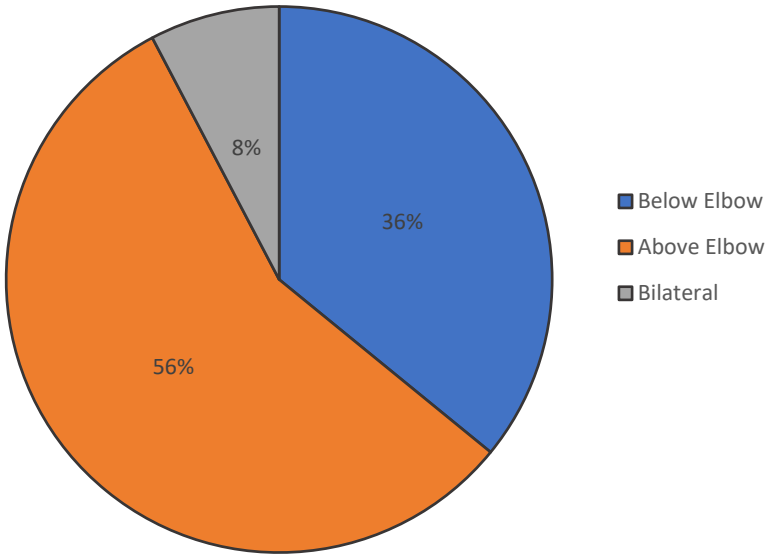

Figure 2.2: Level of Major Upper Limb Amputation in Italy and the United Kingdom [10]

The use of upper limb prostheses has been documented as early as 218 BC by a Roman general named Marcus Sergius, who had a "right hand of iron," which allowed him to return to battle [11]. This iron hand is an example of a passive prosthesis, which involves no moving parts. Documentation of prosthesis use this far back in history is uncommon since the survival with amputation without modern medicine was low. The emergence of active body-powered prostheses came about from a German dentist in 1818 [12].

These devices used leather straps operated by the trunk and torso to open and close the mechanical hand. However, they were quite expensive and not widely adopted. World War I and II resulted in a previously unprecedented number of persons with amputation, 30% of which were upper limb [13]. This increase in people living with limb differences sparked the creation of formal groups dedicated to improving prostheses, such as the U.S. Committee on Prosthetics Research and Development in 1945 and the Canadian Association of Prosthetics and Orthotics in 1955 [14]. In 1948 the first Bowden cables replaced the bulky straps previously actuating the terminal device on body-powered prostheses, a method still commonly used today [11]. Also, in 1948, the first myoelectric prosthesis was created by German Physicist Reinhold Reiter. Electromyographic (EMG) sensors placed on the residual limb's surface actuated the myoelectric hand using electronic motors. This concept did not gain much traction until the 1960's when Russian scientist Alexander Kobrinski began selling them in Britain and Canada [15]. Early myoelectric devices provided on-off control of a single-degree-of-freedom, such as hand-open and hand-close [16]. The first pattern recognition control of myoelectric prostheses was developed in 1975 using auto-regressive-moving-average parameters [17]. However, the computational power in that period could not provide real-time control. As the computational power and size of electronic components advanced, myoelectric devices saw continuous improvement. End effectors also advanced, with the ability to complete complex motions with up to six degrees of freedom [18]. To utilize the available degrees of freedom, pattern recognition based control is now becoming state of the art [19].

(a) (b) (c)

Figure 2.3: (a) Passive Prosthesis, (b) Body-Powered Prosthesis, (c) Myoelectric Prosthesis [20]

Despite significant advances in myoelectric prostheses, both body-powered and passive prostheses are still widely used. An estimated 42.9% of prostheses administered are body-powered, 29.6% passive, and 27.6% myoelectric [9]. Figure 2.3 shows an example of each of these three main types of prostheses. A large meta-study indicated that myoelectric prostheses do not result in higher acceptance than body-

powered prostheses in adults, with mean rejection rates of 26% and 23% for body-powered and myoelectric prostheses, respectively [4]. The same group completed a survey attempting to identify the cause for high rejection rates, finding that 98% of respondents who had rejected the prostheses stated they were more functional without it [3]. Furthermore, 85% of respondents specifically noted a lack of sensory feedback being a significant rejection factor. These survey results indicate that sensory feedback could be critical in reducing the high rejection rate of myoelectric prostheses.

2.2 Sensory Feedback Systems Overview

There are many different sensory feedback signals from the human arm and hand, such as grip force, proprioception, temperature, and texture. Grip force has been ranked as the highest priority sensory input for myoelectric prostheses users [5] and is the focus of this thesis. Our sense of touch is essential for dexterous manipulation using the hands and fingers [21]–[23] and a confident grasp. Augerelle et al. asked non-disabled subjects to slowly shake an object for 30 seconds, which they could do without dropping it [24]. Upon numbing the index and thumb with bupivacaine, subjects dropped the object on 36% of trials. When participants with anesthetized fingers attempted to hold the object stationary, the grasp force became unstable, often over-gripping. This study illustrates the necessity of sensory feedback, even when a healthy limb with complete motor function is available.

With no sensory feedback, prosthesis users must operate in open-loop control, relying only on indirect information to achieve an intended grasp force, such as visual cues and auditory cues. A sensory feedback system can close the loop during grasp force control by indicating the prostheses grip force using a sensitized hand. This information is relayed back to the user in real-time, allowing for grasp force modulation. Figure 2.4 illustrates the control block diagrams for myoelectric prosthesis use with and without a sensory feedback system implemented.

Many different methods of mapping the prostheses grip force to an output for the user have been explored, such as mechanotactile [25]–[27], vibrotactile [28], [29], and electrotactile feedback [30], [31]. Feedback output is described in terms of somatotopic and modality accuracy [7]. Modality matched feedback methods occur when the sensation perceived is the same as through a healthy limb. In the case of grip force input, a modality matched output is perceived as pressure. Somatotopically accurate feedback methods occur when the user perceives the sensation in the same location as the feedback input. For grip force, a somatotopically matched feedback output would be perceived at the fingertips. Somatotopic techniques can be achieved; however, it requires significant resources to implement, such as surgical implants [32], targeted sensory reinnervation [33], or phantom mapping sessions [34]. Having

both modality and somatotopically matched feedback is thought to provide the most intuitive interface for prosthesis users.

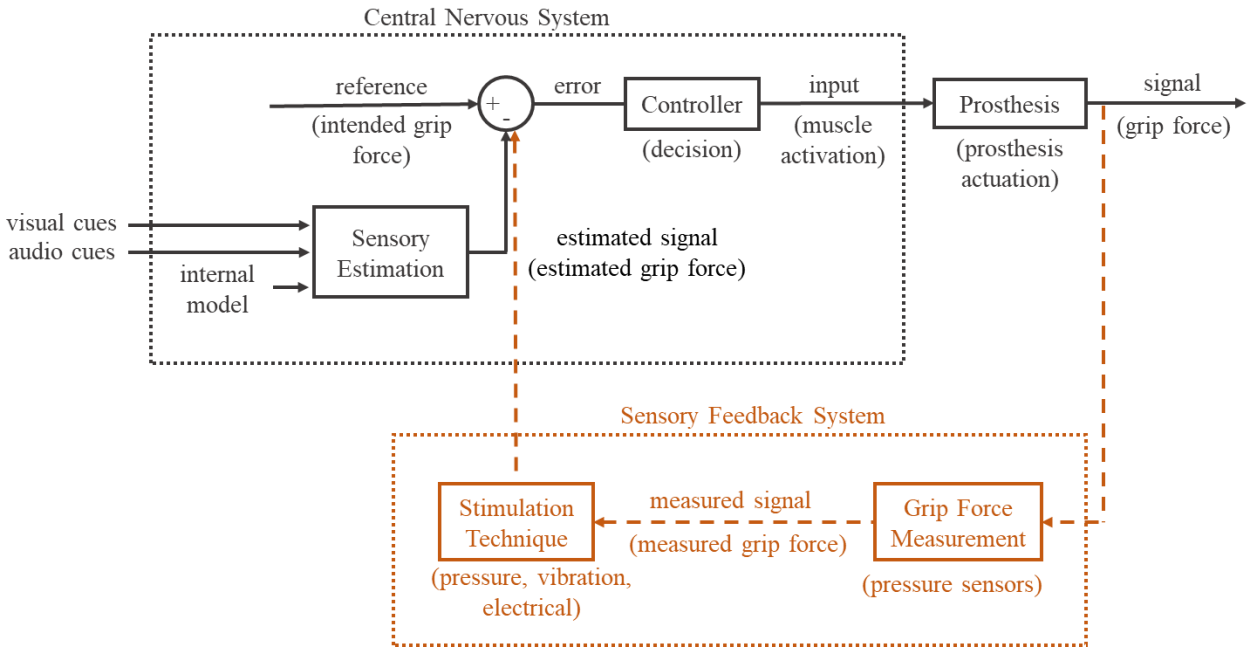

Figure 2.4: Simplified Control Flow Diagram of Grasping With and Without Sensory Feedback Using a Prosthesis

2.3 Somatotopically Matched Methods

Recent advancements have made somatotopically accurate feedback achievable in prosthetic control. This section discusses the main somatotopically accurate feedback techniques.

2.3.1 Phantom Hand Mapping

Most persons with amputation experience sensations of their missing limb, occurring as non-painful feelings such as tingling, itching, or general awareness of the limb's missing part [35]. Often, persons with amputation experience pain in the missing limb referred to as phantom limb pain [36]. Persons with an amputation can also experience non-painful sensations of the missing fingers when specific skin areas on the residual limb are stimulated, referred to as a phantom hand map [37]. These areas can then be targeted by feedback systems to utilize the original afferent pathways to the brain, creating somatotopically accurate feedback. Although not all persons with amputation have a phantom hand map, a previous study showed that 12 out of 18 randomly recruited transradial participants had a distinct representation of the index finger on the residual limb [38]. Phantom hand maps are often not complete, with only partial digits or sensations felt over large areas on the residual limb [37]. Figure 2.5 shows a theoretical illustration of a

phantom hand map for clarity. One group showed that two-point discrimination in the phantom hand map sites was better than corresponding forearm sites in the healthy limb [37].

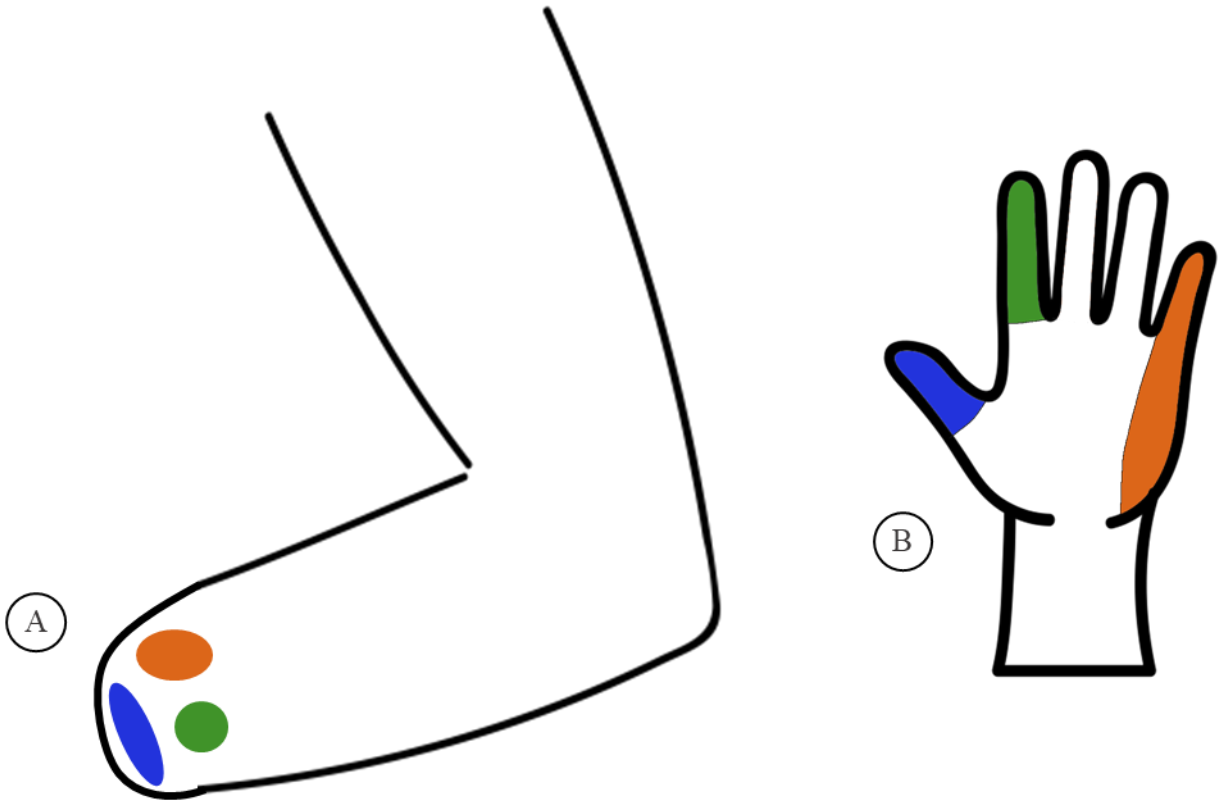

Figure 2.5: Example of Phantom Hand Map on a Transradial Person with Amputation, (A) Stimulation Location (B) Perceived Location

2.3.2 Targeted Muscle Reinnervation

Targeted muscle reinnervation (TMR) is a well-established surgical procedure for improving prosthetic control and reducing nerve pain after amputation [39]. This technique involves redirecting a nerve that previously innervated the hand but was cut due to the amputation surgery to a nearby intact remaining muscle group, thereby creating more available EMG sites. These additional EMG sites act as input signals for more complex myoelectric control techniques [40]–[45]. This surgery incidentally or purposefully re-routes sensory nerve fibers that can reinnervate the surrounding skin resulting in a restored hand map on the residual limb [33], [46], [47]. A touch on this area is perceived as occurring on the lost limb, creating an opportunity for a somatotopically matched feedback site. Like phantom hand mapping, these areas often cover large portions of the missing limb and do not resemble somatotopic organization except by chance [46]. A novel method developed by Hebert et al. allows targeted sensory reinnervated (TSR) regions located away from reinnervated motor sites, making it possible to have both motor control and

sensory feedback devices operating simultaneously [33]. TMR surgery is becoming more common both as a revision and initial surgery due to demonstrated benefits in reducing neuroma formation and PLP [48].

2.3.3 Peripheral Nerve Interfaces

Recent advances in peripheral nerve interfaces allow electrodes to be surgically implanted directly into the peripheral nervous system for long term use [49], [50]. These electrodes can be electrically stimulated in a manner that resembles natural use. Stimulation typically includes using either current modulated or voltage modulated square wave pulse trains. The amplitude and frequency of these square waves can be adjusted to elicit various intensity and spatial selectivity [49], [51]. This technique can produce sensations of touch, joint movement, and position [52]. However, these sensations' level of naturalness has been subjectively stated as limited [53], although recent work has made substantial advances towards invoking a variety of distinct sensory percepts [54]. Current systems use multiple electrodes in a miniature array to increase stimulation channels [55]–[57]. Implanted peripheral nerve interfaces have been used to discriminate object size and stiffness [58]. They have also demonstrated that functional performance increases in longitudinal studies [30], [31], and has shown stability in sensory percepts over long periods [51]. A recent study utilized implanted stimulation to deliver tactile and substituted proprioceptive feedback with high-performance results from transradial persons with amputation [55]. Peripheral nerve interfaces have shown remarkable advances recently, but they are still limited to research applications and require surgical implantation. The remainder of this thesis focuses on non-invasive surface feedback techniques.

2.4 Feedback Output Overview

Many different methods for relaying grip force feedback to prosthesis users have been explored. The primary non-invasive methods used, including mechanotactile, electrotactile, and vibrotactile, are discussed in this section.

2.4.1 Mechanotactile Grip Force Feedback

Mechanotactile feedback applies a force to the user's skin, creating a modality matched feedback system for a grip force sensory input. The mapping of the input to output is typically proportional, providing more force from the device as the measured force at the fingertip increases. Investigation of mechanotactile feedback began as early as 1989. Users could increase their success rate on a fragile object transfer task when mechanotactile feedback was administered to the forearm using a motorized rack and pinion style plunger [27]. An alternative technique uses a hydraulically powered cuff to administer pressure around the upper arm [59]. This device also showed improved grip force accuracy.

Kim et al. designed a miniature haptic device capable of delivering force and vibration, both normal and tangential to the skin, allowing for reduced grip force on a fragile object grasp-and-lift task [60], [26]. Casini et al. designed a cuff-like device that can apply both normal and tangential forces around the residual limb's circumference [61]. Schoepp et al. developed an inexpensive and simple tactor using a rack and pinion style miniature servo to place normal force on the user's residual limb, which also reduced the grasp force when manipulating objects [62].

A phantom hand map or a TMR or TSR site allows for mechanotactile feedback to be modality and somatotopically matched. One study showed that placing tactors on phantom map sites improved multi-site sensory feedback discrimination regardless of modality [34]. Mechanotactile feedback applied to a TSR site resulted in high force and object discrimination with no visual feedback [33]. Another study showed a similar result with reduced grasp force on a fragile object transfer task when mechanotactile feedback was applied to a TSR site [26]. One disadvantage of mechanotactile feedback systems is the need for moving mechanical parts. The larger moving parts typical in mechanotactile feedback systems tend to result in larger overall size and power requirements [7].

2.4.2 Electrotactile Grip Force Feedback

Electrotactile feedback uses an electrical current to stimulate the afferent nervous system from the surface of the skin. Different techniques exist to map the grip force to the stimulus, such as varying current amplitude, frequency, pulse width, and waveform. The current amplitude ranges from 1-20mA with frequencies between 1Hz to 5000Hz [6]. Surface-mounted electrotactile feedback is typically perceived as buzzing, needle-like, or numbness [63]. This modality shift depends on stimulating voltage, current, waveform, electrode size, material, and other factors [64]. Electrotactile feedback has been shown to improve prosthesis grasping force control [65]–[68]. Since electrotactile feedback has no moving parts, it can run with less power, lower mass, and less noise than other methods. However, the inherent electrical current mechanism can interfere with EMG sites, although some mitigating timing strategies have been used [69]. Applying electrotactile feedback to the phantom map can create somatotopically matched feedback [70], [71].

2.4.3 Vibrotactile Grip Force Feedback

Vibrotactile feedback employs miniature actuators that stimulate the afferent network through vibration, typically between 10Hz to 500Hz [6]. Vibrotactile feedback is relatively easy to implement because these actuators are small, inexpensive, and commercially available. The only commercially available prosthesis with incorporated sensory feedback uses a single vibration motor to stimulate proportionally to grip force [72]. Vibration amplitude and frequency can be adjusted to form complex waveforms for additional

communication methods [73]. Vibrotactile feedback has improved grasp force consistency when proportionally mapped to grasp force [74], [75]. Multiple vibration motors can create an additional spatial location parameter to map to the prostheses grasp force [76]. A spatially distributed array of five coin cell vibrotactile tactors has shown improvements over a single pulse-rate modulated site [77]. A significant drawback of vibrotactile feedback is the rise time required before reaching target levels. For one prototype, although the sensory perception level was achieved quickly (1-10ms), the full amplitude took substantially longer (350ms-450ms) [78]. Vibrotactile feedback cannot produce modality matched feedback for a grip force input.

2.4.4 Other

Other methods of feedback output exist, though they are less popular than the three previously discussed. Grip force information has been delivered visually through augmented reality glasses [79], [80]. Another technique uses an actuator pressed into the skin, eliciting a skin stretch feeling, although this is typically used for a proprioception input rather than grip force [81], [82]. Auditory feedback using the EMG control signal as input has increased the user's performance on a grasp and lift task [83]. Researchers have also mapped grasp force to auditory feedback volume, resulting in improved object discrimination [84].

2.4.5 Summary

Figure 2.6 illustrates an example of typical mechanotactile, electrotactile, and vibrotactile feedback implementations. Figure 2.7 summarizes the currently available feedback outputs and locations, with their corresponding somatotopic and modality matched levels.

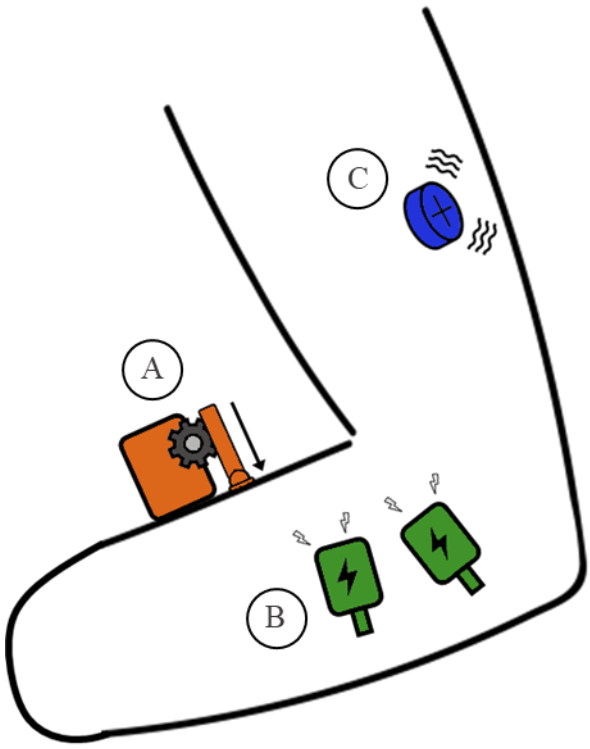

Figure 2.6: Feedback Example Illustration (A), Mechanotactile, (B) Electrotactile, (C) Vibrotactile

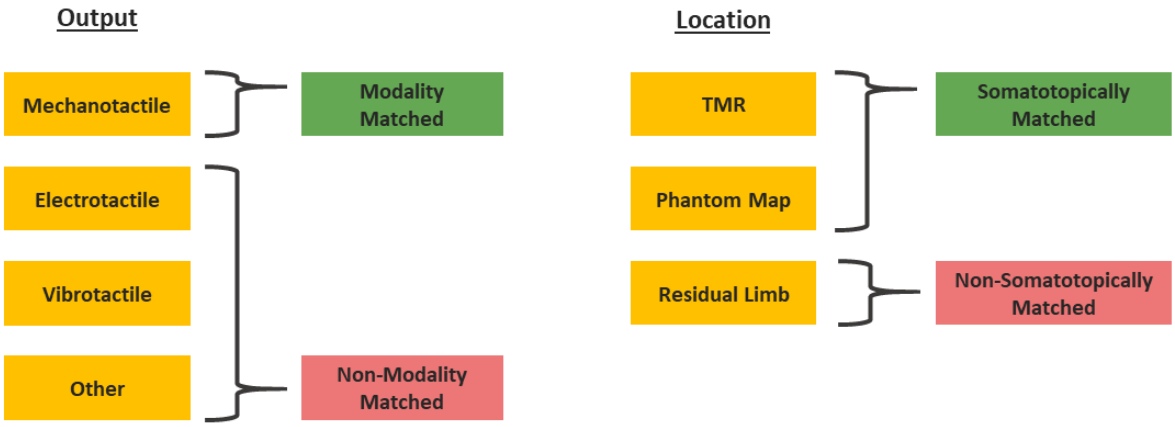

Figure 2.7: Summary of Non-Invasive Grip Force Feedback Options Regarding Modality and Somatotopic Matching

2.5 Sensory Feedback Comparison

Although many different sensory feedback techniques have been investigated, there remains no definitive best method. The majority of the studies discussed previously evaluate specific feedback implementations

against a no-feedback control. However, some studies have compared various implementations to attempt to determine the superior method. Bark et al. found that skin stretch outperformed vibrotactile during a virtual task, although both techniques showed improvement [85]. Tejiero et al. found that both vibrotactile and mechanotactile feedback improved performance on a virtual fragile object task [86]; however, neither technique outperformed the other. In an object discrimination task, Thomas et al. similarly found that both joint-torque feedback (not previously mentioned) and vibrotactile feedback improved performance [87]. Still, no difference was seen between the two techniques. Antfolk et al. found that mechanotactile outperformed vibrotactile in a discrimination task when applied to the phantom map of persons with transradial amputation [34]. A force replication task showed that vibrotactile feedback did not reduce absolute error when added to purely visual feedback, while mechanotactile feedback reduced absolute error [59].

However, each of these studies' implementation is typically unique with a different end effector, sensor, control technique, experimental task, and feedback location. The amount that these parameters contribute to an improvement in prosthetic function is not well understood. Conflicting results from different studies emphasize this issue. Saunders and Vijayakumar found that feedback did not affect grasp force control unless uncertainty was introduced into the feedforward control [88]. One study found that vibrotactile feedback became obsolete when visual feedback was available, although the participants' subjective opinion stated that the vibrotactile feedback was still necessary [89]. Likewise, Chatterjee found no significant differences between a no-feedback group and a feedback group in a force matching task [90]. Furthermore, they found that only experienced participants could use the feedback to their advantage, while the novice participant's performance was reduced. During a grip force accuracy test, the feedback's benefit was significant for low force levels but not for high force levels [75]. Another group found that feedback only improved performance during functional tasks when they were sufficiently complicated [80], [91]. To fully understand the role of feedback systems in prosthesis use, each parameter that can affect results must be isolated and tested. One currently unexplored variable is the effect of feedback stimulus location.

2.6 Sensory Feedback Site Location

Skin properties vary significantly throughout the body. Glabrous skin, found mostly on the hands and feet, is specialized for discriminative touch, determining texture and shape, and providing feedback to the central nervous system for grasp control [92]. Two-point discrimination tests can be conducted to evaluate the spatial resolution of different areas on the body. Two-point discrimination values for the glabrous fingertips typically fall between 2.12mm-2.5mm, while values for forearms are an order of

magnitude higher at 25mm-38mm. Two-point discrimination values are higher still for the upper arm between 45mm-63.5mm. Furthermore, touch sensitivity is also substantially better at the fingertips than on the forearm and upper arm [93], [94]. Previous studies on feedback systems have the stimulation site at many different locations, such as the forearm [27], [68], upper arm [25], [28], toe [95], phantom map on the residual limb [34], as well as to a non-disabled finger [96]. Figure 2.8 was created from a combination of the literature review presented and a recent review paper on non-invasive sensory feedback technique for upper limb prostheses [97], showing the approximate spread of feedback site locations in recent studies across participants with intact arms and those with amputation. However, no studies have examined the impact of the location of feedback on functional myoelectric prosthesis performance.

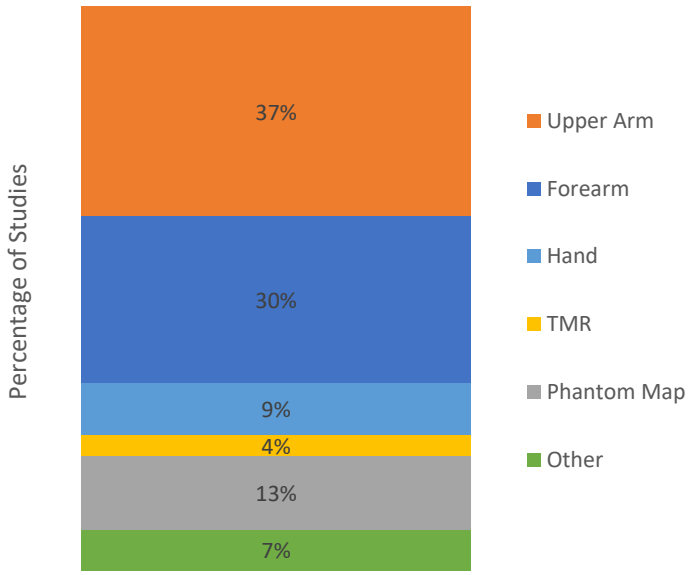

Figure 2.8: Summary of Stimulation Site in Non-Invasive Upper Limb Prostheses Feedback Studies Across Participants with Intact Arms and Those with Amputation [97]

2.7 Conclusions

Many techniques exist for delivering feedback to upper limb prostheses users, though no single method has risen as the best performer. There is some controversy over the impact of sensory feedback in upper limb prosthesis research. This controversy is likely due to the differences between experimental setups between studies. Feedback site location is an often-overlooked parameter in feedback studies. Techniques are available that allow for somatotopically matched feedback sites for upper limb prostheses users. The

functional benefit of utilizing a somatotopically matched feedback site has not been directly compared to a non-somatotopically matched feedback site, such as the commonly used forearm or upper arm. Mechanotactile feedback is the only non-invasive technique capable of achieving modality matched feedback for grip force input, making it the ideal candidate for an experiment isolating somatotopic accuracy. This work addresses a literature gap by developing a method to quantify the effects of somatotopic accuracy on myoelectric performance. The results of this study will inform the future of feedback implementation in prosthetic users, which could lower abandonment rates among prosthesis users.

3 Development of a Modular Simulated Prostheses

3.1 Background

A simulated prosthesis is a device that allows a non-disabled individual to emulate myoelectric control without a limb-amputation. Simulated prostheses are used to study myoelectric control strategies [89], [98]–[103], myoelectric training techniques [104], and sensory feedback techniques [25], [96]. These devices have been shown to effectively reproduce myoelectric users' performance metrics and motion kinematics [105].

As previously discussed, the somatotopic accuracy of feedback location is a currently unexplored parameter in myoelectric control. The available techniques for somatotopically matched feedback for persons with amputation result in spatial regions and sensations that vary in strength and modality unique to each individual. This individuality makes consistency between participants difficult in an experimental study. Additionally, not all persons with amputation have access to somatotopically matched feedback sites, decreasing the number of available participants. With a simulated prosthesis, the participant pool includes non-disabled individuals, and the participant's fingertip can be used as a site for somatotopically accurate feedback. All non-disabled individuals can use the same simulated prostheses, ensuring consistency between participants.

3.2 Device Overview

A Simulated Sensory Motor Prosthesis previously constructed in our lab allowed for somatotopically matched mechanotactile feedback during myoelectric control [106]. However, initial testing with the device showed various issues that justified a revision. The large size, non-modularity, and weight of the device (1.3 kg) made it difficult to move naturally, causing discomfort over short periods. The second iteration of this device, the Modular Simulated Prosthesis (MSP), was designed to optimize the size, weight, and comfort of the Simulated Sensory Motor Prosthesis while maintaining the ability to provide sensory feedback to both the forearm and fingertips. This allows for both modality and somatotopically matched feedback to be used on the same experimental apparatus. An additional focus was placed on modularity to allow for interchangeable components for various user sizes or experimental conditions. The device was fit with a novel implementation of low-cost compliant force sensors to measure the end effector's grip force reliably. These sensors were evaluated and compared to standard sensors under various loading conditions to ensure accurate grip force measurement. Figure 3.1 shows the previously designed simulated prosthesis and the MSP developed as part of this thesis.

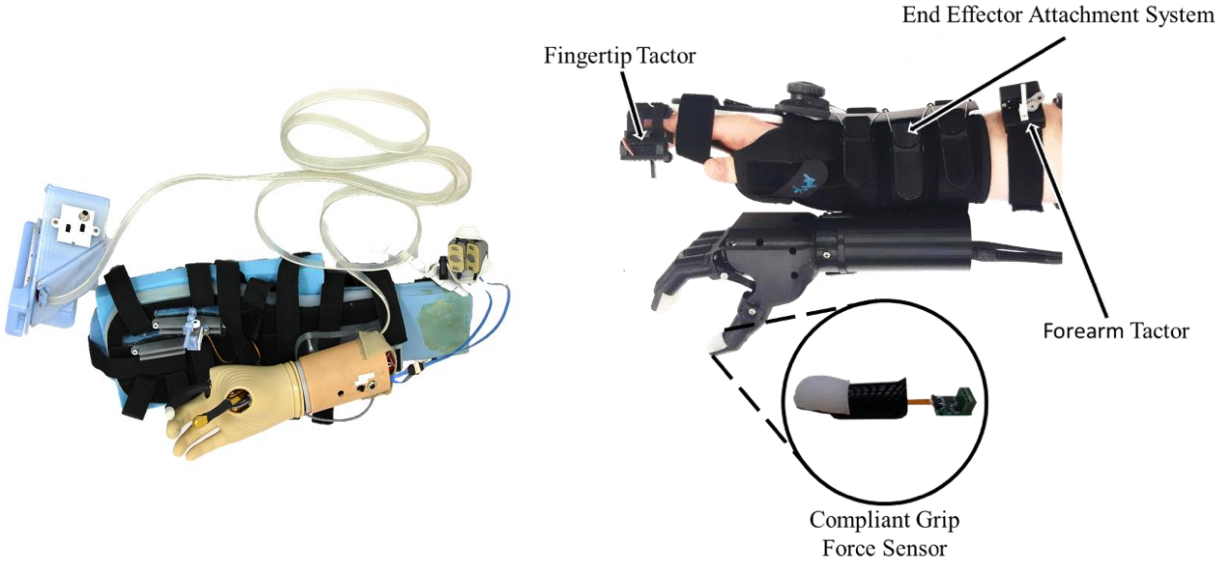

(a) *(b)*

Figure 3.1 (a) Previously Designed Simulated Prosthesis, (b) Modular Simulated Prosthesis

3.3 Hand Restraint Mechanism

A wrist and thumb support brace (MedSpec, USA) restrains the user's hand to ensure isometric contraction during electromyography (EMG) control. This commercially available product is designed to be comfortable, lightweight, adjustable, and leaves adequate space on the proximal forearm for EMG sensors and other devices. Three sizes (small, medium, large) were purchased to accommodate various participant arm/hand sizes. Additional finger flexion restraints were required to prevent the fingertips from colliding with the end effector. The existing metal supports within the brace were extended with 3D printed PLA supports on both sides of the hand. The PLA supports were molded to the ventral and dorsal profile of the arm for additional comfort. PLA's low melting point allows for quick remolding for individual participants by placing the supports in hot water for a short period. The portion of the supports in contact with the skin was covered in closed-cell foam for easy sanitizing between participants. Velcro on the backside allows for the supports to be tightened to the hand using an additional thin piece of Velcro. Figure 3.2 illustrates the components for clarity. Supports were printed in three different sizes to accommodate different participant wrist sizes.

Figure 3.2: (a) Wrist and Thumb Brace (b) 3D Printed PLA Supports (c) Hand Restraint Mechanism

3.4 End Effector Attachment

In simulated prostheses, the end effector must be offset from the user's hand, creating an undesirable torque on the elbow/shoulder joints. See Figure 3.3 for visualization of the anatomical directions. Previously, simulated prostheses designers have designed this offset to be either distal [89], [95], [96], [99], [101], [103], [104], [107], ventral [25], [108]–[110], lateral [111], or medial [79], [100], [102]. Because the human hand width is much smaller than its length and breadth, offsetting the simulated prostheses' added weight in the ventral direction minimizes the added torque. An adjustable offset in the lateral/medial direction was also added to the MSP to resolve any line of sight issues that may arrive for tasks with the palm facing downwards.

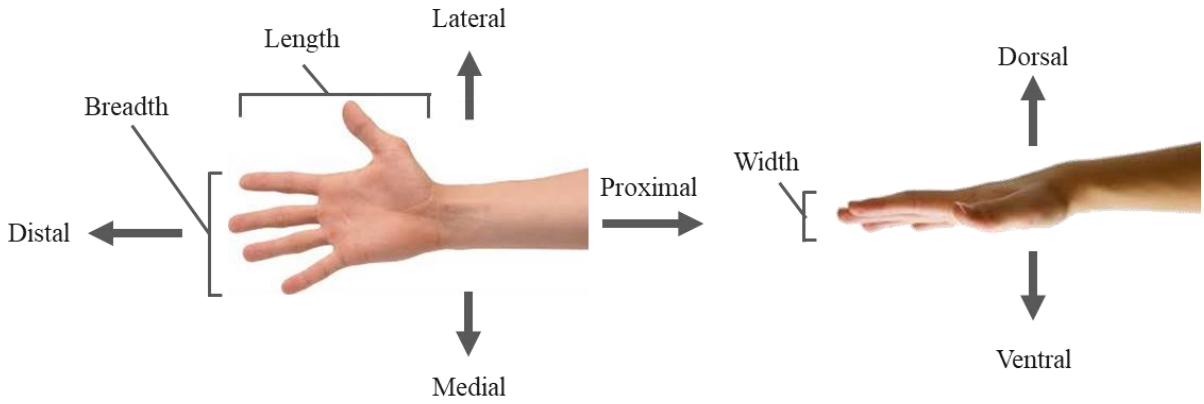

Figure 3.3: (a) Anatomical Direction and Hand Measurement Summary

An end effector attachment system was developed to attach the prosthetic hand to the brace while accommodating various arm shapes and sizes. The system consists of a PLA bracket that rests midline on the wrist brace's ventral surface and an interlocking cable tightening system (BOA, USA) that rests midline on the dorsal surface of the wrist brace. Attached to the bracket is a PLA wrist adapter for end effector mounting. The bracket is temporarily secured to the ventral side of the arm using a large Velcro strip. The cable tightening system is then wrapped around to the dorsal side, where PLA quick-connect clips are connected, completing the loop around the arm. The interlocking cable system is tightened around a flexible TPU (NinjaFlex) plate to create a snug fit between the end effector and the participant's forearm, minimizing the device's relative movement. The end effector attachment system is pictured in Figure 3.4. The hand restraint mechanism and end effector attachment system attached to a participant is shown in Figure 3.5.

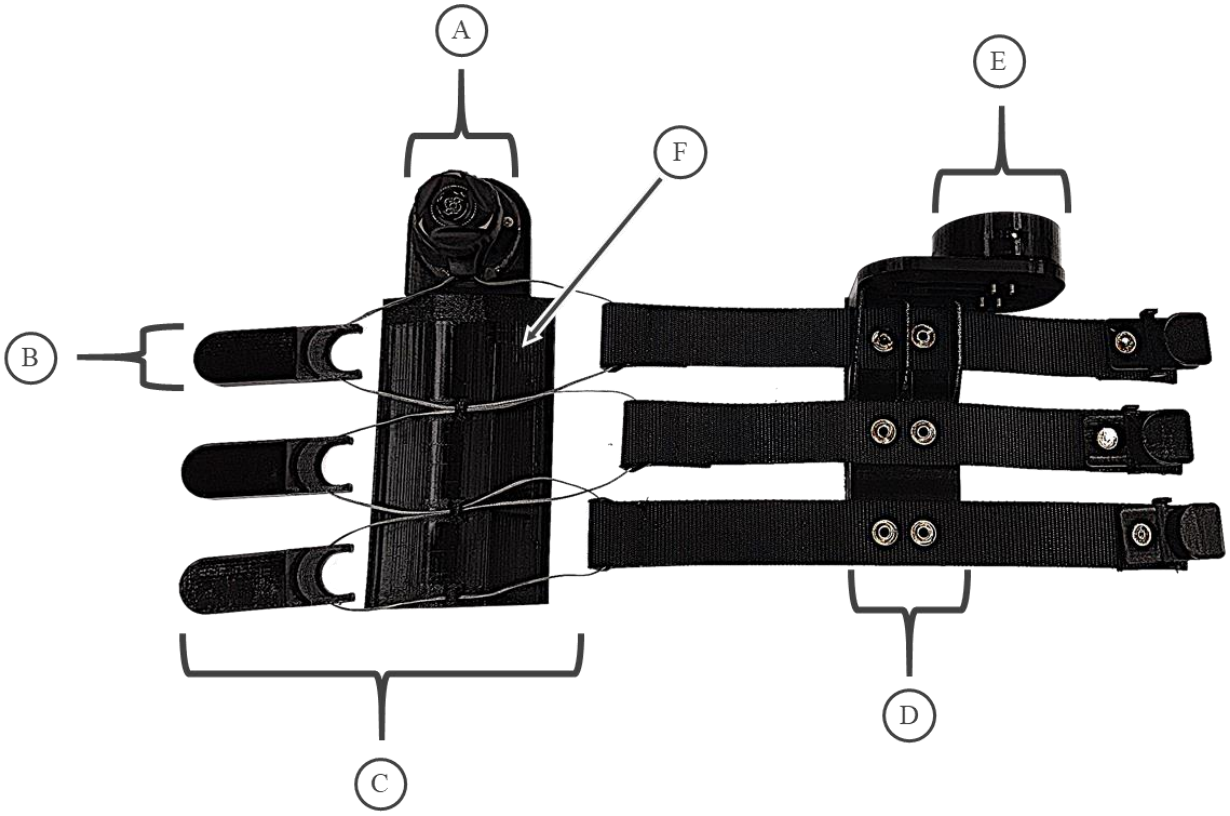

Figure 3.4: End Effector Attachment System, (A) Cable Tightening Knob, (B) Quick Connect Clips, (C) Cable Tightening System, (D) PLA Bracket, (E) Wrist Adapter, (F) Flexible TPU Plate

(a) *(b)*

Figure 3.5: Hand Restraint and End-Effector Attachment System (a) Dorsal View (b) Ventral View

3.5 Mechanotactile Tactor Design

Sensory feedback is integrated into the MSP using small, inexpensive mechanotactile tactors modified from earlier work in the lab [62]. The servo casing was modified to use a lightweight Dymond D47 servo motor (Dymond, USA) with a 3D printed module M0.5 rack and pinion system. An 8mm diameter rounded plunger head optimized for mechanotactile feedback [112] located on the lower end of the rack

applies a linear force to the user. With such a small gear module, tolerance error of 3D printers can cause the center distance between the rack and pinion to be too loose, resulting in tooth slip, or too tight, resulting in binding. Slots were added on the rack gear mount to allow for adjustability of the center distance between the rack and pinion gear, ensuring a proper fit regardless of tolerance errors. A pinion mount was added to support the pinion gear along the rotation axis, reducing transverse forces on the servo motor shaft. A rack gear plug was placed to ensure no debris or fabric from mounting systems contacts the rack gear. The closed-cell foam was placed on areas where the material would contact the skin to allow for sanitization between participants. An overview of the device components is shown in Figure 3.6. Two mounting systems were developed to apply feedback to the fingertips, representing somatotopically accurate feedback, or the forearm, representing modality matched feedback. The tactor slides onto a non-stretchable band wrapped around the user's forearm and clipped in place for the forearm feedback. For the fingertip feedback, two hook Velcro straps wrap around the finger and adhere to a loop Velcro base located on the back of the fingertip. Both devices are shown in Figure 3.7. The tactors can provide up to 12 N of force with a throw of 14 mm.

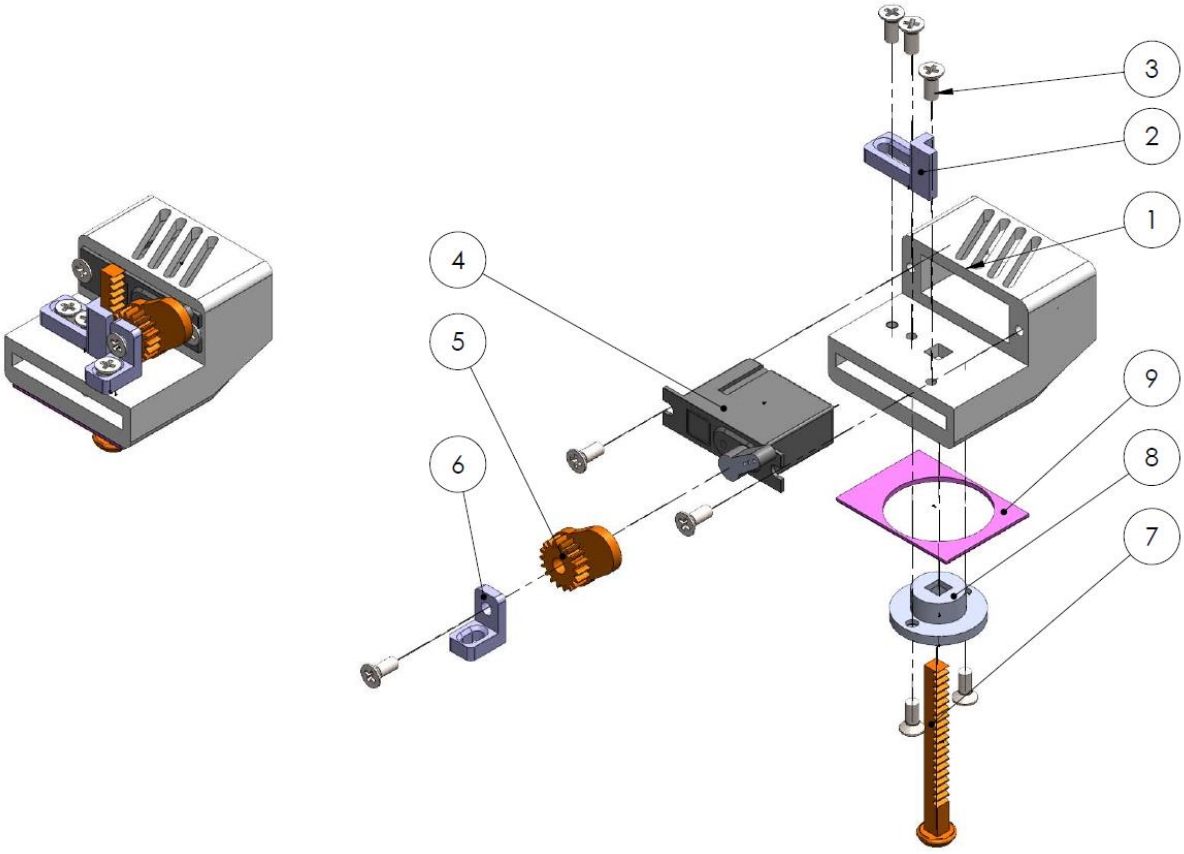

Figure 3.6: Mechanotactile Tactor Components (1) Servo Casing, (2) Rack Gear Mount, (3) M2.5x5mm Screws, (4) D47 Servo Motor, (5) Pinion Gear, (6) Pinion Gear Mount, (7) Rack Gear, (8) Rack Gear Plug, (9) Washable Foam

(a) *(b)*

Figure 3.7: (a) Mechanotactile Tactors on Forearm Mounting System (b) Mechanotactile Tactors on Fingertip Mounting System

3.6 Compliant Fingertip Force Sensor

3.6.1 Introduction

Small force sensors can be placed on the prosthetic hand's fingertip for measurement of grip force. Capacitive force sensors have previously been shown to perform better than commonly used force-sensitive resistors for this application [62]. These sensors are designed to attach to a flat surface, with the force loading evenly distributed across its surface area. Previous testing has shown that these sensors are sensitive to the contact materials curvature and compliance [113]. Previously in the lab, small capacitive force sensors (SingleTact) have been taped directly to the end effector fingertips. However, prosthetic hands undergo various loading conditions that do not represent this ideal situation, as illustrated in Figure 3.8. It was hypothesized that encapsulating a capacitive force sensor in a compliant material would disperse the force evenly throughout the sensor, allowing for more robust measurement to various loading conditions.

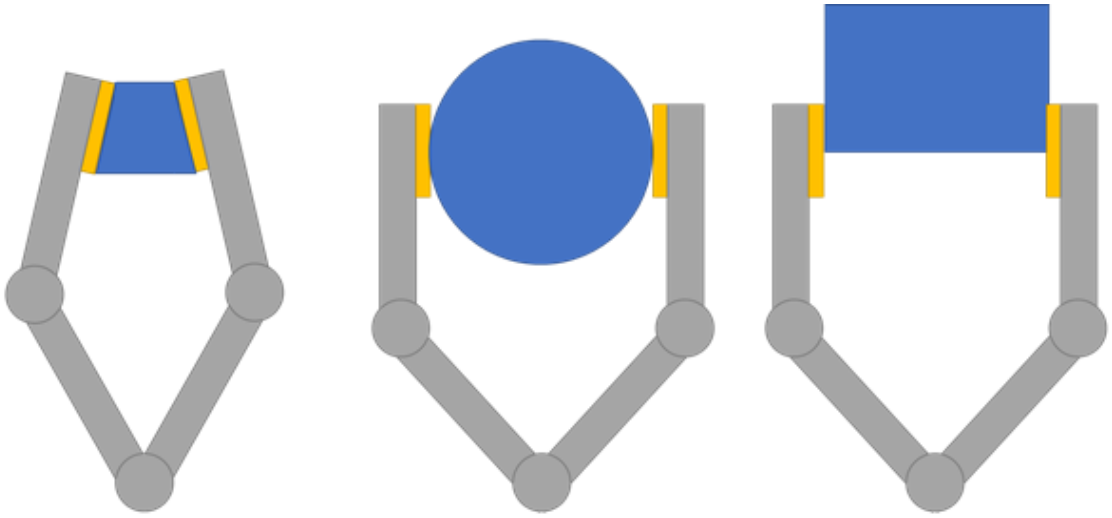

(a) *(b)* *(c)*

Figure 3.8: Varying Loading Conditions: (a) Angled Load, (b) Curved Surface, (c) Shifted Contact Location

3.6.2 Methods

An S8-10 capacitive force sensor (SingleTact, USA) was compared before and after being encased in Dragon Skin 10NV, a compliant silicone rubber-based material (Smooth-On, USA). The apparatus with no compliant material is referred to as the baseline configuration, and the apparatus with compliant material is referred to as the encapsulated configuration. A load cell (Omega LCM703 calibrated to a maximum error of 0.1N) was placed in line with an HS-35HD servo motor (Hitec RCD, USA) to apply force to the sensor through a PLA indenter. The load cell was read using Simulink Real-Time (Matlab 2014a) through a National Instruments data acquisition system (NI PCI6259) at a rate of 2000Hz. A force was applied between 0 and 10 N in a sinusoidal pattern for five total periods, similar to earlier work [62]. Loading periods of 0.5, 1, and 5 seconds were tested to account for dynamic loading effects. Each measurement was repeated three times to ensure repeatability between trials, for a total of 9 trials for each condition. The two configurations, as well as the experimental setup, is shown in Figure 3.9.

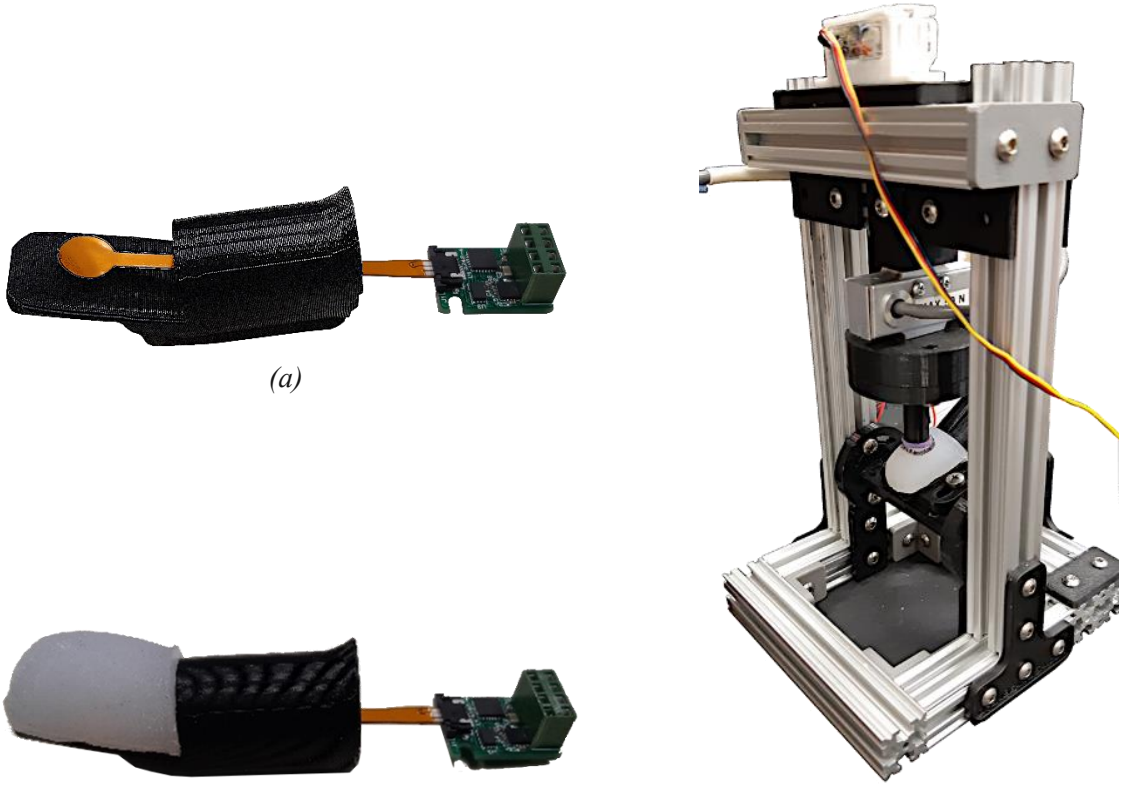

Figure 3.9: Compliant Fingertip Sensor (a) Baseline Configuration, (b) Encapsulated Configuration, (c) Experimental Setup

An ideal indenter was made with a circular flat contact surface (8 mm diameter) and covered in a 2 mm thick foam to ensure even force distribution over the sensor's entire surface area. Loading this indenter aligned with the sensor acted as the ideal condition for both the baseline and the encapsulated configurations. All other conditions were compared to the ideal condition to evaluate the sensor's ability to adapt to various circumstances. The ideal indenter position was moved by 4mm in both the proximal and distal directions to evaluate a non-central loading condition's effect. An indenter with a 10 mm diameter curvature was tested to represent grasping a curved surface. A centred applied loading condition at a 15-degree angle was also evaluated using the ideal indenter for only the encapsulated configuration. To clarify, the force line of action for this loading condition still passed through the center of the sensor but was applied 15-degrees perpendicular to the sensor. Table 3.1 shows a summary of the different loading conditions for each configuration and images of the indenter types.

Table 3.1: Compliant Fingertip Sensor Experiment Overview

	Baseline Configuration 	**Encapsulated Configuration** 
Ideal Indenter 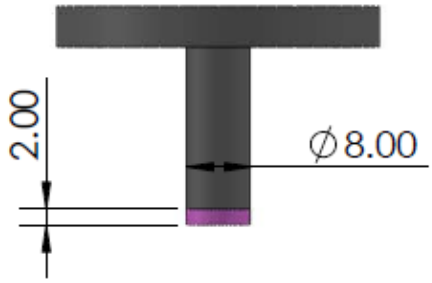	• Centered (Ideal Condition) • 4mm Proximal Offset • 4mm Distal Offset	• Centered (Ideal Condition) • 4mm Proximal Offset • 4mm Distal Offset • 15 Degree Angle
Curved Indenter 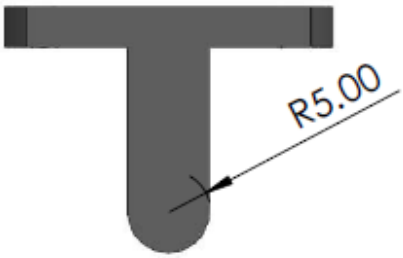	• Centered	• Centered

3.6.3 Results

Note that the SingleTact force sensor has a reported hysteresis of 4% full-scale range, equating to 0.4N of error for the selected 10N range sensor.

Ideal Condition

The baseline and encapsulated sensors were calibrated using the ideal flat indenter in a centered loading condition at a zero-degree angle. All trials were used to create a polynomial calibration curve relating the sensor output voltage to the applied force. Polynomial fits of increasing degrees were evaluated, as shown in Figure 3.10 and Figure 3.11. The root-mean-squared error (RMSE) was calculated using the following formula.

$$RMSE = \sqrt{\frac{1}{n}\sum_{i=1}^{n}(y_i - \hat{y}_i)^2}$$

Where y_i is the measured force value of data point i and $\hat{y}_i$ is the predicted force value from the polynomial curve fit of data point i. n corresponds to the total number of data points in the nine combined trials. RMSE was used to evaluate the goodness of fit of the polynomial curves created. RMSE was chosen over Mean Absolute Error (MAE), as the square term makes RMSE more sensitive to large errors, which is undesirable in a prostheses application.

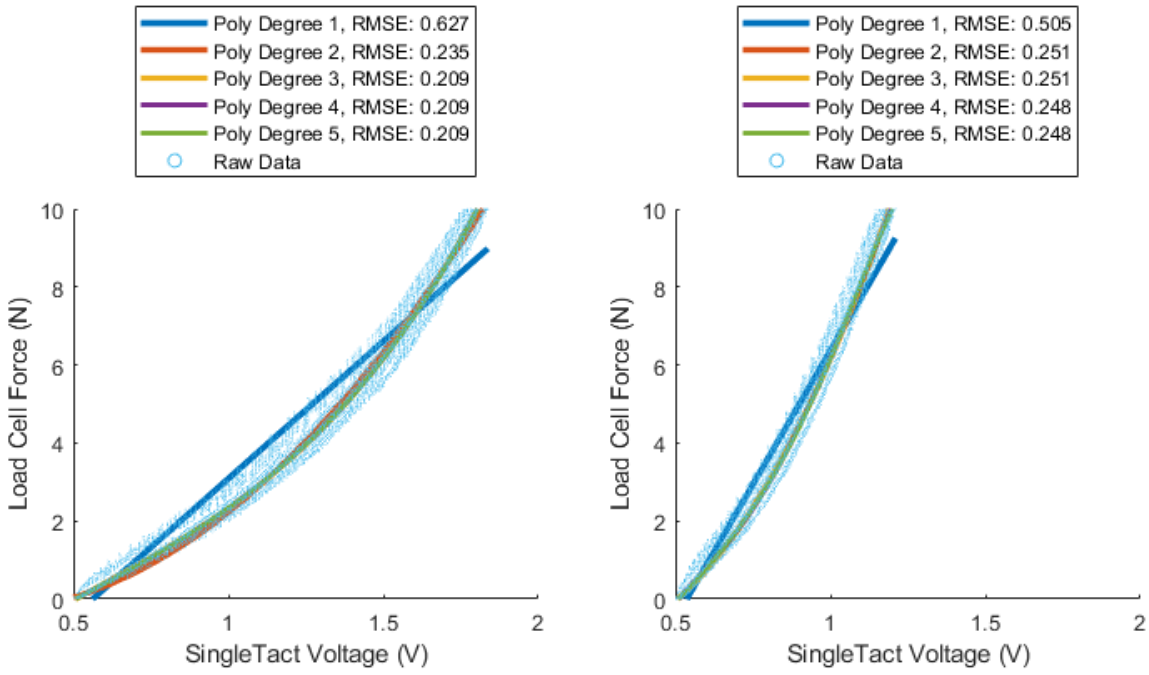

(a) *(b)*

Figure 3.10: Polynomial Curve Fitting Analysis on Ideal Conditions with (a) Baseline Sensor and (b) Encapsulated Sensor

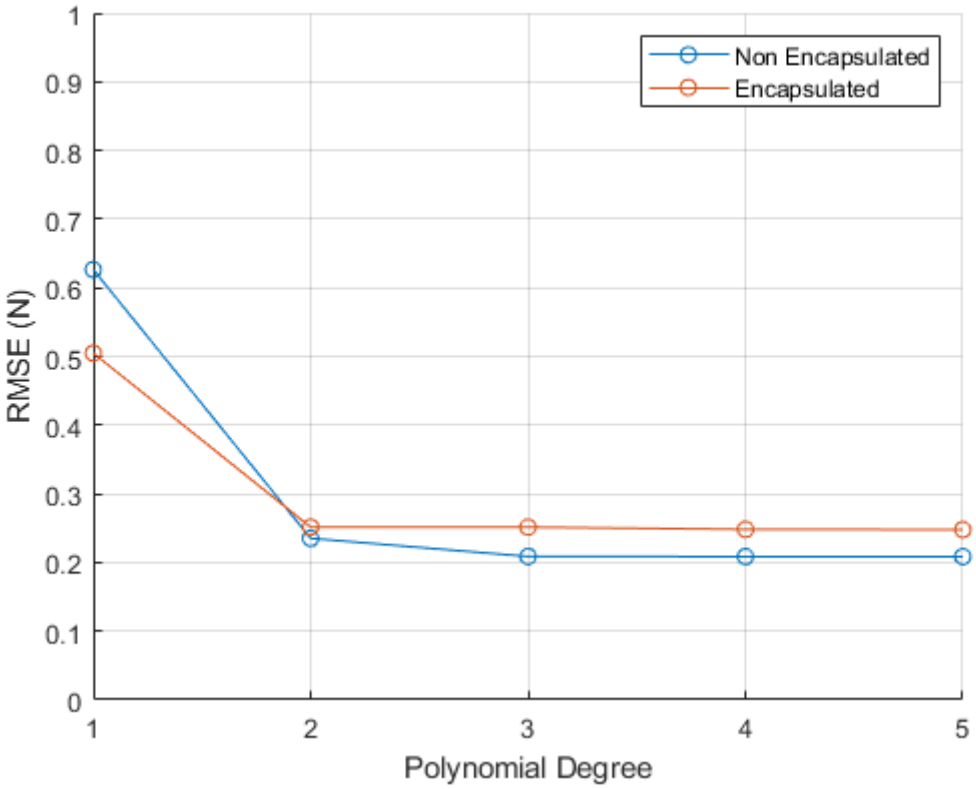

Figure 3.11: Polynomial Curve Fitting RMSE Summary

The RMSE plateaus around the 3rd order at 2.1% full-scale range for the baseline sensor and 2.5% full-scale range for the encapsulated sensor. Also, note that the RMSE for both configurations is below the reported 4% full-scale range hysteresis error reported on the SingleTact datasheet, indicating the sensors perform as expected during the ideal loading condition. The 5th order polynomial curve fit was used as the calibration curve for the baseline and encapsulated sensors for comparison to the non-ideal configurations.

Curved Indenter Condition

The results using the curved indenter is pictured in Figure 3.12.

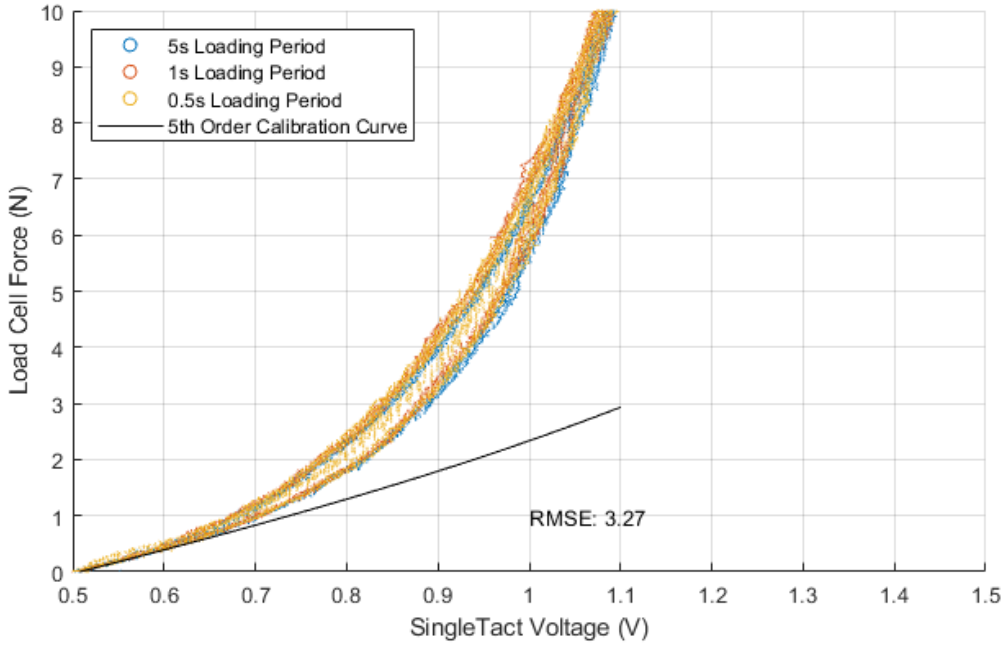

(a)

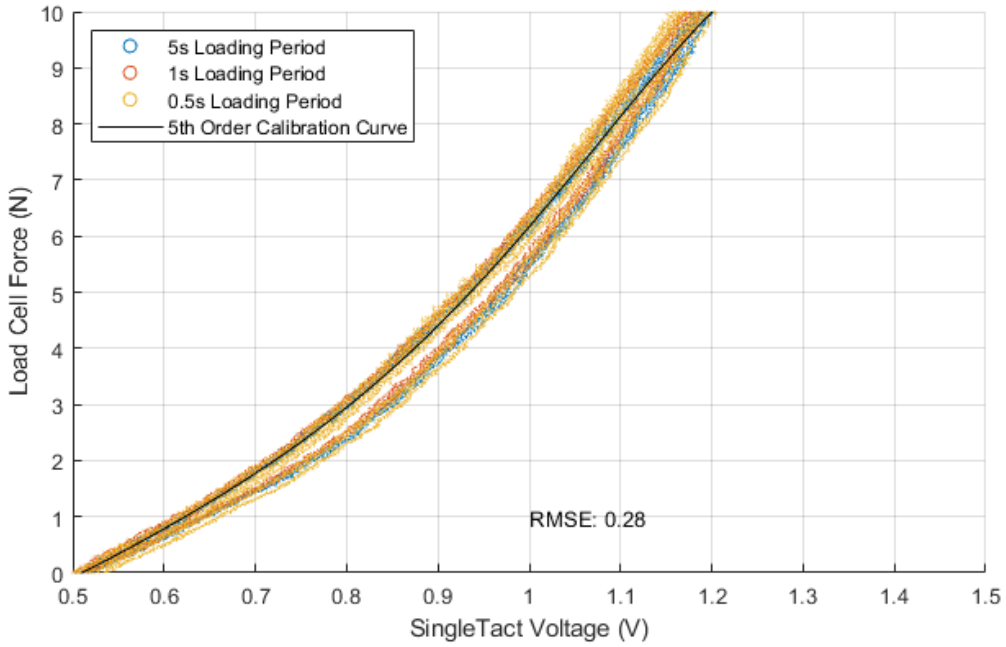

(b)

Figure 3.12: Results For 10mm Diameter Curved Indenter (a) Baseline Sensor and (b) Encapsulated Sensor

The baseline configuration showed a substantial increase in RMSE to 32.7% of full-scale range, while the encapsulated configuration was relatively unaffected, showing an RMSE increase to 2.8% full-scale

range. The high RMSE of the baseline configuration indicates that it cannot adapt to varying indenter shapes using a single calibration curve. The large error for the baseline configuration is caused by the curved indenter contacting only a portion of the SingleTact sensor's surface area. The encapsulated sensor disperses the indenter's force throughout the soft material, resulting in consistent readings agnostic of indenter shape.

Indenter Position Offset Condition

The results when moving the ideal indenter position 4mm in the distal direction is pictured in Figure 3.13.

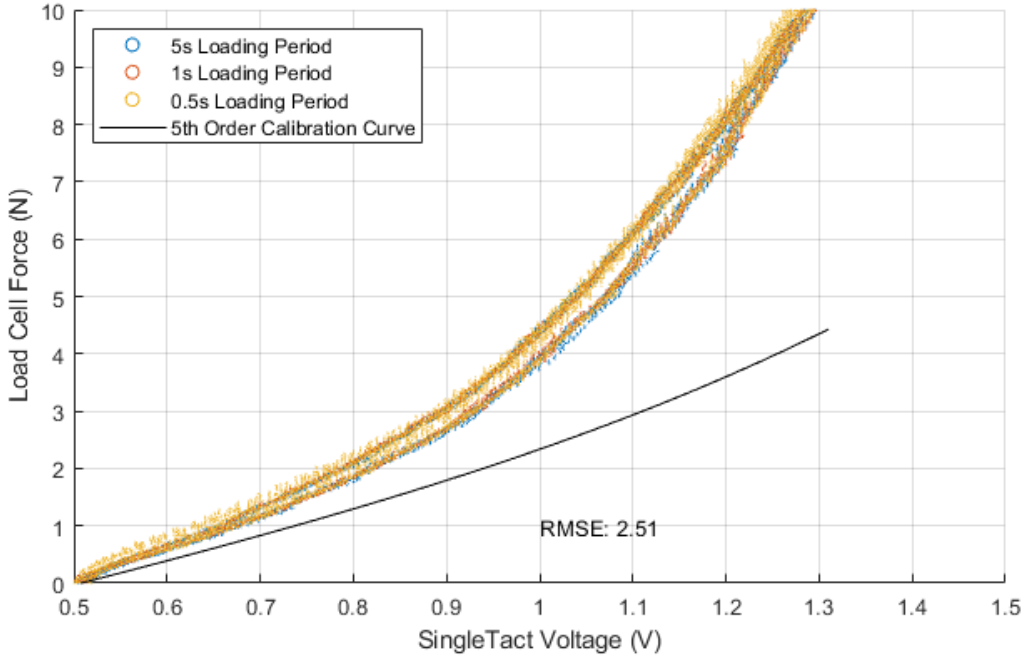

(a)

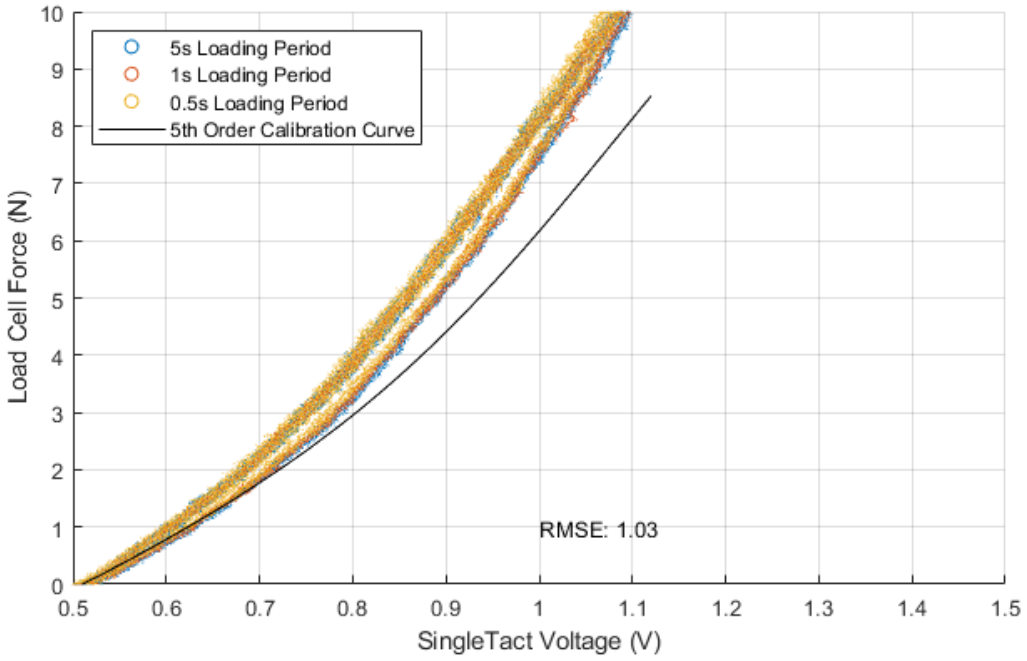

(b)

Figure 3.13: Results For Ideal Indenter Offset 4mm Distally (a) Baseline Sensor and (b) Encapsulated Sensor

The results when moving the ideal indenter position 4mm in the proximal direction are pictured in Figure 3.14.

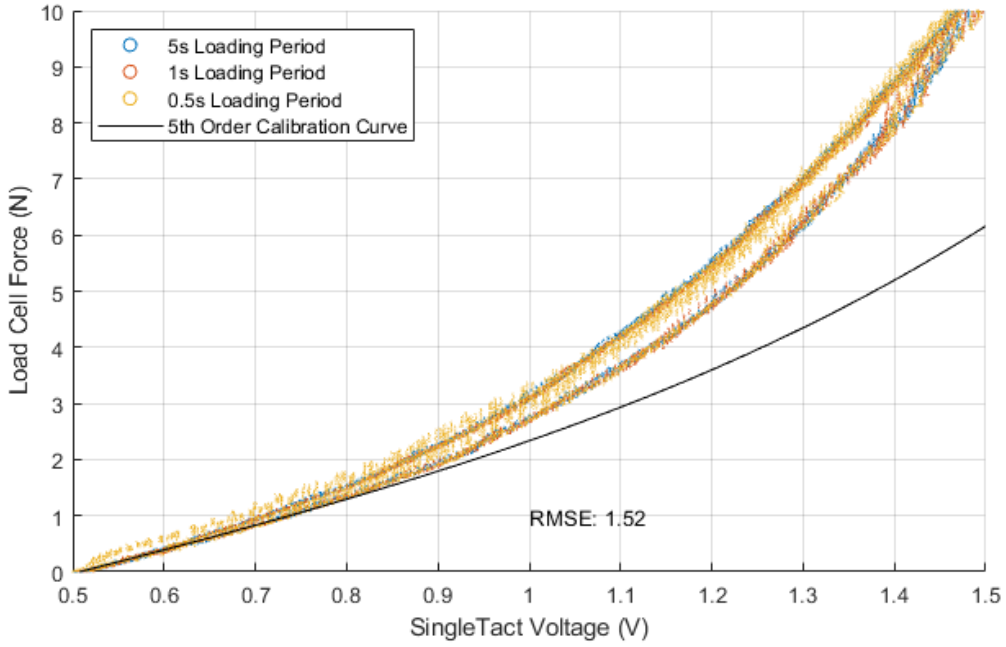

(a)

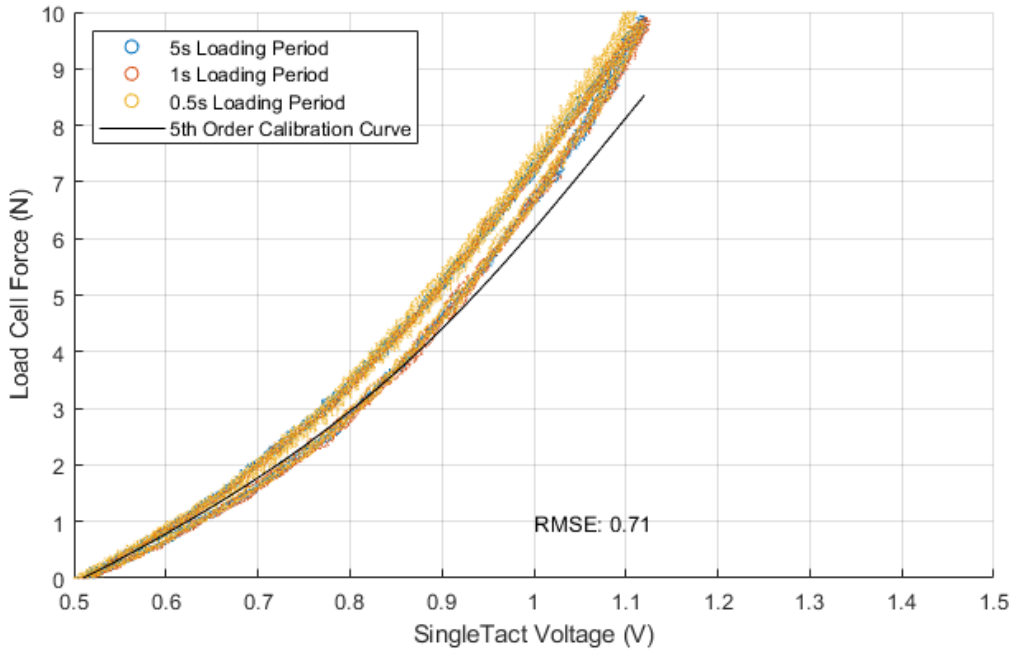

(b)

Figure 3.14: Results For Ideal Indenter Offset 4mm Proximally (a) Baseline Sensor and (b) Encapsulated Sensor

The baseline configuration showed an RMSE of 25.1% and 15.2% full-scale range when the ideal indenter was varied by 4mm distally and proximally, respectively. The encapsulated configuration showed an RMSE of 10.3% and 7.1% full-scale range when the ideal indenter was varied by 4mm proximally and distally. These results show that the encapsulated sensor much less susceptible to an indenter location shift than the baseline sensor.

Angular Loading of Encapsulated Sensor

The results when applying the ideal indenter at an angle of 15 degrees is pictured in Figure 3.15.

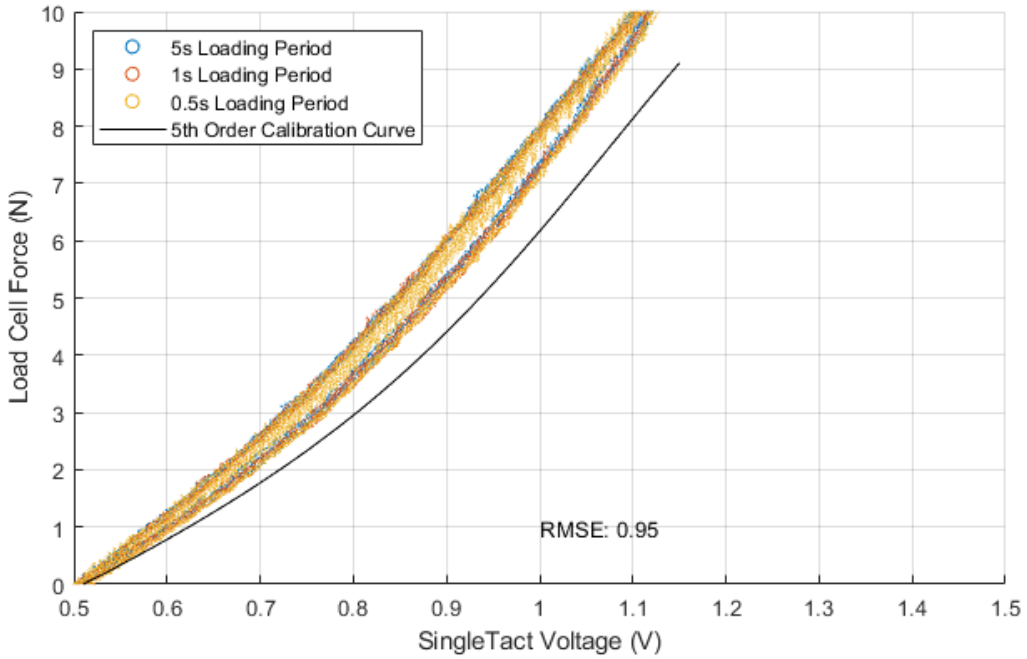

Figure 3.15: Results For Ideal Indenter Offset 15 Degrees for Encapsulated Sensor

The results show an RMSE of 9.5% full-scale range, indicating that the encapsulated sensor remains functional at reduced accuracy for angled loading scenarios.

3.6.4 Sensor Summary

Table 3.2 and Figure 3.16 summarize all results for the compliant fingertip force sensor evaluation. In the ideal condition, both configurations performed within the manufacturer's specifications at root mean square error (RMSE) of 2.1% and 2.5% of full-scale range for the baseline and encapsulated configuration. The RMSE of the baseline configuration was much more sensitive to changing conditions than the encapsulated configuration. The curved indenter condition produced a substantial decrease in the baseline configuration performance, giving an RMSE of 32.7% full-scale range. The encapsulated configuration was relatively unaffected with an RMSE of 2.8% full-scale range. Similarly, when the ideal indenter was shifted by 4mm, the RMSE for the baseline configuration rose to 25.1% full-scale range (distal offset) and 15.2% full-scale range (proximal offset). The encapsulated configuration RMSE increased to 10.3% full-scale range (distal offset) and 7.1% full-scale range (proximal offset). Finally, the encapsulated configuration showed an RMSE error of 7.6% full-scale range during the 15-degree angled loading scenario. Figure 3.16 shows each configuration's loading curve fit with a 5th-degree polynomial curve. The baseline configuration's loading curves are much more varied than the encapsulated sensor, illustrating the dependency on environmental conditions. For example, at a 10 N load, the baseline configuration voltage output varies by 0.72 V (50.7% full-scale range over 10 N) depending on the

condition. In comparison, the encapsulated configuration only varies by 0.11 V (14.4% full-scale range over 10 N). In conclusion, the encapsulated configuration is much more robust to changes in environmental conditions, producing substantially more accurate results than the baseline configuration. Therefore, the encapsulated configuration was implemented in the MSP end effector.

Table 3.2: Summary of Experimental Results for Grip Force Sensor Comparison

Loading Condition	Baseline Sensor RMSE (N)	Encapsulated Sensor RMSE (N)
Ideal	0.21	0.25
Rounded	3.27	0.28
4 mm Distal Offset	2.51	1.03
4 mm Proximal Offset	1.52	0.71
15 Degree Angle	-	0.95

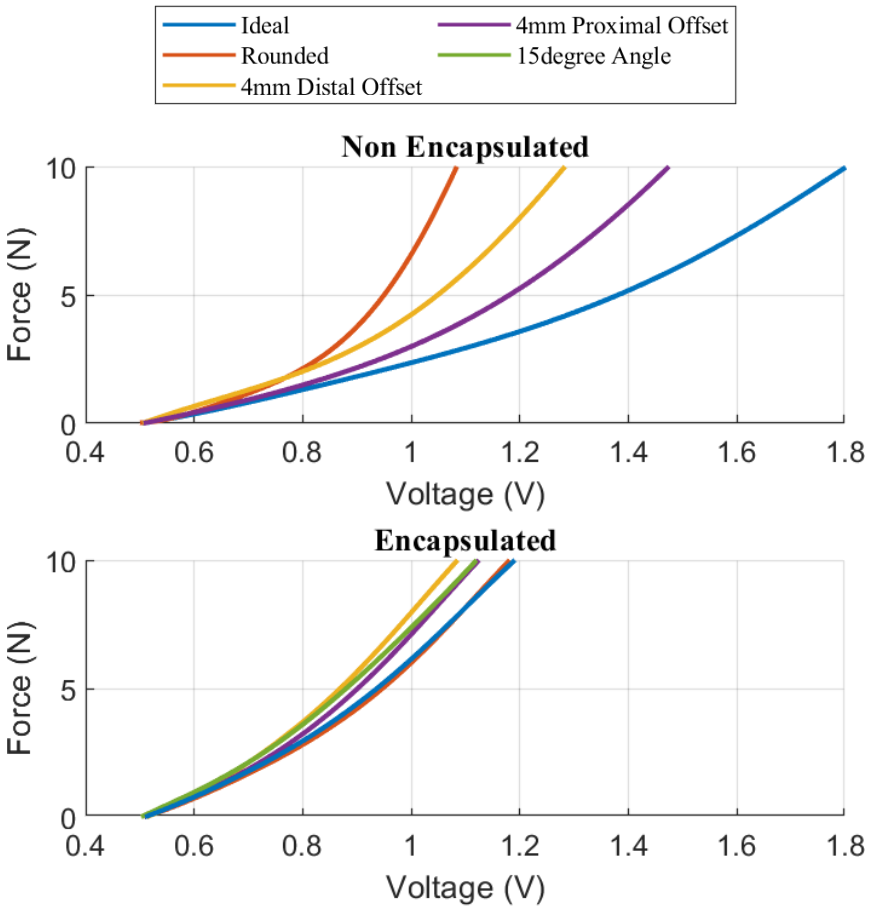

Figure 3.16: Loading Curve Comparison Between Various Conditions

3.7 End Effector

A 3D printed PLA, anthropometric, single-degree-of-freedom (hand open, hand close) end effector was designed (Solidworks, 2018) titled the Powerhand. The Powerhand is driven by a Dynamixel MX-64AT servo motor (Robotis, Inc.). The four fingers are rigidly connected and attach directly to the Dynamixel rotation point. The fingers and thumb are actuated simultaneously through a linked bar mechanism, as illustrated in Figure 3.17.

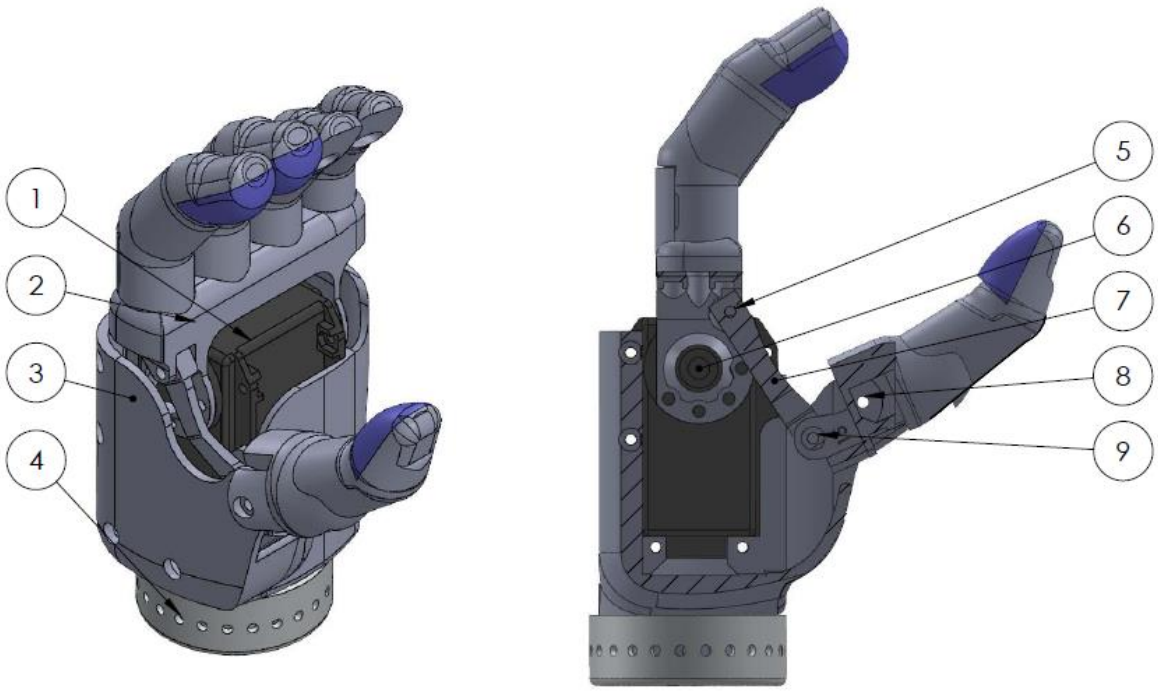

(a) *(b)*

Figure 3.17: (a) Isometric View of Powerhand, (b) Cutaway View of Linked Bar Mechanism, (1) Dynamixel MX-64AT, (2) Rigid Finger Brace, (3) Hand Casing, (4) Wrist Adapter, (5) Linked Bar Finger Rotation Point (6) Dynamixel Rotation Point, (7) Linked Bar Mechanism (8) Fixed Thumb Rotation Point (9) Linked Bar Thumb Rotation Point

The previously discussed compliant force sensors were added to the index finger, middle finger, and thumb of the end effector to measure contact pressure. The SingleTact sensors require an attached analog-to-digital converter (ADC) located approximately 5cm from the sensor pad. This distance is too short to locate the ADC externally from the hand. Therefore, the ADC board must be placed within the finger of the end effector. The fingers were hollowed out to create a cavity for the electronics box and SingleTact wires. A snap-fit lid allows for installment and access to the embedded ADC box. The details of a compliant sensor within a Powerhand finger are shown in Figure 3.18.

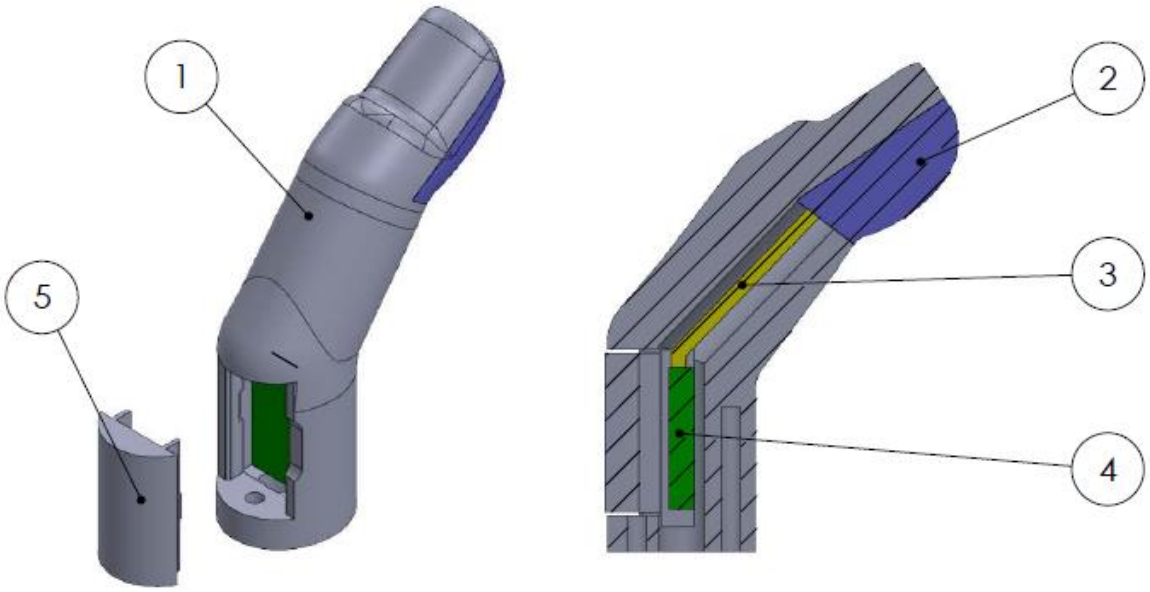

Figure 3.18: Exploded and Section View of Powerhand Finger With Compliant Sensor, (1) PLA Finger, (2) Compliant Sensor, (3) SingleTact Wire, (4) ADC Board, (5) Snap-Fit Lid

There is little inherent compliance in the PLA material used for the fingers, and all fingers are rigidly coupled. When grasping without the compliant fingertip sensors, only two contact points are made on the object, with a minimal surface area. Having only two contact points makes the grasp unstable as the object can easily be rotated along the axis between the two points of contact. Furthermore, the PLA material is quite slippery, resulting in low friction between these contact points and the object. The compliant fingertip sensors also helped solve this problem, creating a more stable grasp by allowing three contact points, increased contact surface area, and higher friction between the fingertips and the object.

The specifications of the end effector are summarized in Table 3.3. The completed device can be seen in Figure 3.19. It is important to note that many anthropomorphic end effectors exist [18]. However, using an end effector with a Dynamixel motor allows the MSP to integrate with BrachIOplexus [114], an open-source graphical user interface (GUI) designed in the BLINC lab for myoelectric prosthesis control experiments.

Table 3.3: Specifications for End Effector

Mass (g)	298
Maximum Grip Aperture (mm)	125
Maximum Grip Strength (N)	11
Degrees of Freedom	Hand (open/close)
Maximum Grip Speed (deg/s)	180
Maximum Current Draw (A)	4.1
Operating Voltage (V)	12
Cost ($CAD)	$550

Figure 3.19: PowerHand End Effector

3.8 Electrical/Software Design

BrachI/Oplexus, an open-source graphical user interface (GUI) designed for myoelectric prosthesis control [114], enables the EMG signal interpretation and end-effector motion. A microcontroller (Arduino Uno, R3) controls the mechanotactile tactors through PPM signals and reads the SingleTact sensors through the I2C communication protocol. Data logging capability is enabled at a frequency of 50 Hz. A custom GUI (Visual Studio C#, 2015) was created to communicate with the microcontroller to customize

tactor parameters, as pictured in Figure 3.20 quickly. This GUI had been previously designed in the lab for use with a force-sensitive resistor based tactor. However, it was modified to include streamlined data logging capabilities, more robust data packet protocols, capacitive sensor measurement capabilities and optional feedback delay.

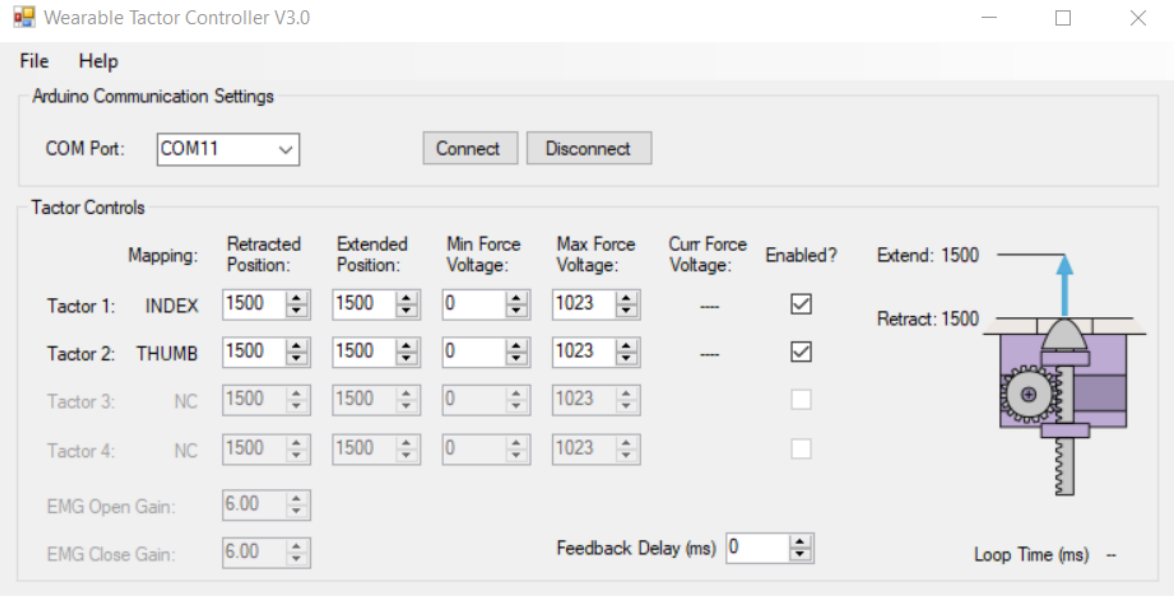

Figure 3.20: Mechanotactile Tactor User Interface

3.9 Conclusion

A lightweight, modular, simulated prosthesis was developed with both modality and somatotopically matched mechanotactile feedback systems. Pressure sensors used to measure grip force were compared before and after being encapsulated in a compliant material under various loading conditions. In all non-standard loading conditions, the encapsulated sensors outperformed the baseline sensor. This device will help researchers study feedback and control techniques in myoelectric prosthetics by providing a reliable test apparatus that easily allows for manipulating various parameters. The MSP's total mass is 691 g with the end effector included, can be comfortably worn for 3 hours, and costs less than CAD $1000. The end effector, feedback devices, and attachment system are all independent units creating a highly modular design that can be easily customized to fit specific needs. An image of the MSP donned on a participant is shown in Figure 3.21.

Figure 3.21: Modular Simulated Prosthesis with Forearm and Fingertip Tactors on Participant

4 Pilot Study

4.1 Introduction

The prosthetic hand's grip force is a high priority sensory signal for prosthesis users [5]. Many different feedback techniques exist to relay grip force information to the user that differs in modality and somatotopic accuracy [7], [97]. Persons with an amputation can experience non-painful sensations on the missing fingers when specific skin areas on the residual limb are stimulated, referred to as a phantom hand map [37]. Targeted muscle reinnervation (TMR) is a well-established surgical procedure for improving prosthetic control by re-routing efferent nerves from the lost limb to nearby intact muscle groups [39]. This surgery also re-routes sensory nerve fibers that can reinnervate the surrounding skin resulting in a restored hand map at the TMR location. Targeted sensory reinnervated (TSR) regions can be located away from reinnervated motor sites, making it possible to have both motor control and sensory feedback devices operating simultaneously [33]. The functional benefits of utilizing a somatotopically matched feedback site have not been compared to a non-somatotopically matched feedback site. Modality matched grip force feedback can be restored non-invasively through a mechanotactile feedback system [62]. Mechanotactile feedback is the only non-invasive technique capable of achieving modality matched feedback for grip force input, making it the ideal candidate for an experiment isolating somatotopic accuracy.

This pilot study's primary purpose was to validate an experimental protocol to compare the myoelectric performance of non-somatotopically accurate grip force feedback to somatotopically matched grip force feedback. Within-participant effect sizes were analyzed to evaluate chosen outcome measures, and between-participant effect sizes were used to inform an a-priori power analysis for a more extensive future study. Additionally, the presented pilot study serves to evaluate the effectiveness of the previously described MSP system. It was hypothesized that both feedback conditions would result in improved myoelectric performance, however, neither condition would outperform the other.

4.2 Methods

4.2.1 Materials

The experimental protocol consisted of non-disabled participants using the Modulated Simulated Prosthesis (MSP) to perform a grasp and lift task with a fragile object, pictured in Figure 4.1a. The fragile object was a 3D printed (PLA) cylinder previously designed in the lab instrumented with a 9-degree-of-freedom (DOF) inertial measurement unit (IMU) for orientation and acceleration measurement. Flat edges were designed along the cup's edges to ensure consistent and repeatable contact of the MSP fingertips. The cup weighed 272g, and with the compliant fingertips of the MSP took approximately 2N of grip force

to create enough friction to lift the fragile object without slipping. Note that the MSP's maximum grip force value is 11 N. Three participants underwent preliminary testing to determine the fragile object's breakage threshold. They were asked to lift the object while grasping as lightly as possible. Each participant underwent 20 trials without feedback and 20 trials with finger feedback. The results can be seen in Appendix A. Large variability in grasp forces between-participants was observed. A break force threshold value between 6.5N and 7.5N was chosen to ensure that the average participant could complete the task with a success rate between 60%-80%. Upon exceeding this threshold, the fragile object would emit a glass-shattering sound indicating to the user that the fragile object had broken.

Participants were fit with the MSP, with grip force fingertip measurement and mechanotactile tactors described in the MSP section previously. There were two feedback location conditions: finger and forearm. For the finger feedback condition, tactors were placed on the thumb and index fingers of the participant. The thumb tactor was mapped to the grip force sensor in the thumb of the MSP. The index tactor was mapped to the sum of the grip force sensor in the MSP index and middle finger. This mapping allowed for the utilization of three contact points of compliant digits when grasping the fragile object while maintaining sensor accuracy. For the forearm feedback condition, two tactors were placed approximately 10 cm apart on the forearm's volar surface between the Myo armband and the MSP wrist brace. This positioning is similar to a study conducted previously on mechanotactile discrimination [115] and ensures that the tactors are further apart than the noted two-point discrimination distance on the forearm of 38mm [93], [94]. A study using identical tactor plunger heads found the two-point discrimination to be 5mm higher than regular calipers [112]; the 10 cm distance used was enough to allow the two tactors to be independently discerned.

The MSP's conventional control was calibrated by monitoring the eight EMG signals from the Myo Armband while the participant underwent a series of wrist flexion and extension isometric muscle contractions. The two channels with the highest activation were mapped to open and close the hand. Special care was taken to ensure that additional weight from lifting an object did not result in EMG activation of the two chosen electrodes. This lift activation check was done by monitoring the signals while placing a vertical load on the end-effector and adjusting the minimum and maximum thresholds and gains accordingly.

Once set up and comfortable wearing the MSP with the mechanotactile feedback in place, the participants were instructed to move the fragile object from the starting position to the 10cm high shelf position with the lightest grasp force possible. A 20 second time limit was invoked to keep experiment time to under 3 hours. Participants were instructed to focus on grasping lightly rather than task speed, as 20 seconds was

more than enough time to complete the task (only one trial of all participant trials went over time). The task setup can be seen in Figure 4.1b.

(a) (b)

Figure 4.1: (a) Fragile Object (b) Experimental Setup

4.2.2 Experimental Protocol

A total of three non-disabled participants were recruited for an individual 3-hour long session. This experiment was approved by the University of Alberta Research Ethics Board (Pro00077893), and written informed consent was obtained from all participants before the experiment. The experiment was organized into four separate blocks corresponding to the four feedback conditions presented. Each participant fell into one of two categories that alternated the arm and finger feedback conditions' presentation order. The first and third block for all participants was a no-feedback condition. The second and fourth block contained either the arm or finger feedback condition, depending on which presentation order the participant underwent. An overview of the presentation order is shown in Figure 4.2a.

During each block, participants were administered a 5-minute training segment to practice using the MSP system. The first 3 minutes consisted of grasping and lifting various objects such as a foam ball and a stackable cup. The final 2 minutes were dedicated to manipulating the fragile object. The fragile object was set to administer the break sound feedback each time the break threshold was exceeded, allowing the participant to gain familiarity with the system. Commands were given to ensure the participants were performing similar motions during the training segment. After the training segment, the task completion segment commenced. The task completion segment was split into two identical sets of 15 trials. The first

set is referred to as the familiarization set, and the second set is referred to as the testing set. The outcome measures were calculated using only the testing set, similar to previous work [76]. Using only the testing set for calculation was done to reduce any confounding learning effects throughout the task completion segment. An overview of the protocol within each block is shown in Figure 4.2b.

Participants used noise-canceling headphones to ensure no sound from the MSP, and tactor motors could be used as incidental feedback. Participants were given mandatory 1-minute rest periods after each training segment and after each 15-trial set during task completion segments. Additional breaks were provided whenever requested by the participants. A protective sensation test was conducted with a 10 g monofilament to ensure that each participant had normal sensation in their forearm before beginning the experiment. Two-point discrimination tests were conducted to ensure the participant could discriminate between the two tactor positions before each feedback block.

Note that the fragile object breaking threshold for the first participant was set to 6.5N rather than 7.5N. Although the first participant still had a success rate in the desired range, they were an experienced myoelectric user. The following two participants were not experienced myoelectric users, and so the threshold was raised to 7.5N to ensure enough successful trials occurred. Additionally, the first participant completed fewer trials (~20 for each feedback condition) than the other participants. The number of trials per block was raised from 20 to 30 to increase the number of trials available for data analysis. For the first participant, the task completion segment was split into 10-trial sets rather than 15-trial sets. However, all metrics used were calculated within-participant, so this participant's data was still included for this pilot study.

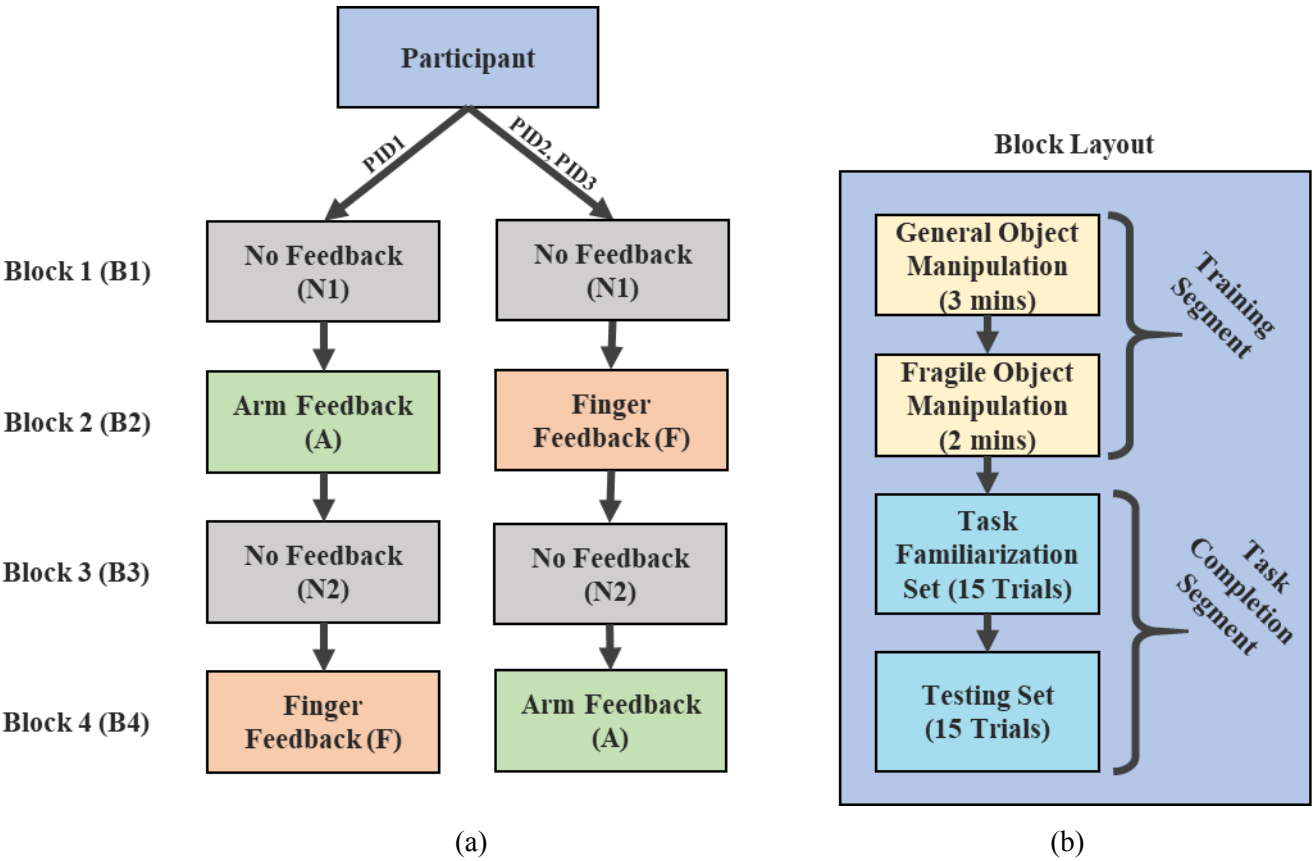

Figure 4.2: Experimental Protocol (a) Block Presentation Order Summary (b) Block Layout Summary

4.2.3 Data Processing

Data was collected at 50 Hz from the tactor system, fragile object, and the MSP through three independent GUIs (C#, Visual Studio Express 2015). The tactor system automatically logged grasp force from each digit, tactor positions, and timestamps. The fragile object automatically logged quaternion information representing orientation, raw accelerometer values in the x, y, and z directions, and timestamps. BrachIOplexus automatically logged all 8 EMG signals, the MSP hand position, velocity, torque, temperature, current draw, and timestamps.

4.2.4 Participants

PID1 was very experienced with myoelectric control and feedback systems. PID3 was moderately experienced, having completed myoelectric control experiments as a participant before. PID2 was unfamiliar with myoelectric control.

4.3 Outcome Measures

Success rate, maximum grasp, completion time, and grasp time were primary outcome measures as they directly represent functional performance in terms of consistency, accuracy, and speed. Adjustments were a secondary metric that showed how often a participant would adjust their grip. Learning effects within each testing were also explored. These metrics are discussed in further detail in the following sections.

The repeated measures experimental design allowed each participant to act as their own baseline or control, reducing the impact of inherent variation between-participants by allowing for relative improvements to be analyzed. It was initially planned to compare each feedback condition to the previous no-feedback condition. However, during experimentation, participants would make significant task completion strategy changes between blocks during the training segments, potentially causing large performance variations between the two no-feedback blocks. Thus, it was decided that averaging both no-feedback blocks would obtain the best estimate for each participant's baseline. The *A* label represents the arm feedback, *F* represents the finger feedback, and *Navg* represents the average between the two no-feedback conditions. The *A-N* label is used to indicate the difference between the arm feedback condition and *Navg*. The *F-N* label is used to indicate the difference between the finger feedback condition and *Navg*. Additionally, the *F-A* label represents the difference between the finger feedback condition and the arm feedback condition. To clarify, the 2nd abbreviation is subtracted from the first abbreviation; for example, a positive *A-N* value indicates that the arm condition had a higher value than the *Navg* condition. The comparison and label structure are visualized in Figure 4.3.

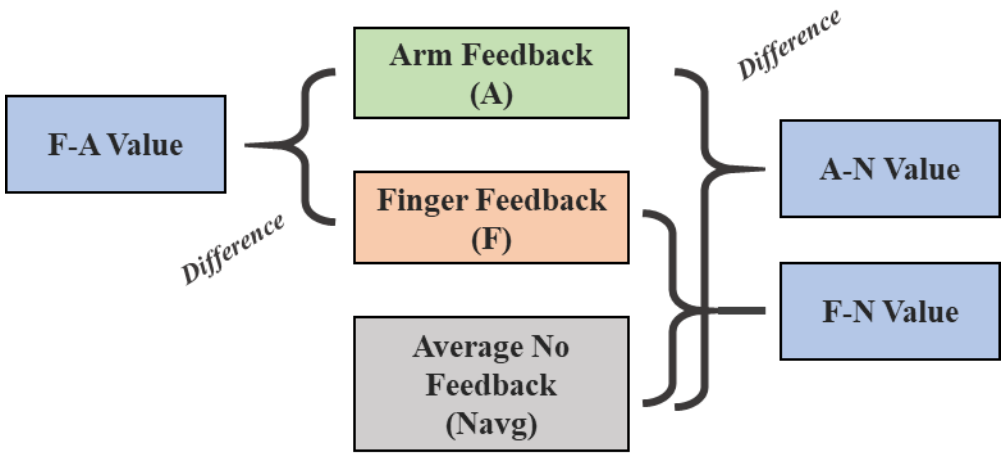

Figure 4.3: Outcome Measure Overview

4.3.1 Primary Outcome Measures

Success rate

A trial was deemed successful if the participant transferred the fragile object to the shelf without breaking or dropping it within the 20 second time limit. The ratio of successful trials to total trials in a testing set is the block's success rate. This metric indicates task performance consistency. The added information provided by the feedback was hypothesized to result in an improved success rate for both feedback conditions.

Maximum Grasp

The largest value measured by the fingertip force sensors on each trial was recorded as the maximum grasp force, similar to previous work [62], [76]. The average maximum grasp for each block was calculated from all successful trials in the testing set to provide a single value for each block. A lower value indicates better grasp force control as the participants were explicitly told to grip the cup as lightly as possible. The added information provided by the feedback was hypothesized to reduce the maximum grasp force for both feedback conditions.

Completion Time and Grasp Time

The time taken from task start to object release was defined as the completion time. The average task completion time for each block was calculated from all successful trials in the testing set to provide a single value for each block. The time taken from first contacting the object to first lifting the object was defined as grasp time. The average grasp time was calculated from all successful trials in each set to provide a single value for each feedback condition. The added information provided by the feedback was hypothesized to increase the completion and grasp time for both feedback conditions, as the participants would be more focused on the task.

The contact point was calculated as the first instance where the grasp force exceeded 0.3N. The lift point was defined when the z-acceleration of the fragile object first exceeded 1m/s. The release point was calculated as the first point where the grip force fell below 0.3N after the lift point. An example of these points extracted from a successful trial is shown in Figure 4.4. The X's indicate the contact point, lift point, and release point in a typical successful trial. Grasp force increases just before the defined contact point at around 3.8s. After the grasp force increases to a stable level just after 5s, the lift point is identified by an initial increase in z-acceleration. As the object is released, the grasp force decreases, marking the release point. Additionally, the z-acceleration is seen to jump to very high values as the object hits the shelf's bottom.

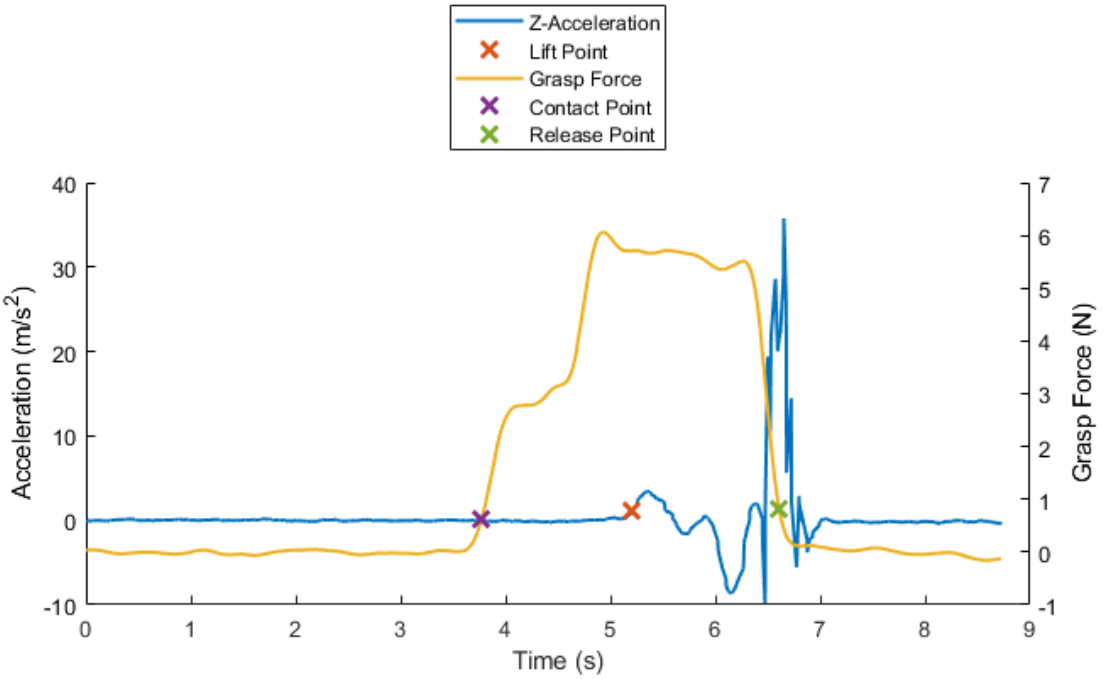

Figure 4.4: Contact Point, Lift Point, and Release Point Extraction Example

4.3.2 Secondary Outcome Measures

Hand Aperture Adjustments

A hand aperture adjustment was defined as a direction change in the prosthesis hand open/close velocity. The calculation of this value becomes problematic when the participant's EMG signal is very close to the minimum motion threshold. The noise in the EMG signal results in the hand aperture velocity signal oscillating over the minimum threshold creating artificial zero crossings in the hand aperture velocity at a frequency much faster than is capable by a human. The hand velocity signal was low pass filtered using a moving average filter designed to have -3dB of attenuation at 7Hz to mitigate these motion artifacts. 7 Hz was chosen as it represents the average frequency exerted by humans during a fast tapping motion [116]. 7 Hz is a conservative estimate of what gesture frequency a human could generate since participants in the current study were activating wrist flexion and extension rather than fast finger motion. The moving average filter was chosen over other filtering techniques since it does not cause signal overshoot, which could manifest as artificial motion changes upon the signal returning to zero. An example of the adjustments extracted from a successful trial is shown in Figure 4.5. A positive hand velocity corresponds to the hand-close direction. The X's indicate that an adjustment was made (i.e., a direction change of the prosthesis hand aperture velocity). Around the 3.5s mark, the unfiltered hand aperture velocity can be seen to oscillate rapidly. However, this oscillation only results in one adjustment after the signal is filtered

as described. This metric was chosen to provide insight into the impact of feedback condition on grasp modulation during the fragile object task. The total number of adjustments from task start to object release was calculated from all successful trials in each set to provide a single metric for each feedback condition. The number of adjustments was hypothesized to increase for both feedback conditions due to an increased focus on the task.

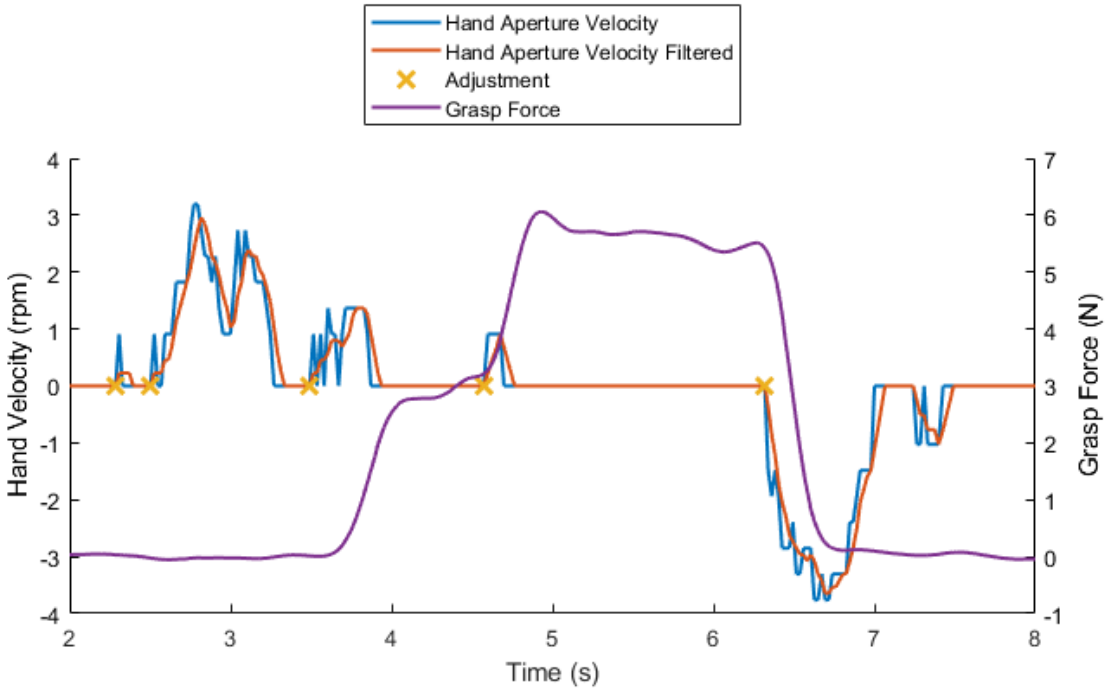

Figure 4.5: Adjustment Calculation Example (PID 1 during Block 1)

4.3.3 Learning Effect

The repeated measures experimental design allowed each participant to act as their baseline or control, reducing the inherent variation between-participants by allowing for relative improvements to be analyzed. A problem that arises anytime human participants are involved in a sequential task study is the possibility of a learning effect, making results dependent on the presentation order. The presentation order has shown to be a substantial factor in feedback experiments involving fragile objects [117], [118]. Often this is overcome by pseudo-randomizing the presentation order between-participants. Due to the low number of participants, randomization could not be effectively used in this pilot study; therefore, individual repeated measures were used rather than group comparisons. The training segment and task familiarization set were to provide the participant with enough time to become accustomed to the myoelectric control to mitigate learning during the testing set. A linear regression analysis was used to

quantify the learning occurring within the testing set by comparing each outcome measure to the trial number. If the training segment and task familiarization set provided sufficient experience for each participant, there would be little or no correlation between the trial number and each outcome measure.

4.3.4 Effect Sizes

Standardized effect sizes provide a unitless measurement of the experimental effect's magnitude that can be interpreted between studies. Many researchers argue that effect sizes are a more important value for interpretation than the more commonly used p-value [119]–[121]. The p-value can inform whether there is a difference between the two means; however, it provides no information about the difference's size. Furthermore, statistically significant p-values can almost always be obtained through an increased sample size (unless the effect size is zero). This thesis focuses on Cohen's D effect size, which compares two means [122]. The following formula gives Cohen's D:

$$d = \frac{M_1 - M_2}{s} \quad [1]$$

Where d is the effect size, M_1 and M_2 are the means of two different groups, and s is the standardizer. Note that the standardizer choice depends on the comparison being made and the experimental context. The standardizer for Cohen's D is always a standard deviation [123]. More specifically, the value of d represents the number of standard deviations that separate the two means.

In this study, individual effect sizes were computed on a per-participant basis to analyze each participant separately for the A-N, F-N, and F-A comparisons. These individual effect sizes were calculated using the mean difference and pooled standard deviation between both conditions being compared for each participant separately. The formula for pooled standard deviation is given below:

$$SD_{pooled} = \sqrt{\frac{(N_1 - 1)SD_1^2 + (N_2 - 1)SD_2^2}{N_1 + N_2 - 2}} \quad [2]$$

Where SD_1 and SD_2 are the sample standard deviations for each group, and N_1 and N_2 are the number of samples in each group.

The previously discussed individual effect sizes are not useful for doing a power analysis, as they are unique to each participant. For power analyses, between-participant effect sizes were computed using the group mean difference and standard deviation of difference scores for the A-N, F-N, and F-A comparisons. While the standard deviation of difference scores are not the best standardizer for reporting

effect sizes of results for paired designs, it is the proper standardizer for power analysis as it is the same value used for conducting the t-test during null-hypothesis testing [123]. A better standardizer for reporting effect sizes in a more extensive study would be a pooled standard deviation of group means from both conditions being compared [123]. This standardizer would allow for results to be used in meta-analysis more readily.

4.3.5 Power Analysis

The power of a study indicates the probability of detecting an effect given that one exists. A power analysis can be completed before recruitment for a study to determine the number of participants required to detect a specific effect size based on the desired error tolerances. The calculation is a function of four key variables: α-level (Type I error), β-level (Power), d (effect size), and n (number of participants). If any three of these values are known, the fourth can be calculated. Before recruitment, the α and β values are chosen by the researcher. For prosthesis research, an α-level of 0.05 is standard. Cohen outlines a generally accepted β-level of 0.8 [122].

The effect size depends on what statistical test is conducted after the study is completed. For this study, the statistical test to be used compares group means of the A-N, F-N, and F-A metrics using a one-sample t-test, making Cohen's D the appropriate effect size statistic. Note that completing a paired samples t-test between two group means is mathematically identical to completing a one-sample t-test on difference scores [124]. However, effect sizes are unknown before a study and must be estimated to conduct the power analysis. A search in the literature can sometimes yield experiments similar enough to the study being done that an idea of these missing parameters can be found to compute a likely effect size. For prosthesis research, experiments are often variable in the materials and tasks, making this difficult. Alternatively, a pilot study with a smaller sample size can be run before recruitment to give a rough estimate of these missing parameters. Third, if none of the above parameters are known, the effect size can be directly asserted by the researcher, in the absence of knowing the underlying mean and standard deviation values in the specific application. However, this technique considers no experimental context and should only be used when no other technique is available to gather better estimates [125]. Cohen's recommendations state that an effect size of 0.25 is considered small, 0.5 medium, and 0.8 large [122].

This study's power analysis was completed using G*Power, a commonly used software package built for this application [126]. For the F-N, A-N, and F-A metrics, a two-tailed one-sample t-test power analysis was used. Plots of the interaction between effect size and required sample size are shown in Figure 4.6 for a two-tailed one-sample t-test of the chosen α and β values.

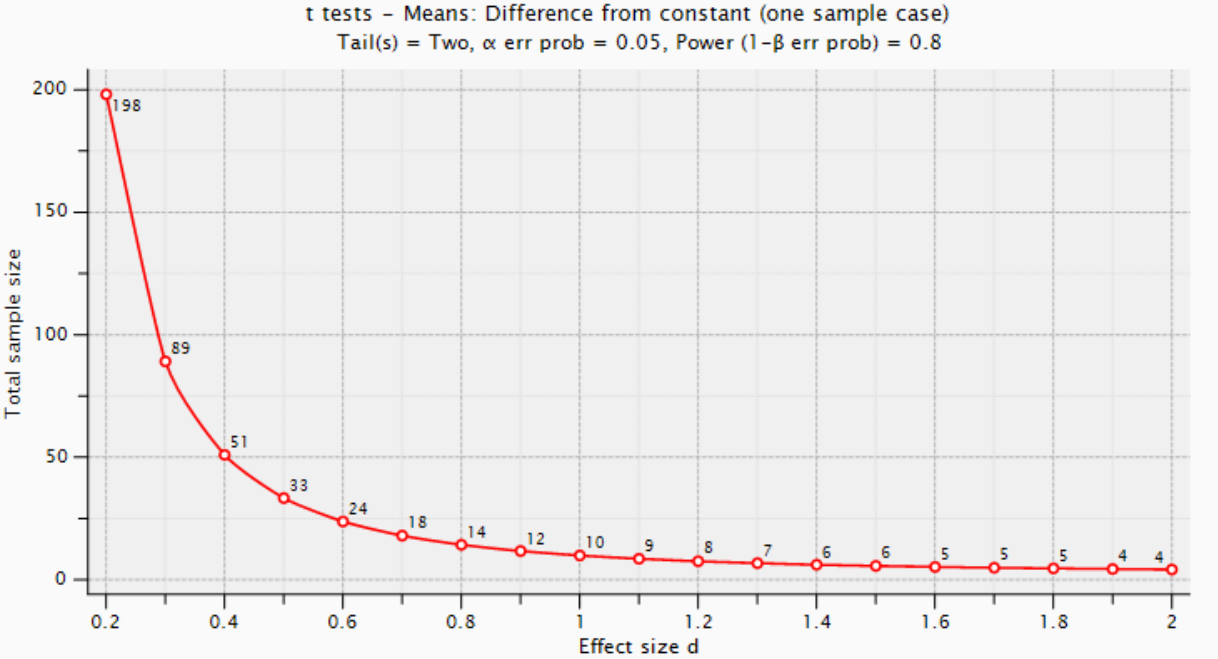

Figure 4.6: Total Sample Size as a Function of Effect Size for Various Power Levels During a One-Sample Two-Tailed T-Test

Note that participant pools are inherently small for prosthesis research and often limited to less than 20 participants. An effect size of approximately 0.7 would be required to ensure statistical significance could be achieved with a participant pool of this size.

4.4 Results

4.4.1 Absolute Values

As discussed previously, the critical comparison to be made is the relative difference of each feedback condition compared to the average of the two no-feedback conditions. However, the absolute values are still relevant for gauging the relative values' magnitude and for visualizing the data. The absolute values for each feedback condition are shown in Figure 4.7. *F* and *A* represent the finger and arm feedback condition, while *N1* and *N2* represent the first and second no-feedback conditions. The success rate metric requires all trials in a set to calculate, resulting in a single value on each testing set. Therefore, there are no descriptive statistics available for the success rate metric. For this reason, the success rate was visualized using a standard bar plot. All other metrics were visualized using box and whisker plots to help show how each participant differed during the various conditions. Each box represents the 25^{th}-75^{th} percentile of the data; each horizontal line within the box represents the median; the whiskers represent the minimum and maximum values, and the circular dot markers represent outliers. Data points were defined as outliers if they were greater than $q_3 + 1.5IQR$ or less than $q_1 - 1.5IQR$ where q_1 and q_3 are

the 25th and 75th percentiles, and IQR is the interquartile range. Note that outliers were used for visualization only and were not removed from the dataset. All descriptive statistics can be seen in Appendix B. All per-trial metrics were found to be normally distributed for each testing set by the Kolmogorov-Smirnov method using Matlab 2018b [127].

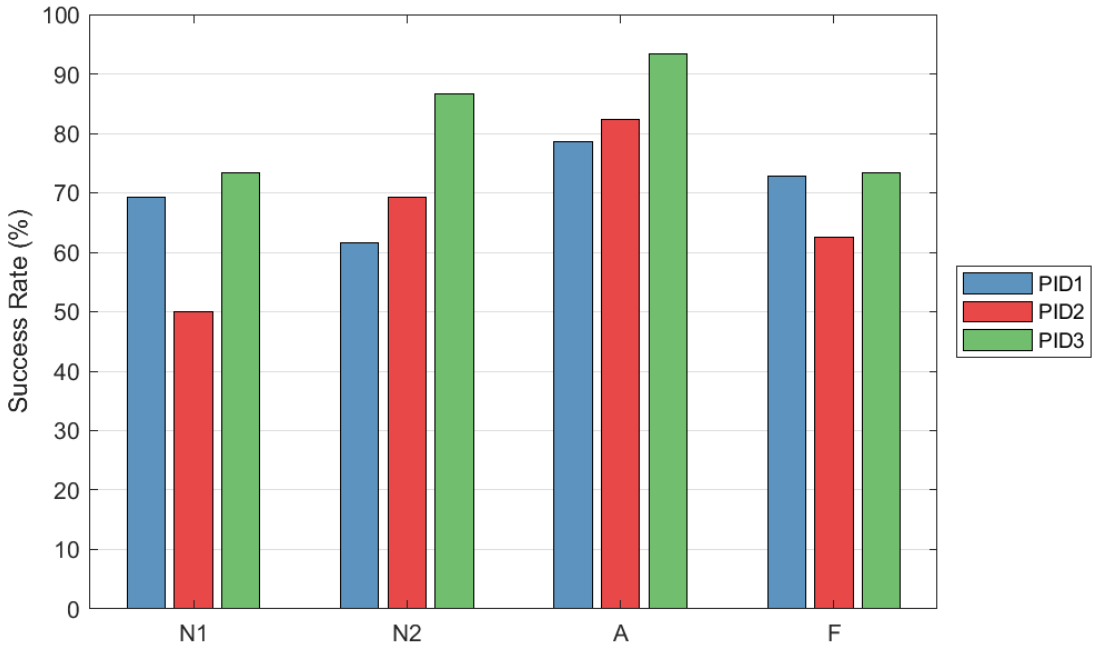

(a)

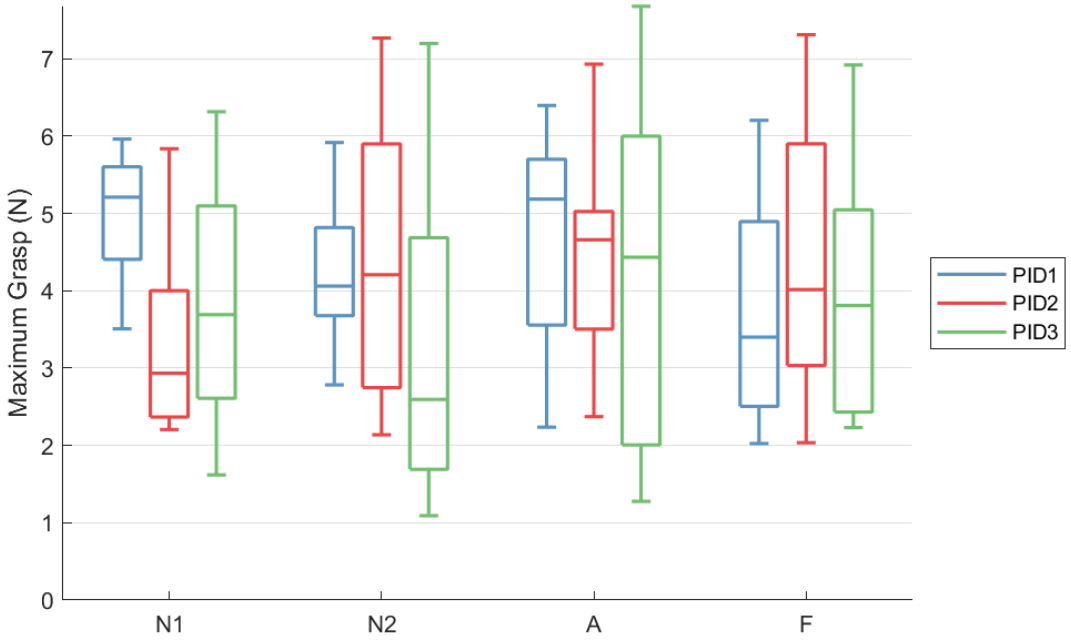
Maximum Grasp (N)
0
1
2
3
4
5
6
7
N1
N2
A
F
PID1
PID2
PID3

(b)

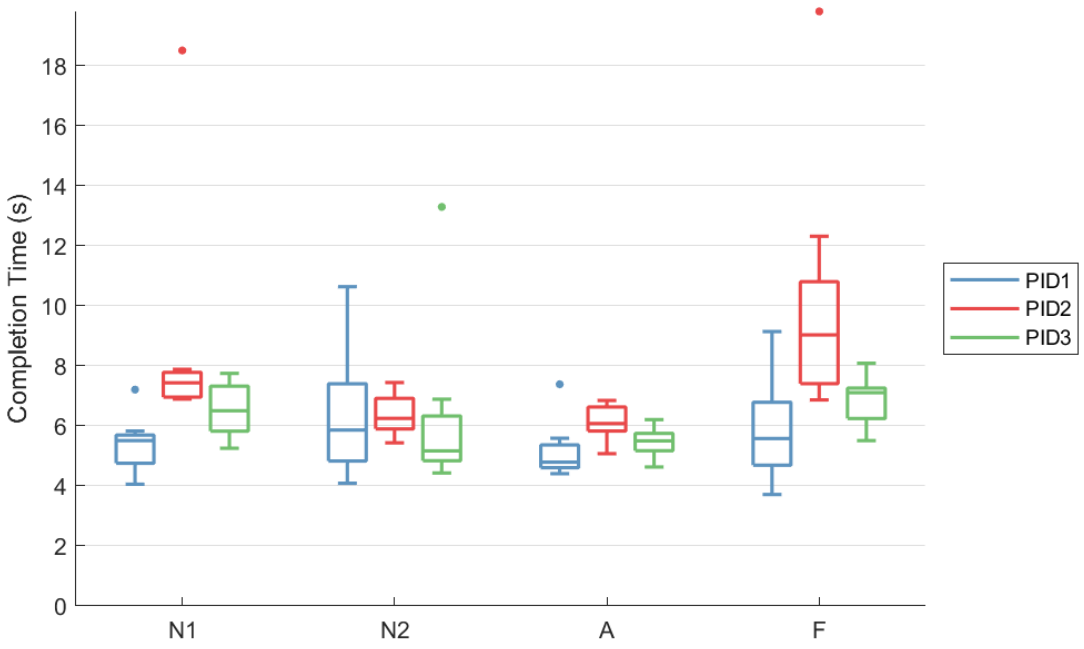
Completion Time (s)
0
2
4
6
8
10
12
14
16
18
N1
N2
A
F
PID1
PID2
PID3

(c)

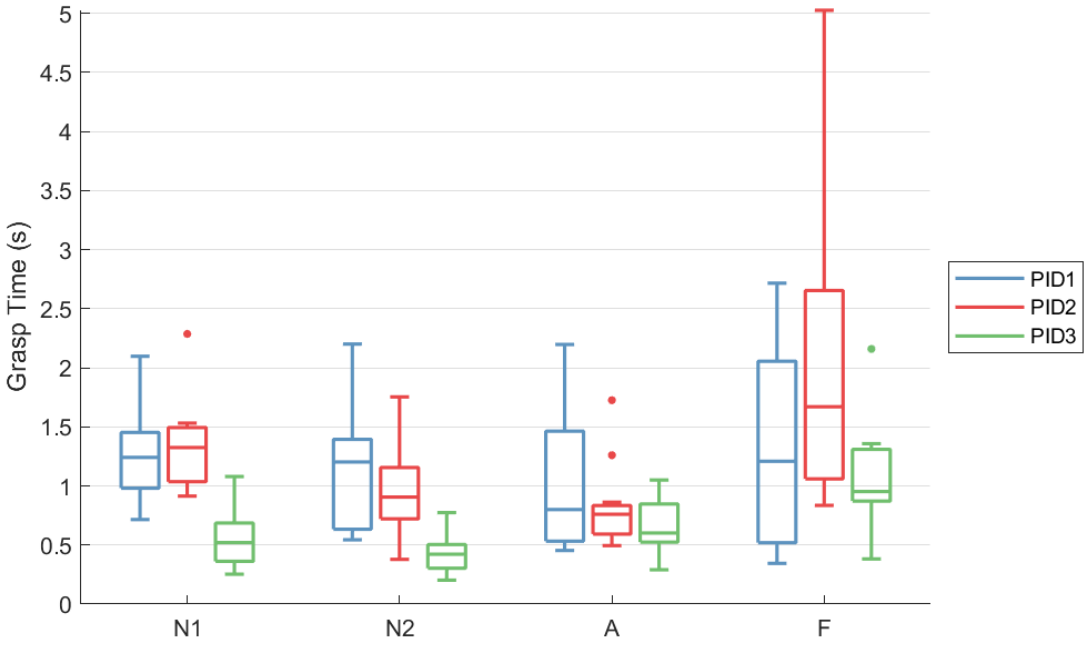

(d)

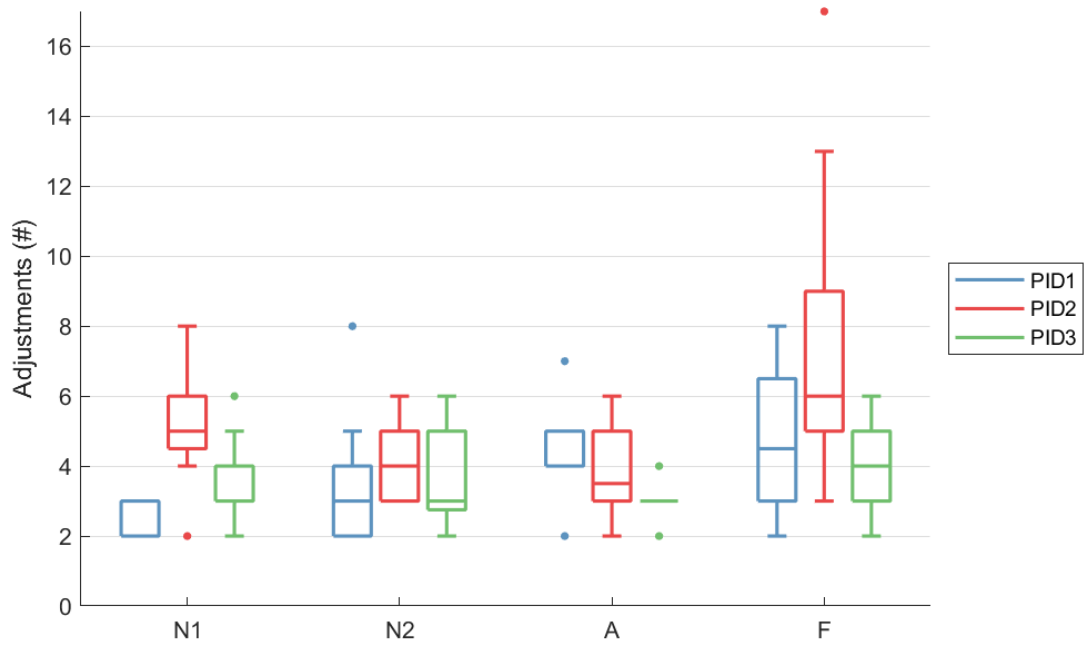

(e)

Figure 4.7: Absolute Value Results for (a) Success Rate, (b) Maximum Grasp, (c) Completion Time, (d) Grasp Time, (e) Adjustments

The absolute success rate results are shown in Figure 4.7a. The lowest success rate between all participants and all conditions was 50% (PID2, Block N1), while the highest was 93% (PID3, Block A). Each participant's range of success rate was 17%, 32%, and 20% for PID1, PID2, and PID3. This large difference in range highlights the skill variation between-participants. PID2's increased range could be due to inexperience with myoelectric control, as noted earlier, resulting in more potential for improvement gains.

The absolute maximum grasp force results are shown in Figure 4.7b. The lowest average maximum grasp force between all participants was 3.3N (PID2, Block N1), while the highest was 5.0N (PID1, Block N1). The range of average maximum grasp force for each participant individually was 1.3N, 1.2N, and 1.1N for PID1, PID2, and PID3. This range was more similar between-participants than the success rate. Each block's variation was relatively high for this metric, with IQR values larger than the range between blocks for all participants. This high variation demonstrates that the grasp was not performed very consistently by any of the participants. Median values for PID1 did not appear to be consistently lower (better performance) than PID2 or PID3, indicating that myoelectric experience did not affect this metric's absolute values.

The absolute completion time results are shown in Figure 4.7c. The lowest average completion time between all participants was 5.4s (PID1, Block N1), while the highest was 10.1s (PID2, Block F). The range of average completion time for each participant individually was 1.2s, 4.0s, and 1.3s for PID1, PID2, and PID3. Note the presence of several outliers, specifically for PID2, which lie very far outside the IQR. The median values for PID2 were higher than PID1 and PID3 in all blocks.

The absolute grasp time results are shown in Figure 4.7d. The lowest average grasp time between all participants was 0.43s (PID3, Block N2), while the highest was 2.1s (PID2, Block F). The average grasp time range for each participant was 0.3s, 1.3s, and 0.6s for PID1, PID2, and PID3. The variation for PID2 in Block F was substantially higher than any others. The magnitude and frequency of outliers for PID2 lend further evidence that the myoelectric control experience played a factor in the consistency of grasp time.

The absolute adjustment results are shown in Figure 4.7e. The lowest average adjustments between all participants were 2.4 (PID1, Block N1), while the highest was 7.6 (PID2, Block F). The range of average adjustments for each participant individually was 2.3, 3.7, and 1.2 for PID1, PID2, and PID3. Again, it can be noted that the variation for PID2 during the finger feedback condition was much higher than in the other blocks.

4.4.2 Within-Participant Results

All the within-participant comparison results can be seen in Figure 4.8. Error bars represent the pooled standard deviation of each metric calculated using Equation [2]. Note again that the success rate metric was calculated using all trials from each set; therefore, error bars are not present. For all metrics excluding success rate, effect sizes were computed per participant using their individual mean and standard deviation. The effect sizes are summarized in Table 4.1. The strength of the shading represents the magnitude of the effect size value. *A-N* represents the difference between the arm feedback condition and the average of the two no-feedback conditions, *F-N* represents the difference between the finger feedback condition and the average of the two no-feedback conditions, and *F-A* represents the difference between the finger and arm feedback condition. To clarify, a positive value for *A-N* indicates that *A* resulted in a larger value than *N*. All descriptive statistics can be seen in Appendix B.

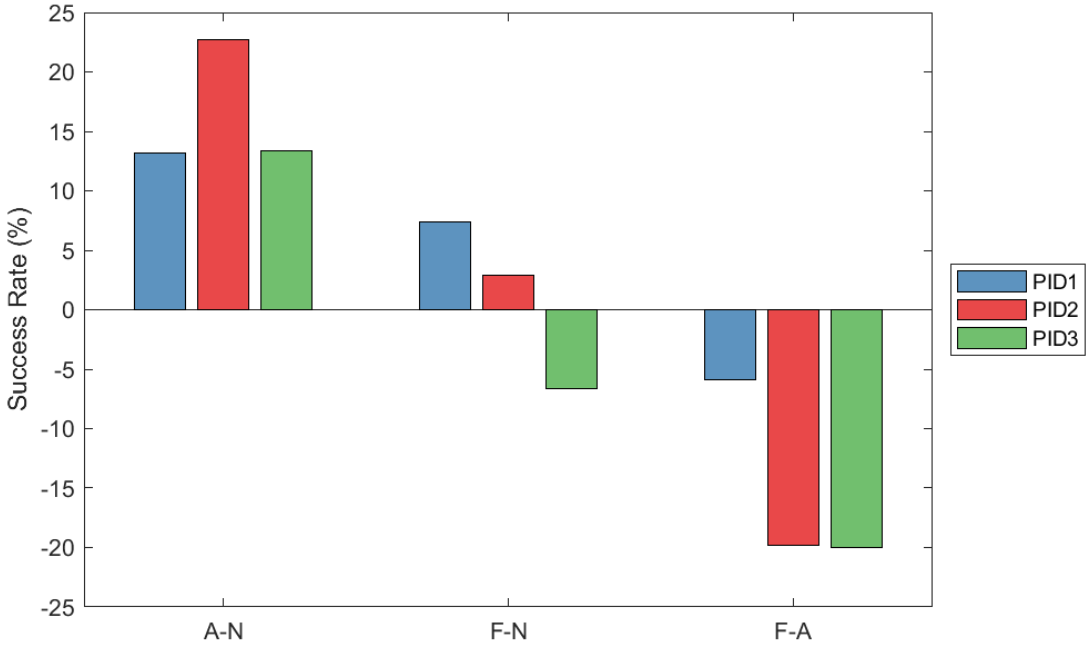

(a)

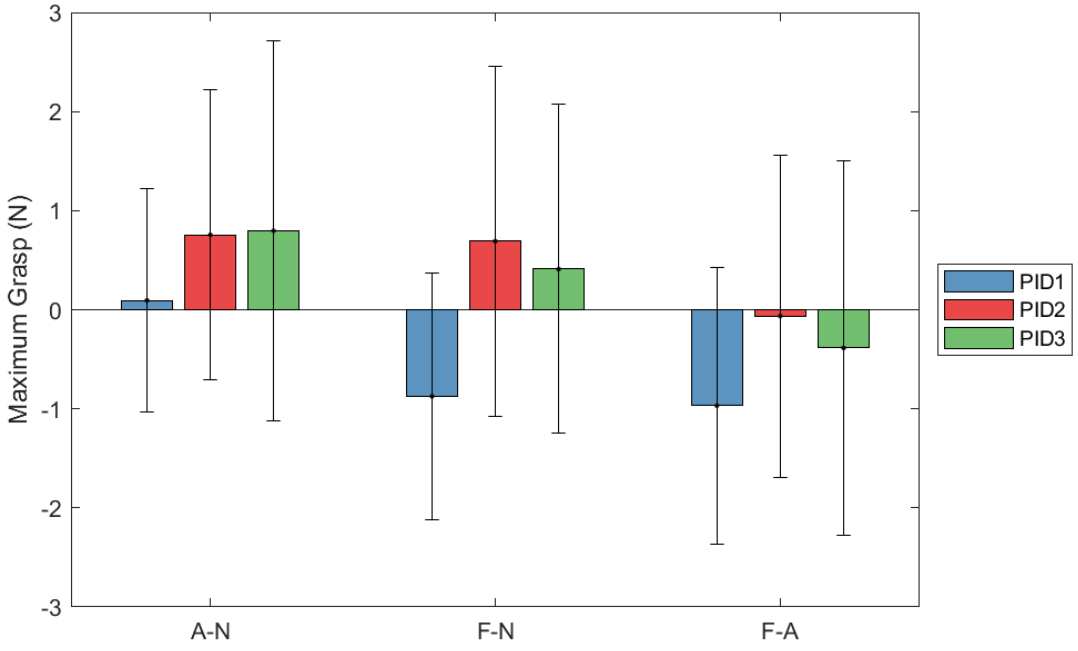
Maximum Grasp (N)
3
2
1
0
-1
-2
-3
A-N
F-N
F-A
PID1
PID2
PID3

(b)

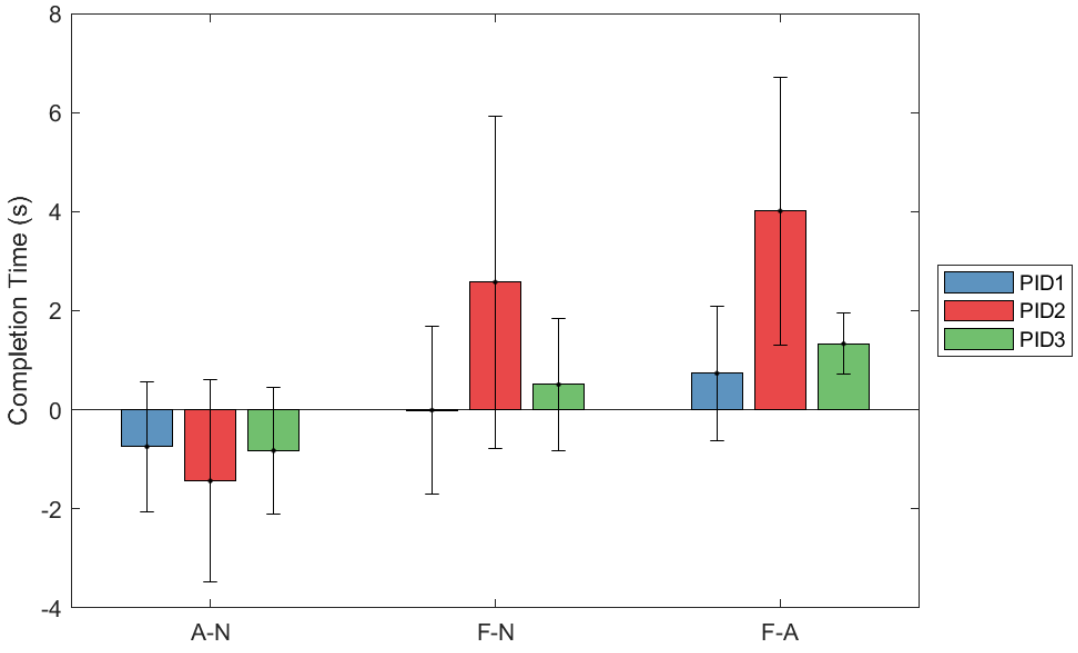
Completion Time (s)
8
6
4
2
0
-2
-4
A-N
F-N
F-A
PID1
PID2
PID3

(c)

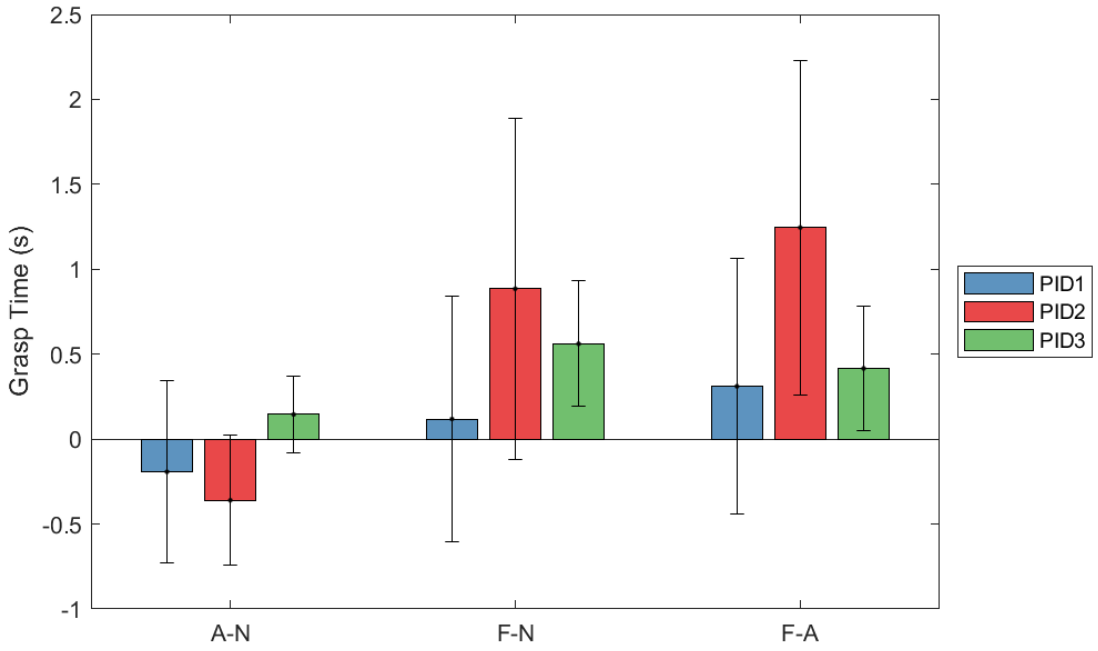

(d)

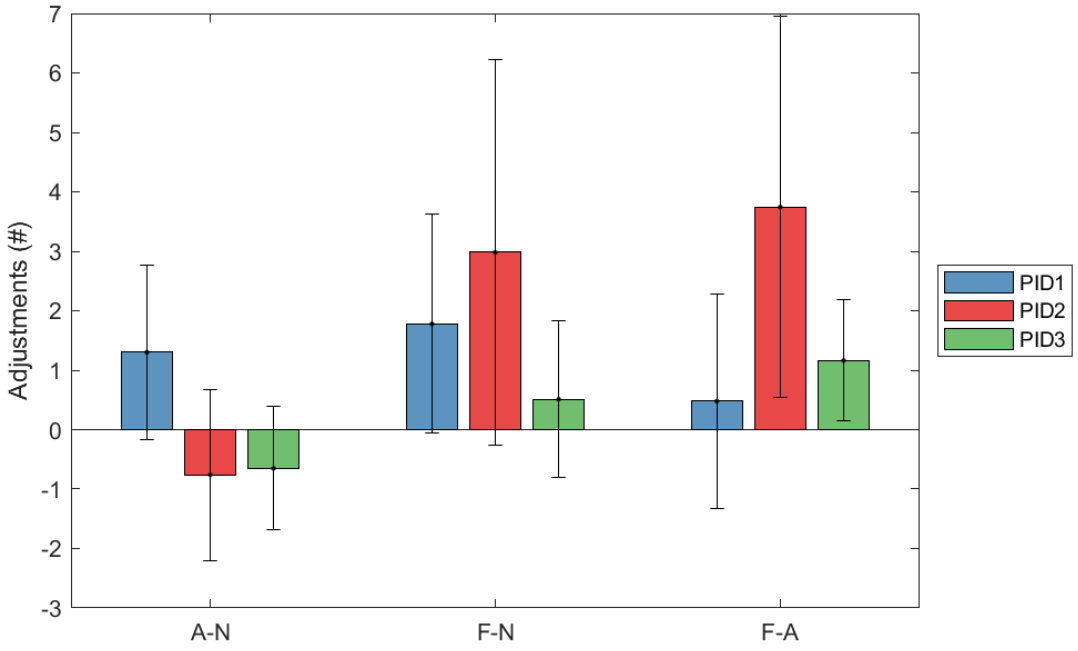

(e)

Figure 4.8: Within-participant Results for (a) Success Rate, (b) Maximum Grasp, (c) Completion Time, (d) Grasp Time, (e) Adjustments

Table 4.1: Effect Sizes for Relative Within-Participant Results (green shading represents a positive value, red shading represents a negative value, strength of shading represents the magnitude of value)

	Maximum Grasp			Completion Time			Grasp Time			Adjustments		
	A-N	F-N	F-A	A-N	F-N	F-A	A-N	F-N	F-A	A-N	F-N	F-A
PID1	0.08	-0.7	-0.69	-0.57	-0.01	0.54	-0.36	0.16	0.41	0.89	0.97	0.26
PID2	0.51	0.39	-0.04	-0.7	0.77	1.49	-0.94	0.88	1.27	-0.53	0.92	1.17
PID3	0.42	0.25	-0.2	-0.64	0.38	2.18	0.64	1.51	1.13	-0.63	0.39	1.14

The *A-N* comparison's success rate between all participants had a minimum of 13.2% (PID1) and a maximum of 22.7% (PID2). All participants showed an increase in the success rate upon receiving the arm feedback condition compared to the no-feedback condition. The *F-N* comparison's success rate was much less consistent, with values ranging from -6.7% (PID3) to 7.3% (PID1). Interestingly, PID3 decreased in performance upon receiving the finger feedback. The *F-A* values show that the finger feedback condition resulted in lower success rates than the arm feedback condition for all participants.

All participants showed a higher average maximum grasp upon receiving the arm feedback condition than the no-feedback condition. PID2 and PID3 showed a moderate increase of 0.76N (d = 0.51) and 0.80N (d = 0.42), while PID 1 had a very small increase of about 0.10N (d = 0.08). The *F-N* values for maximum grasp were much less consistent between-participants. Again, PID2 and PID3 showed an increase in maximum grasp of 0.69N (d = 0.39) and 0.41N (d = 0.25). PID1 was the only participant to decrease maximum grasp with a value of -0.87N and a relatively large effect size of -0.70. The *F-A* values revealed that all participants displayed a lighter maximum grasp force when interfacing with the finger feedback than the arm feedback. PID2 and PID3 had very small differences of -0.06N (d = -0.04) and -0.39N (d = -0.2), while PID1 had a higher difference of -0.97N with a relatively large effect size of -0.69. PID1's high myoelectric experience could have resulted in leveraging the finger feedback without losing control of the grasp force.

All participants showed a lower completion time when receiving the arm feedback condition than the no-feedback condition with *A-N* values of -0.7s, -1.4s, and -0.82s for PID1, PID2, and PID3. All participants had similar medium-to-large negative effect sizes of -0.57, -0.7, and -0.64 for PID1, PID2, and PID3. The finger feedback to no feedback comparison generally had opposite results. PID2 showed a large increase in the completion time of 2.6s with a large effect size of 0.77. PID3 showed a smaller increase of 0.5s with a moderate effect size of 0.38. PID1, however, showed no change with an effect size of

approximately zero. The opposite effects of the arm and finger feedback conditions were highlighted by the *F-A* metric, where all participants showed higher completion time values for the finger feedback condition. PID1 was the least affected by feedback location, with an *F-A* value of 0.7s and a moderate effect size of 0.54. PID2 had a much larger change in the completion time of 4.0s, with a very large effect size of 1.49. PID3 had a smaller change in the completion time of 1.33s; however, the small standard deviation led to an extremely large effect size of 2.18. This value was the largest within-participant effect size for any metric.

PID1 spent slightly less time in the grasp phase during the arm feedback condition than the no-feedback condition with a value of -0.19s and a moderate effect size of -0.36. PID2 also spent slightly less time in the grasp phase during the arm feedback condition than the average no-feedback condition with a value of -0.36s; however, the effect size was quite large at -0.94. PID3 showed the opposite trend for the *A-N* metric with a small increase in grasp time of 0.14s with a moderate effect size of 0.51. All participants showed an increase in grasp time during the finger feedback condition than the no-feedback condition. PID2 showed the largest increase at 0.89s, with a large effect size of 0.88. PID3 showed an increase in grasp time of 0.56s with a very large effect size of 1.51. PID1 showed the lowest increase in grasp time of 0.12s with a small effect size of 0.16. Again, the difference between the finger feedback and arm feedback condition for grasp time was highlighted by the *F-A* metric, where all participants showed a positive value. PID2's grasp time was 1.00s higher for the finger feedback condition, with a very large effect size of 1.27. PID3's grasp time was 0.56s higher for the finger feedback condition, with a large effect size of 1.13. PID1 showed a smaller change of only 0.12s higher for the finger feedback with a small effect size of 0.41.

The *A-N* comparison for adjustments showed that PID1 increased the number of adjustments by 1.3 during the arm feedback condition compared to the average no feedback condition with a large effect size of 0.89. PID2 and PID3 showed a small decrease in adjustments of -0.8 and -0.7 with corresponding moderate effect sizes of -0.53 and -0.63. All participants agreed for the *F-N* metric, with more adjustments for the finger feedback condition than the average no-feedback condition. PID1 and PID2 showed increases of 1.8 and 3.0, with large effect sizes of 0.97 and 0.92, respectively. PID3 had a much smaller increase in adjustments of 0.5 with a small-to-moderate effect size of 0.39. The *F-A* values for adjustments were positive for all participants, showing more adjustments during the finger feedback condition than the arm feedback condition. PID1 showed a very small difference of 0.5 with a small effect size of 0.26. PID2 showed a much larger difference of 3.7 with a large effect size of 1.17. PID3 showed a difference of 1.13, also with a large effect size of 1.14.

4.4.3 Between-Participant Power Analysis

Between-participant effect sizes and the corresponding number of required participants computed using the described power analysis are shown in Table 4.2. Full descriptive statistics can be found in Appendix B.

Table 4.2: Between-participant Power Analysis Summary (green shading represents a positive value, red shading represents a negative value, strength of shading represents the magnitude of value)

	Effect Size			**Required Participants for Significance**		
	A-N	F-N	F-A	A-N	F-N	F-A
Success Rate	3.67	0.20	-2.29	3	>100	4
Maximum Grasp	1.70	0.11	-1.26	5	>100	8
Completion Time	-3.24	0.92	1.42	4	12	7
Grasp Time	-0.65	1.65	1.57	21	6	6
Adjustments	-0.04	1.74	1.27	>100	5	8

The largest between-participant effect size seen was for the *A-N* comparison's success rate, requiring only three participants to achieve statistical significance. This study had three participants, making this result statistically significant ($t = 6.35$, $p=0.024$). This very large effect size was caused by all participants improving by a similar amount, creating a small standard deviation in difference scores. The between-participant effect size for the *F-N* comparison of success rate was very small, requiring over 100 participants to achieve statistical significance. The *F-A* comparison for success rate resulted in a large negative between-participant effect size, requiring an estimated four participants to achieve statistical significance. Results were similar for the maximum grasp, requiring only 5 participants to obtain significance for the *A-N* comparison, 8 participants for the *F-A* comparison, and over 100 participants for the *F-N* comparison. Completion time also yielded high between-participant effect sizes, requiring an estimated 4 participants to achieve significance for the *A-N* comparison, 7 participants for the *F-A* comparison, and 12 participants for the *F-N* comparison. Grasp time showed a large sample of 21 participants required for the *A-N* comparison and only 6 participants for the *F-N* and *F-A* comparison. Finally, the *A-N* comparison adjustments had an effect size of almost zero, requiring much more than 100 participants to achieve significance. However, the *F-N* and *F-A* comparisons had high between-participant effect sizes resulting in an estimated 5 and 8 participants to reach significance.

It is important to note that the estimated between-participant effect sizes' standard error is very high due to the low number of participants. The data for between-participant effect sizes with 95% confidence intervals are presented in Table 4.3, [119].

Table 4.3: Between-participant Effect Size With 95% Confidence Interval Summary

	Effect Size (95% CI)		
	A-N	**F-N**	**F-A**
Success Rate	3.67 [1.05, 6.29]	0.2 [-1.4, 1.8]	-2.29 [-4.35, -0.23]
Maximum Grasp	1.7 [-0.17, 3.57]	0.11 [-1.49, 1.71]	-1.26 [-3.01, 0.49]
Completion Time	-3.24 [-5.67, -0.81]	0.92 [-0.76, 2.6]	1.42 [-0.37, 3.21]
Grasp Time	-0.65 [-2.29, 0.99]	1.65 [-0.2, 3.5]	1.57 [-0.26, 3.4]
Adjustments	-0.04 [-1.64, 1.56]	1.74 [-0.14, 3.62]	1.27 [-0.48, 3.02]

4.4.4 Learning Effects Within Trials

A linear regression analysis was used to analyze the relationship between the trial number and each primary outcome measure. Linear regression analysis was not possible for success rate since this metric is computed once per set rather than per trial. The analysis was done for each block and participant separately using Matlab 2018b [127]. The normality of residuals assumption was upheld for all tests. The p-value for this analysis indicates the level of evidence for rejecting the null hypothesis (no correlation between variables) in the usual manner. The R-value represents the percentage of variation explained by the linear relationship between trial number and outcome metric. The regression coefficient (M) indicates the fitted line's slope, or the outcome measure rate-of-change per trial. All results are tabulated and visualized in Appendix C; however, only maximum grasp will be discussed in-depth as it displayed the highest regression coefficients and R-squared values. The linear regression results for maximum grasp are shown in Table 4.4 and Figure 4.9.

*Table 4.4: Linear Regression Summary for Maximum Grasp Force of Testing Set, M=slope, R=R-Squared Value, p=p-value, * indicates significant correlation*

	Block 1	**Block 2**	**Block 3**	**Block 4**
PID 1	M=0.008 R=-0.141 p=0.927	M=0.156 R=0.086 p=0.197	M=-0.054 R=-0.093 p=0.549	M=0.002 R=-0.167 p=0.993
PID 2	**M=-0.194** **R=0.641** **p=0.010***	M=0.034 R=-0.120 p=0.853	M=-0.160 R=-0.035 p=0.420	M=-0.064 R=-0.031 p=0.450
PID 3	M=-0.076 R=-0.062 p=0.535	M=0.206 R=0.226 p=0.079	M=-0.004 R=-0.091 p=0.974	M=0.014 R=-0.082 p=0.917

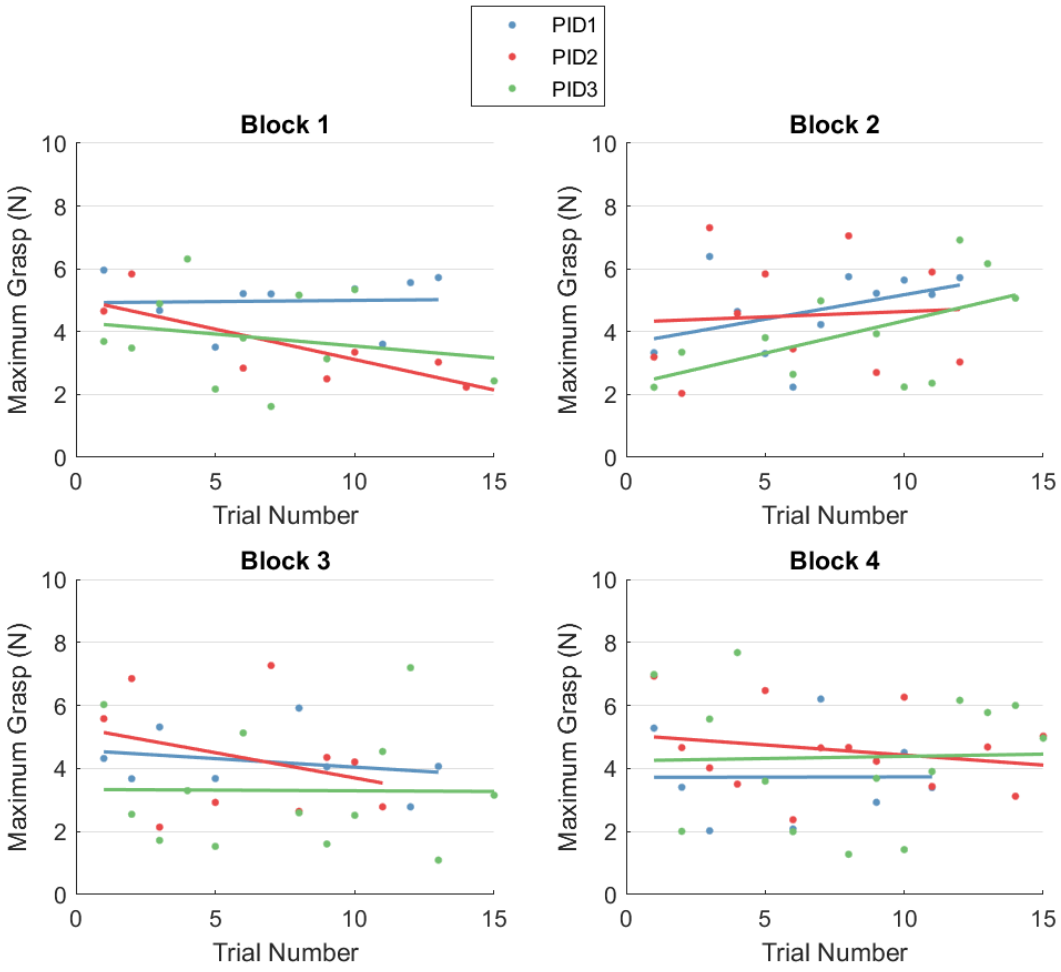

Figure 4.9: Linear Regression Models for Maximum Grasp Metrics Over Testing Set

The only statistically significant p-value observed was for PID2 during block 1, indicating that the null hypothesis of no correlation was false. The R-squared value indicated that 64.1% of the observed variation could be explained using the trial number as a predictor, with a correlation coefficient of 0.2N/trial. These values could be due to PID2 being the least experienced with myoelectric control of the three participants, requiring more trials to become familiar with the device. No significant p-values or large R-squared values are observed for PID2 in the remaining blocks. It seems apparent that learning effects were occurring for PID1 in block 2 and PID3 in blocks 1 and 2 when visually inspecting the regression lines. However, the R-squared values were minimal, and p-values were not significant.

4.5 Discussion

4.5.1 Absolute Values

Substantial variation was seen between-participants for the absolute values of all outcome measures, excluding maximum grasp. The absolute value range between-participants was much higher than each participant range, making the within-participant values much more consistent. This difference in variation highlights the importance of using relative within-participant values to eliminate individual participants' inherent performance differences. The repeated measure design eliminates much of the variance between-participants allowing for recruitment sizes to be smaller. A minimum recruitment size is necessary specifically to the prosthesis community, where participant pools are inherently small.

The maximum grasp values had a high individual variation for all participants during all testing conditions. PID1 did not have consistently lower maximum grasp values than the other participants, despite having more myoelectric experience and a lower breaking threshold (6.5N vs. 7.5N). The high individual variation relative to between-participant differences could indicate a lack of control over slight adjustments of the grasp force, reinforced by all participants' anecdotal statements. A potential reason for this lack of control is explored in the limitations section.

Different strategies emerged among the participants. PID2 tended to have more outliers and typically higher median values for completion time, grasp time, and adjustment metrics. The higher median values may indicate a slower, more focused strategy or could be a result of lack of experience. PID3 exhibited a quick grasp strategy, highlighted by their consistently lower grasp time values and lower adjustment values. Interestingly, this strategy had the highest success rate of all participants for all blocks, and the variation in maximum grasp was not substantially larger than other participants.

4.5.2 Results

The within-participant success rate values showed the efficacy of the arm feedback condition over no feedback. Even in this small pilot study, statistical significance was obtained for this metric. The range of success rate increase values for the arm feedback condition over the no-feedback condition (13.2% to 22.7%) was consistent with the literature. Meek et al. conducted a similar myoelectric fragile object transfer task with mechanotactile feedback delivered to the forearm, which resulted in a success rate increase of 5%-20% [27]. Although exact values were not reported, Clemente et al. found success rate increases of up to 6% using discrete vibrotactile feedback delivered to the upper arm on a similar task [28]. Consistency of success rate with the literature demonstrates the MSP’s efficacy as an experimental platform. The finger feedback did not appear to benefit the success rate over the no-feedback condition. Consequently, when compared directly with the arm feedback condition, the finger feedback condition

had a much lower success rate with a very large effect size of -2.29. These results run contrary to the hypotheses made that both feedback cases would improve the success rate. From this pilot study, the success rate appears to be affected by the sensory feedback location.

Within-participant effect sizes for average maximum grasp were small due to the large variances in each testing set. However, the average maximum grasp difference values between conditions were consistent for all participants. The consistency in difference values produced large between-participant effect sizes indicating that the arm feedback condition resulted in higher grasp forces than the no-feedback and finger feedback conditions. However, all within-participant difference values were less than 1N in magnitude, representing about 10% of the MSP's maximum grasp force. Although the MSP's compliant fingertip sensor had a resolution of ~0.03N, the system's noise was ~0.3N due to the long cables required for mobility. The small within-participant values were of a similar magnitude of the sensor noise and small compared with the variance for any participant on any individual block. This result is reflected in a previous study where the max value of generated forces for a myoelectric target acquisition task did not change significantly with added feedback, although this was done with discrete vibrotactile feedback [76]. Other studies have reported a much larger decrease in grasp force magnitude when presented with sensory feedback during fragile object transfer tasks for proportional mechanotactile and proportional vibrotactile feedback. Kim et al. found that maximum grasp decreased between 28%-43% when mechanotactile feedback was administered to TMR sites [26]. Pylatiuk et al. found that the grasp force decreased by an average of 54% when mechanotactile feedback was provided to the upper arm of five persons with amputation [74]. Schoepp et al. similarly found a maximum grasp force decrease of 21% when mechanotactile feedback was provided to the upper arm of a person of amputation [62]. It is hypothesized that the lack of fine control in this pilot study was due to the MSP grasp force changing too quickly for the participants to react. The delay from grasp force measurement to tactor actuation compounded with human reaction time was too long for participants to use the feedback for fine grasp control. This idea is analyzed further in the limitations section.

General trends of decreased completion time and decreased grasp time were observed for the arm feedback condition over the no-feedback condition, while the opposite was observed for the finger feedback condition. A recent study found an increase of ~13% in task completion time when implanted electrotactile feedback was presented [30]; however, while this feedback's perceived location was in the missing limb, the perceived modality was not reported. In another study, proportional somatotopically matched feedback, similar to the finger feedback case, also increased task completion time [26]. Another study with proportional modality matched feedback, similar to the arm feedback case, showed an increase in task completion time, contrary to this pilot study [62]. In contradiction, Meek et al. found a decrease in

completion time for the same feedback strategy [27]. Clemente et al. found no change in task completion time using discrete vibrotactile feedback on a fragile object task [28]. Different values reported throughout the literature show the experimental setup's impact on the task timing outcome measures. The comparisons made in this study between the arm feedback condition and the finger feedback condition are more informative about the effect of feedback location due to the data being recorded with the same apparatus, with the only changed variable being feedback location. The finger feedback condition resulted in higher completion time and grasp time for all participants than the no-feedback condition and the arm feedback condition, with large within-participant effect sizes from 0.54 to 2.18 for completion time and 0.41 to 1.27 for grasp time. This consistently slower movement was likely caused by an increased focus on the task from the more sensitive finger feedback site. The between-participant effect size for the finger feedback to arm feedback comparison produced for both completion time and grasp time were large, requiring an estimated 7 participants to obtain statistical significance. These results indicate that both completion time and grasp time are sensitive outcome measures to the somatotopic accuracy of feedback.

The adjustments outcome measure was newly introduced in this study. It showed mixed results for the arm feedback condition compared to the no-feedback condition, with two participants decreasing the number of adjustments and one participant increasing. The finger feedback condition had more adjustments than the no-feedback and the arm feedback condition for all participants. A recent study showed that participants adjusted their control signals significantly more when given continuous audio feedback than when given discrete vibrotactile feedback delivered to the forearm [29]. Although the audio feedback used myoelectric control as an input, the information could be considered a lot richer than that of the vibrotactile, which only output a short burst during discrete events. The rich audio feedback could be likened to the finger feedback in this study, conveying more information than the arm feedback condition due to the increased sensitivity at the fingertip. The proposed total adjustments outcome measure proved sensitive to the somatotopic accuracy of feedback. Large between-participant effect sizes were observed between finger feedback and both no feedback and arm feedback. The power analysis revealed that a participant pool of 8 would be required to obtain statistical significance for this metric. While this metric does not directly relate to functionality, it provides insight into how the participant uses the prosthesis that may not be easily seen through other outcome measures.

4.5.3 Learning Effects

The linear regression analysis showed that there was very little learning occurring throughout each testing set. The first block of PID2 was the only exception, which could likely be attributed to their low myoelectric experience level. Testing sets on subsequent blocks for PID2 did not exhibit learning effects. Despite finding minimal learning effects within blocks, learning effects between blocks could have been a

factor in this experiment. While it is possible to quantify differences between both no feedback blocks, there would be no way to tell whether any differences seen were caused by a between-block learning effect or residual effects from the previous feedback block. A previous study specifically showed that performance increases gained from feedback could remain during open-loop control during single session testing [118]. Visually inspecting the absolute value plots in Figure 4.7, the differences between blocks *N1* and *N2* do not seem to follow any pattern, with different participants' values going in different directions. If a more extensive study were to be conducted, pseudo-randomizing all participants' presentation orders would remove confounding results caused by block learning effects.

4.6 Limitations

4.6.1 Small Sample Size

A priori pilot studies for power analysis aim to estimate the effect size with a smaller number of participants before the main study is conducted. This method results in a small sample size, translating to a large standard error of the effect size. This large error can lead to a substantial probability that the effect size is underestimated, which can result in the study being abandoned. Conversely, it can lead to a substantial probability that the effect size is overestimated, which results in an underpowered main study and a higher type II error [128]. This emphasis should be especially noted in prosthesis research as sample sizes are inherently small due to the small population of persons with amputation. The 95% confidence intervals on the between-participant effect sizes demonstrate the high sample error with such a small participant pool. All recommended sample sizes should be interpreted with the high confidence intervals in mind.

While the confidence intervals could be greatly reduced by gathering additional participants, recruitment was postponed due to the arrival of the COVID-19 pandemic. The protocol requires the experimenter to be in physical contact with the participants (e.g., fitting the MSP, placing tactors, conducting two-point discrimination tests, placing the fragile object), breaking the research restrictions set out by the University of Alberta. To ensure participants' and researchers' safety, further recruitment for this pilot study and initial recruitment for a full study was postponed until it is deemed safe to continue.

4.6.2 MSP Grasp Speed

In this study, the maximum grasp force showed a high variation for each participant individually. This variation is hypothesized to be caused by the MSP's grasp force increasing faster than the participants could react. This speed of force increase is rarely reported in studies but plays a critical role in utilizing real-time feedback. When the MSP hand is closing at minimum velocity (i.e., EMG just hovering on the threshold line), the force increases at a rate of 7.6N/s. A system with identical hardware previously used in the lab showed a delay of 92ms from initial sensor input to tactor motion. The human reaction time from pressure on the fingertip is around 270ms [129]. This force ramp in combination with human and system delay results in a change in grasp force of 2.75N before the participant can react to the feedback from the tactor. On average, participants moved the MSP hand faster than the minimum speed during grasping, resulting in an even quicker change in grasp force. Such a large force delay results in the participant unable to utilize the feedback systems' added information in a closed-loop manner. A similar study comparing feedback condition and learning effects of vibrotactile feedback similarly stated that the end effector (Michelangelo Hand, Ottobock) was too high for the feedback to be used until after the trial

was complete [130]. In this case, the force ramp was at a rate of around 500N/s. This study found that the added vibrotactile feedback did not provide any performance increase over the provided implicit audio feedback. Raspopovic et al. adjusted the hand closing velocity unbeknownst to the participants to ensure the participants did not use learned timing to achieve the desired force level [31]. They found a higher error with the higher hand velocity in a force target acquisition task. Pena et al. also noted hand velocity as an issue in their study on vibrotactile feedback for myoelectric grasp control [77]. The force ramp parameter is essential to utilizing feedback in a real-time manner. A recent study adopted a dual gain system in which the EMG gain would be reduced once the grasp force started to increase, which substantially increased performance on an object transfer task [131]. For future studies, the dual gain technique is suggested to ensure participants can utilize the provided feedback in a closed-loop manner.

4.7 Recommendations

4.7.1 Protocol Adjustments

All the outcome measures used (excluding success rate) could only be calculated on successful trials. Since the number of trials was fixed for each testing set, the number of samples to calculate each outcome measure depended on the number of successful trials in each set. The higher the success rate, the lower the standard error of each testing set's calculated mean. It is recommended to run each testing set until a fixed number of successful trials is obtained. With a fixed number of successful trials, calculating mean values on each testing set would be consistent across the different blocks. A downside that arises is that participants with lower success rates would have more total trials per block. However, during each block, learning effects were observed to be non-significant for most cases, making this tradeoff a worthwhile endeavor.

In the current experimental design, the overall learning effect is difficult to calculate. This difficulty is partly due to the feedback conditions (B2 and B4) appearing consistently later than the no-feedback blocks (B1 and B3). Since we can expect outcome measures to be affected by the two feedback blocks, any attempt at observing overall trends caused by presentation order can become skewed. It is recommended to remove the second no feedback block from the experimental protocol and revert to a standard repeated measures design. This would involve three blocks, one for each feedback condition (no-feedback, arm-feedback, finger-feedback), with the order pseudo-randomized for each participant. A larger sample would be required to ensure an even participant number in each of the six groups. Within-participant values could still easily be calculated by comparing both feedback conditions to each participant's no-feedback condition as done previously.

Although the linear regression results revealed very little learning within each testing set, there was still one exception with the least skilled participant in the first block. It is recommended to increase the training segment’s duration from 5 minutes to 7.5 minutes to ensure that even low-skilled participants are out of the learning phase for the first block testing. This time increase would only add 10 minutes to the total experiment.

4.7.2 Experimental Setup

An internal accelerometer was used to calculate the lift point of the fragile object. Accelerometers are prone to high signal to noise ratios in the presence of vibration. In this experiment, digital filtering was required to remove the accelerometer noise. Additionally, some hand-tuning of parameters was still necessary to calculate the lift point consistently. A camera is recommended to be added to the setup in place of the accelerometer. If the fragile object were made to be a distinct solid color, a simple color-

filtering image processing algorithm could then determine the z-position of the fragile object eliminating the need for the accelerometer.

4.7.3 Target Grasp Force

In this experiment, participants were asked to grasp the fragile object as lightly as possible without dropping it. This instruction can lead to a conflict between these two objectives. If the participant emphasizes not dropping the object rather than gripping lightly, their target grasp force value could be close to the breaking threshold to ensure that their grip is secure. If the participant put more emphasis on grasping lightly, they could have dropped the object more often. Giving a target force value of halfway between the required lift and break threshold would ensure a secure grip on the cup during transfer. Grasp values could then be compared to this target level rather than to the minimum required grasp force. The difficulty comes with indicating the target level to the user. Target levels would have to be shown during the training phase and removed during testing, as whatever method used would provide incidental feedback to the participant.

4.7.4 Feedback Sites

A feedback site on the index finger and thumb during the finger feedback condition replicated the same forces seen on the prosthetic hand. Likewise, there were two sites for the forearm feedback condition to be the fairest comparison to the finger feedback condition. Having multiple sites adds a variable that could demand a higher cognitive load from the participant. It is recommended to switch to a single feedback site for both the finger and forearm feedback conditions to keep the experiment as simple as possible.

5 Conclusion

Despite many advancements related to myoelectric prostheses, rejection rates remain high. A lack of sensory feedback is commonly cited as a reason for rejection. Although many different non-invasive techniques exist to replace grip force feedback, there is no consensus on which method yields the best results. Most studies are completed on different experimental hardware, making comparisons between studies difficult. The impact of the feedback site location had previously not been investigated. A literature review was conducted summarizing the history of prostheses and an overview of current feedback stimulation techniques focusing on feedback site location.

A modular simulated bypass prosthesis (MSP) was developed to deliver modality and somatotopically matched mechanotactile feedback to non-disabled participants. The device can be worn for long periods due to the focus on comfort and weight reduction. Since each component is modular, components can be easily interchanged for different experiments. Encapsulated pressure sensors used to measure the grip force of the end effector were designed and evaluated. These compliant fingertips allowed for a substantial reduction in error for all non-standard loading conditions typical to prosthesis use. The MSP will help researchers study feedback and control techniques in myoelectric prostheses by providing a reliable test apparatus that easily allows for manipulating various parameters. In collaboration with Rhodes College in Memphis, Tennessee, this device has been used to study ownership of a prosthesis [132]. The encapsulated pressure sensors and end-effector are currently being used for international collaboration between the University of Alberta, the German Aerospace Institute, and Aalborg University.

A pilot study was conducted to compare modality matched mechanotactile grip force feedback in a somatotopically matched and non-matched location during a fragile object transfer task. A range of effect sizes for a variety of performance outcome measures were calculated. The importance of using within-participant values in a repeated measures design was highlighted by large between participant effect sizes even when absolute values varied between participants substantially. All participants showed similar difference values in the comparison between the finger feedback condition and the arm feedback condition, creating large between-participant effect sizes for all outcome measures. Contrary to the hypothesis presented, the arm feedback's success rate was higher than that of the finger feedback. This decreased success rate of the finger feedback condition could be potentially attributed to the finger's higher sensitivity resulting in an increased focus on the feedback rather than the prostheses' control. The completion time, grasp time, and adjustments from all participants during the finger feedback were substantially higher than the arm feedback, indicating that more attention was on the task. A lack of fine control over the maximum grasp force was exhibited by all participants, characterized by the considerable

variation during all feedback conditions. This variation was hypothesized to be caused by the MSP's grasp force increasing quicker than the participants' reaction time. It is recommended that for future studies, brachIOplexus be modified to decrease the MSP's force ramp. Despite high variation in absolute maximum grasp values for each participant, between-participant comparisons revealed that the finger feedback condition resulted in decreased grasp force with a large effect size. Additional recommendations were made on the experimental protocol to make for a more standardized statistical analysis and better account for learning effects.

These preliminary results indicate that the feedback location could play a factor in functional prostheses' control. The power analysis revealed that an estimated participant pool of n=8 would be enough to achieve significance for comparing the arm and finger feedback conditions for all proposed metrics. However, due to this pilot study's low recruitment, the 95% confidence intervals of the between-participant effect sizes (and subsequently required number of participants) are considerable. The difference in the arm feedback's success rate to the no-feedback's success rate was comparable to similar values reported in the literature, lending credibility to the MSP as a standardized experimental apparatus. This pilot study showed the feasibility of the proposed experimental task, confirmed sensitive outcome measures, and discovered potential error sources to be improved before a larger experiment. Data analysis techniques were also established that would scale to a future more extensive study.

References

[1] M. Asghari Oskoei and H. Hu, "Myoelectric control systems—A survey," *Biomedical Signal Processing and Control*, vol. 2, no. 4, pp. 275–294, Oct. 2007, doi: 10.1016/j.bspc.2007.07.009.

[2] E. Scheme and K. Englehart, "Electromyogram pattern recognition for control of powered upper-limb prostheses: State of the art and challenges for clinical use," *Journal of Rehabilitation Research & Development*, vol. 48, no. 6, pp. 643–659, Sep. 2011, doi: 10.1682/JRRD.2010.09.0177.

[3] E. Biddiss and T. Chau, "Upper-Limb Prosthetics: Critical Factors in Device Abandonment," *American Journal of Physical Medicine & Rehabilitation*, vol. 86, no. 12, p. 977, Dec. 2007, doi: 10.1097/PHM.0b013e3181587f6c.

[4] E. A. Biddiss and T. T. Chau, "Upper limb prosthesis use and abandonment: A survey of the last 25 years," *Prosthet Orthot Int*, vol. 31, no. 3, pp. 236–257, Sep. 2007, doi: 10.1080/03093640600994581.

[5] B. Peerdeman *et al.*, "Myoelectric forearm prostheses: state of the art from a user-centered perspective," *Journal of Rehabilitation Research & Development*, vol. 48, no. 6, pp. 719–738, 2011.

[6] C. Antfolk, M. D'Alonzo, B. Rosén, G. Lundborg, F. Sebelius, and C. Cipriani, "Sensory feedback in upper limb prosthetics," *Expert Review of Medical Devices*, vol. 10, no. 1, pp. 45–54, Jan. 2013, doi: 10.1586/erd.12.68.

[7] J. S. Schofield, K. R. Evans, J. P. Carey, and J. S. Hebert, "Applications of sensory feedback in motorized upper extremity prosthesis: a review," *Expert Review of Medical Devices*, vol. 11, no. 5, pp. 499–511, Sep. 2014, doi: 10.1586/17434440.2014.929496.

[8] K. Ziegler-Graham, E. J. MacKenzie, P. L. Ephraim, T. G. Travison, and R. Brookmeyer, "Estimating the Prevalence of Limb Loss in the United States: 2005 to 2050," *Archives of*

Physical Medicine and Rehabilitation, vol. 89, no. 3, pp. 422–429, Mar. 2008, doi: 10.1016/j.apmr.2007.11.005.

[9] E. National Academies of Sciences *et al.*, "Upper-Extremity Prostheses," in *The Promise of Assistive Technology to Enhance Activity and Work Participation.*, National Academies Press (US), 2017.

[10] F. Cordella *et al.*, "Literature Review on Needs of Upper Limb Prosthesis Users," *Front Neurosci*, vol. 10, May 2016, doi: 10.3389/fnins.2016.00209.

[11] K. J. Zuo and J. L. Olson, "The evolution of functional hand replacement: From iron prostheses to hand transplantation," *Plast Surg (Oakv)*, vol. 22, no. 1, pp. 44–51, 2014.

[12] R. H. Meier, "History of Arm Amputation, Prosthetic Restoration, and Arm Amputation Rehabilitation," *New York: Demos Medical Publishing*, p. 8, 2004.

[13] R. P. Petri and E. Aguila, "The military upper extremity amputee," *Physical Medicine and Rehabilitation Clinics of North America*, vol. 13, no. 1, pp. 17–43, Feb. 2002, doi: 10.1016/S1047-9651(03)00070-6.

[14] D. S. Childress, "Historical Aspects of Powered Limb Prostheses | O&P Virtual Library," *Digital Resource Foundation for the Orthotics & Prosthetics Community*, vol. 9, no. 1, pp. 2–13, 1985.

[15] E. D. Sherman, "A Russian Bioelectric-Controlled Prosthesis," *Can Med Assoc J*, vol. 91, no. 24, pp. 1268–1270, Dec. 1964.

[16] D. S. Dorcas and R. N. Scott, "A three-state myo-electric control," *Med. & biol. Engng.*, vol. 4, no. 4, pp. 367–370, Jul. 1966, doi: 10.1007/BF02476154.

[17] D. Graupe and W. K. Cline, "Functional Separation of EMG Signals via ARMA Identification Methods for Prosthesis Control Purposes," *IEEE Transactions on Systems, Man, and Cybernetics*, vol. SMC-5, no. 2, pp. 252–259, Mar. 1975, doi: 10.1109/TSMC.1975.5408479.

[18] J. T. Belter, J. L. Segil, A. M. Dollar, and R. F. Weir, "Mechanical design and performance specifications of anthropomorphic prosthetic hands: A review," *Journal of Rehabilitation Research & Development*, vol. 50, no. 5, pp. 599–617, Sep. 2013.

[19] P. Geethanjali, “Myoelectric control of prosthetic hands: state-of-the-art review,” *Med Devices (Auckl)*, vol. 9, pp. 247–255, Jul. 2016, doi: 10.2147/MDER.S91102.

[20] Ottobock, “Myoelectric Prosthetics,” *Myoelectric Prostheses*, 2020. https://www.ottobockus.com/prosthetics/upper-limb-prosthetics/solution-overview/myoelectric-prosthetics/.

[21] R. S. Johansson, “Sensory and Memory Information in the Control of Dexterous Manipulation,” in *Neural Bases of Motor Behaviour*, F. Lacquaniti and P. Viviani, Eds. Dordrecht: Springer Netherlands, 1996, pp. 205–260.

[22] D. A. Nowak and J. Hermsdörfer, “Predictive and reactive control of grasping forces: on the role of the basal ganglia and sensory feedback,” *Exp Brain Res*, vol. 173, no. 4, pp. 650–660, Sep. 2006, doi: 10.1007/s00221-006-0409-7.

[23] A. G. Witney, A. Wing, J.-L. Thonnard, and A. M. Smith, “The cutaneous contribution to adaptive precision grip,” *Trends in Neurosciences*, vol. 27, no. 10, pp. 637–643, Oct. 2004, doi: 10.1016/j.tins.2004.08.006.

[24] A.-S. Augurelle, A. M. Smith, T. Lejeune, and J.-L. Thonnard, “Importance of Cutaneous Feedback in Maintaining a Secure Grip During Manipulation of Hand-Held Objects,” *Journal of Neurophysiology*, vol. 89, no. 2, pp. 665–671, Feb. 2003, doi: 10.1152/jn.00249.2002.

[25] S. B. Godfrey, M. Bianchi, A. Bicchi, and M. Santello, “Influence of force feedback on grasp force modulation in prosthetic applications: A preliminary study,” in *2016 38th Annual International Conference of the IEEE Engineering in Medicine and Biology Society (EMBC)*, Aug. 2016, pp. 5439–5442, doi: 10.1109/EMBC.2016.7591957.

[26] K. Kim and J. E. Colgate, “Haptic Feedback Enhances Grip Force Control of sEMG-Controlled Prosthetic Hands in Targeted Reinnervation Amputees,” *IEEE Transactions on Neural Systems and Rehabilitation Engineering*, vol. 20, no. 6, pp. 798–805, Nov. 2012, doi: 10.1109/TNSRE.2012.2206080.

[27] S. G. Meek, S. C. Jacobsen, and P. Goulding, “Extended physiologic taction: design and evaluation of a proportional force feedback system.,” *Journal of rehabilitation research and development*, vol. 26, no. 3, pp. 53–62, 1989.

[28] F. Clemente, M. D’Alonzo, M. Controzzi, B. B. Edin, and C. Cipriani, “Non-Invasive, Temporally Discrete Feedback of Object Contact and Release Improves Grasp Control of Closed-Loop Myoelectric Transradial Prostheses,” *IEEE Transactions on Neural Systems and Rehabilitation Engineering*, vol. 24, no. 12, pp. 1314–1322, Dec. 2016, doi: 10.1109/TNSRE.2015.2500586.

[29] L. F. Engels, A. W. Shehata, E. J. Scheme, J. W. Sensinger, and C. Cipriani, “When Less Is More – Discrete Tactile Feedback Dominates Continuous Audio Biofeedback in the Integrated Percept While Controlling a Myoelectric Prosthetic Hand,” *Front. Neurosci.*, vol. 13, 2019, doi: 10.3389/fnins.2019.00578.

[30] E. L. Graczyk, L. Resnik, M. A. Schiefer, M. S. Schmitt, and D. J. Tyler, “Home Use of a Neural-connected Sensory Prosthesis Provides the Functional and Psychosocial Experience of Having a Hand Again,” *Scientific Reports*, vol. 8, no. 1, Dec. 2018, doi: 10.1038/s41598-018-26952-x.

[31] S. Raspopovic *et al.*, “Restoring Natural Sensory Feedback in Real-Time Bidirectional Hand Prostheses,” *Science Translational Medicine*, vol. 6, no. 222, pp. 222ra19-222ra19, Feb. 2014, doi: 10.1126/scitranslmed.3006820.

[32] S. Micera, J. Carpaneto, and S. Raspopovic, “Control of Hand Prostheses Using Peripheral Information,” *IEEE Reviews in Biomedical Engineering*, vol. 3, pp. 48–68, 2010, doi: 10.1109/RBME.2010.2085429.

[33] J. S. Hebert *et al.*, “Novel Targeted Sensory Reinnervation Technique to Restore Functional Hand Sensation After Transhumeral Amputation,” *IEEE Transactions on Neural Systems and Rehabilitation Engineering*, vol. 22, no. 4, pp. 765–773, Jul. 2014, doi: 10.1109/TNSRE.2013.2294907.

[34] C. Antfolk *et al.*, "Artificial Redirection of Sensation From Prosthetic Fingers to the Phantom Hand Map on Transradial Amputees: Vibrotactile Versus Mechanotactile Sensory Feedback," *IEEE Transactions on Neural Systems and Rehabilitation Engineering*, vol. 21, no. 1, pp. 112–120, Jan. 2013, doi: 10.1109/TNSRE.2012.2217989.

[35] J. P. Hunter, J. Katz, and K. D. Davis, "Stability of phantom limb phenomena after upper limb amputation: A longitudinal study," *Neuroscience*, vol. 156, no. 4, pp. 939–949, Oct. 2008, doi: 10.1016/j.neuroscience.2008.07.053.

[36] L. Nikolajsen and T. S. Jensen, "Phantom limb pain," *British Journal of Anaesthesia*, vol. 87, no. 1, pp. 107–116, Jul. 2001, doi: 10.1093/bja/87.1.107.

[37] A. Bjorkman, U. Wijk, C. Antfolk, I. Bjorkamn-Burtscher, and B. Rosen, "Sensory qualities of the phantom hand map in the residual forearm of amputees," *Journal of Rehabilitation Medicine*, vol. 48, no. 4, pp. 365–370, 2016, doi: 10.2340/16501977-2074.

[38] H. H. Ehrsson, B. Rosén, A. Stockselius, C. Ragnö, P. Köhler, and G. Lundborg, "Upper limb amputees can be induced to experience a rubber hand as their own," *Brain*, vol. 131, no. 12, pp. 3443–3452, Dec. 2008, doi: 10.1093/brain/awn297.

[39] T. A. Kuiken, A. K. Barlow, L. J. Hargrove, and G. A. Dumanian, "Targeted Muscle Reinnervation for the Upper and Lower Extremity," *Techniques in Orthopaedics*, vol. 32, no. 2, pp. 109–116, Jun. 2017, doi: 10.1097/BTO.0000000000000194.

[40] J. E. Cheesborough, L. H. Smith, T. A. Kuiken, and G. A. Dumanian, "Targeted Muscle Reinnervation and Advanced Prosthetic Arms," *Semin Plast Surg*, vol. 29, no. 1, pp. 62–72, Feb. 2015, doi: 10.1055/s-0035-1544166.

[41] T. A. Kuiken, L. A. Miller, R. D. Lipschutz, B. A. Lock, and G. A. Dumanian, "Targeted reinnervation for enhanced prosthetic arm function in a woman with a proximal amputation: a case study," *The Lancet*, 2007, doi: 10.1016/S0140-6736(07)60193-7.

[42] T. A. Kuiken *et al.*, “Targeted Muscle Reinnervation for Real-Time Myoelectric Control of Multifunction Artificial Arms,” *JAMA*, vol. 301, no. 6, pp. 619–628, Feb. 2009, doi: 10.1001/jama.2009.116.

[43] L. A. Miller *et al.*, “Control of a six degree of freedom prosthetic arm after targeted muscle reinnervation surgery,” *Arch Phys Med Rehabil*, vol. 89, no. 11, pp. 2057–2065, Nov. 2008, doi: 10.1016/j.apmr.2008.05.016.

[44] L. A. Miller, K. A. Stubblefield, R. D. Lipschutz, B. A. Lock, and T. A. Kuiken, “Improved Myoelectric Prosthesis Control Using Targeted Reinnervation Surgery: A Case Series,” *IEEE Transactions on Neural Systems and Rehabilitation Engineering*, vol. 16, no. 1, pp. 46–50, Feb. 2008, doi: 10.1109/TNSRE.2007.911817.

[45] K. D. O’Shaughnessy, G. A. Dumanian, R. D. Lipschutz, L. A. Miller, K. Stubblefield, and T. A. Kuiken, “Targeted Reinnervation to Improve Prosthesis Control in Transhumeral Amputees: A Report of Three Cases,” *JBJS*, vol. 90, no. 2, pp. 393–400, Feb. 2008, doi: 10.2106/JBJS.G.00268.

[46] J. S. Hebert, K. Elzinga, K. M. Chan, J. Olson, and M. Morhart, “Updates in Targeted Sensory Reinnervation for Upper Limb Amputation,” *Curr Surg Rep*, vol. 2, no. 3, p. 45, Jan. 2014, doi: 10.1007/s40137-013-0045-7.

[47] J. S. Hebert, K. M. Chan, and M. R. Dawson, “Cutaneous sensory outcomes from three transhumeral targeted reinnervation cases,” *Prosthet Orthot Int*, vol. 40, no. 3, pp. 303–310, Jun. 2016, doi: 10.1177/0309364616633919.

[48] L. M. Mioton and G. A. Dumanian, “Targeted muscle reinnervation and prosthetic rehabilitation after limb loss,” *Journal of Surgical Oncology*, vol. 118, no. 5, pp. 807–814, 2018, doi: 10.1002/jso.25256.

[49] C. Pasluosta, P. Kiele, and T. Stieglitz, “Paradigms for restoration of somatosensory feedback via stimulation of the peripheral nervous system,” *Clinical Neurophysiology*, vol. 129, no. 4, pp. 851–862, Apr. 2018, doi: 10.1016/j.clinph.2017.12.027.

[50] K. A. Yildiz, A. Y. Shin, and K. R. Kaufman, “Interfaces with the peripheral nervous system for the control of a neuroprosthetic limb: a review,” *Journal of NeuroEngineering and Rehabilitation*, vol. 17, no. 1, p. 43, Mar. 2020, doi: 10.1186/s12984-020-00667-5.

[51] D. W. Tan, M. A. Schiefer, M. W. Keith, J. R. Anderson, J. Tyler, and D. J. Tyler, “A neural interface provides long-term stable natural touch perception,” *Science Translational Medicine*, vol. 6, no. 257, pp. 257ra138-257ra138, Oct. 2014, doi: 10.1126/scitranslmed.3008669.

[52] G. S. Dhillon, S. M. Lawrence, D. T. Hutchinson, and K. W. Horch, “Residual function in peripheral nerve stumps of amputees: implications for neural control of artificial limbs,” *The Journal of Hand Surgery*, vol. 29, no. 4, pp. 605–615, Jul. 2004, doi: 10.1016/j.jhsa.2004.02.006.

[53] G. Valle *et al.*, “Biomimetic Intraneural Sensory Feedback Enhances Sensation Naturalness, Tactile Sensitivity, and Manual Dexterity in a Bidirectional Prosthesis,” *Neuron*, vol. 100, no. 1, pp. 37-45.e7, Oct. 2018, doi: 10.1016/j.neuron.2018.08.033.

[54] J. A. George *et al.*, “Long-term performance of Utah Slanted Electrode Arrays and intramuscular electromyographic leads implanted chronically in human arm nerves and muscles,” *J Neural Eng*, Oct. 2020, doi: 10.1088/1741-2552/abc025.

[55] E. D’Anna *et al.*, “A closed-loop hand prosthesis with simultaneous intraneural tactile and position feedback,” *Science Robotics*, vol. 4, no. 27, Feb. 2019, doi: 10.1126/scirobotics.aau8892.

[56] T. S. Davis *et al.*, “Restoring motor control and sensory feedback in people with upper extremity amputations using arrays of 96 microelectrodes implanted in the median and ulnar nerves,” *J. Neural Eng.*, vol. 13, no. 3, p. 036001, Mar. 2016, doi: 10.1088/1741-2560/13/3/036001.

[57] I. Strauss *et al.*, “Characterization of multi-channel intraneural stimulation in transradial amputees,” *Scientific Reports*, vol. 9, no. 1, Art. no. 1, Dec. 2019, doi: 10.1038/s41598-019-55591-z.

[58] K. Horch, S. Meek, T. G. Taylor, and D. T. Hutchinson, “Object Discrimination With an Artificial Hand Using Electrical Stimulation of Peripheral Tactile and Proprioceptive Pathways

With Intrafascicular Electrodes," *IEEE Transactions on Neural Systems and Rehabilitation Engineering*, vol. 19, no. 5, pp. 483–489, Oct. 2011, doi: 10.1109/TNSRE.2011.2162635.

[59] P. E. Patterson and J. A. Katz, "Design and evaluation of a sensory feedback system that provides grasping pressure in a myoelectric hand," *JRRD*, vol. 29, no. 1, p. 1, 1992, doi: 10.1682/JRRD.1992.01.0001.

[60] K. Kim, J. E. Colgate, J. J. Santos-MunnÉ, A. Makhlin, and M. A. Peshkin, "On the Design of Miniature Haptic Devices for Upper Extremity Prosthetics," *IEEE/ASME Transactions on Mechatronics*, vol. 15, no. 1, pp. 27–39, Feb. 2010, doi: 10.1109/TMECH.2009.2013944.

[61] S. Casini, M. Morvidoni, M. Bianchi, M. Catalano, G. Grioli, and A. Bicchi, "Design and realization of the CUFF - clenching upper-limb force feedback wearable device for distributed mechano-tactile stimulation of normal and tangential skin forces," in *2015 IEEE/RSJ International Conference on Intelligent Robots and Systems (IROS)*, Sep. 2015, pp. 1186–1193, doi: 10.1109/IROS.2015.7353520.

[62] K. R. Schoepp, M. R. Dawson, J. S. Schofield, J. P. Carey, and J. S. Hebert, "Design and Integration of an Inexpensive Wearable Mechanotactile Feedback System for Myoelectric Prostheses," *IEEE Journal of Translational Engineering in Health and Medicine*, vol. 6, pp. 1–11, 2018, doi: 10.1109/JTEHM.2018.2866105.

[63] K. Li, Y. Fang, Y. Zhou, and H. Liu, "Non-Invasive Stimulation-Based Tactile Sensation for Upper-Extremity Prosthesis: A Review," *IEEE Sensors Journal*, vol. 17, no. 9, pp. 2625–2635, May 2017, doi: 10.1109/JSEN.2017.2674965.

[64] K. A. Kaczmarek, J. G. Webster, P. Bach-y-Rita, and W. J. Tompkins, "Electrotactile and Vibrotactile Displays for Sensory Substitution Systems," *IEEE Transactions on Biomedical Engineering*, vol. 38, no. 1, pp. 1–16, 1991, doi: 10.1109/10.68204.

[65] G. Chai, J. Briand, S. Su, X. Sheng, and X. Zhu, "Electrotactile Feedback with Spatial and Mixed Coding for Object Identification and Closed-loop Control of Grasping Force in Myoelectric

Prostheses," in *2019 41st Annual International Conference of the IEEE Engineering in Medicine and Biology Society (EMBC)*, Jul. 2019, pp. 1805–1808, doi: 10.1109/EMBC.2019.8856508.

[66] S. Dosen *et al.*, "Multichannel Electrotactile Feedback With Spatial and Mixed Coding for Closed-Loop Control of Grasping Force in Hand Prostheses," *IEEE Transactions on Neural Systems and Rehabilitation Engineering*, vol. 25, no. 3, pp. 183–195, Mar. 2017, doi: 10.1109/TNSRE.2016.2550864.

[67] M. Isaković *et al.*, "Electrotactile feedback improves performance and facilitates learning in the routine grasping task," *European Journal of Translational Myology*, vol. 26, no. 3, Art. no. 3, Sep. 2016, doi: 10.4081/ejtm.2016.6069.

[68] N. Jorgovanovic, S. Dosen, D. J. Djozic, G. Krajoski, and D. Farina, "Virtual Grasping: Closed-Loop Force Control Using Electrotactile Feedback," *Computational and Mathematical Methods in Medicine*, vol. 2014, p. e120357, Jan. 2014, doi: https://doi.org/10.1155/2014/120357.

[69] R. N. Scott, R. H. Brittain, R. R. Caldwell, A. B. Cameron, and V. A. Dunfield, "Sensory-feedback system compatible with myoelectric control," *Med. Biol. Eng. Comput.*, vol. 18, no. 1, pp. 65–69, Jan. 1980, doi: 10.1007/BF02442481.

[70] G. Chai, D. Zhang, and X. Zhu, "Developing Non-Somatotopic Phantom Finger Sensation to Comparable Levels of Somatotopic Sensation through User Training With Electrotactile Stimulation," *IEEE Transactions on Neural Systems and Rehabilitation Engineering*, vol. 25, no. 5, pp. 469–480, May 2017, doi: 10.1109/TNSRE.2016.2580905.

[71] D. Zhang, H. Xu, P. B. Shull, J. Liu, and X. Zhu, "Somatotopical feedback versus non-somatotopical feedback for phantom digit sensation on amputees using electrotactile stimulation," *Journal of NeuroEngineering and Rehabilitation*, vol. 12, no. 1, p. 44, May 2015, doi: 10.1186/s12984-015-0037-1.

[72] Psyonic, "The Ability Hand™," *The Ability Hand*, 2020. https://www.psyonic.co/ability-hand (accessed Jul. 20, 2020).

[73] C. E. Stepp and Y. Matsuoka, “Vibrotactile Sensory Substitution for Object Manipulation: Amplitude Versus Pulse Train Frequency Modulation,” *IEEE Transactions on Neural Systems and Rehabilitation Engineering*, vol. 20, no. 1, pp. 31–37, Jan. 2012, doi: 10.1109/TNSRE.2011.2170856.

[74] C. Pylatiuk, A. Kargov, and S. Schulz, “Design and Evaluation of a Low-Cost Force Feedback System for Myoelectric Prosthetic Hands,” *JPO: Journal of Prosthetics and Orthotics*, vol. 18, no. 2, pp. 57–61, Apr. 2006.

[75] T. Rosenbaum-Chou, W. Daly, R. Austin, P. Chaubey, and D. A. Boone, “Development and Real World Use of a Vibratory Haptic Feedback System for Upper-Limb Prosthetic Users,” *JPO: Journal of Prosthetics and Orthotics*, vol. 28, no. 4, pp. 136–144, Oct. 2016, doi: 10.1097/JPO.0000000000000107.

[76] A. M. De Nunzio *et al.*, “Tactile feedback is an effective instrument for the training of grasping with a prosthesis at low- and medium-force levels,” *Exp Brain Res*, vol. 235, no. 8, pp. 2547–2559, 2017, doi: 10.1007/s00221-017-4991-7.

[77] A. E. Pena, L. Rincon-Gonzalez, J. J. Abbas, and R. Jung, “Effects of vibrotactile feedback and grasp interface compliance on perception and control of a sensorized myoelectric hand,” *PLOS ONE*, vol. 14, no. 1, p. e0210956, Jan. 2019, doi: 10.1371/journal.pone.0210956.

[78] C. Cipriani, M. D’Alonzo, and M. C. Carrozza, “A Miniature Vibrotactile Sensory Substitution Device for Multifingered Hand Prosthetics,” *IEEE Transactions on Biomedical Engineering*, vol. 59, no. 2, pp. 400–408, Feb. 2012, doi: 10.1109/TBME.2011.2173342.

[79] F. Clemente, S. Dosen, L. Lonini, M. Markovic, D. Farina, and C. Cipriani, “Humans Can Integrate Augmented Reality Feedback in Their Sensorimotor Control of a Robotic Hand,” *IEEE Transactions on Human-Machine Systems*, vol. 47, no. 4, pp. 583–589, Aug. 2017, doi: 10.1109/THMS.2016.2611998.

[80] M. Markovic, H. Karnal, B. Graimann, D. Farina, and S. Dosen, “GLIMPSE: Google Glass interface for sensory feedback in myoelectric hand prostheses,” *J. Neural Eng.*, vol. 14, no. 3, p. 036007, Mar. 2017, doi: 10.1088/1741-2552/aa620a.

[81] E. Battaglia, J. P. Clark, M. Bianchi, M. G. Catalano, A. Bicchi, and M. K. O’Malley, “The Rice Haptic Rocker: Skin stretch haptic feedback with the Pisa/IIT SoftHand,” in *2017 IEEE World Haptics Conference (WHC)*, Jun. 2017, pp. 7–12, doi: 10.1109/WHC.2017.7989848.

[82] J. Wheeler, K. Bark, J. Savall, and M. Cutkosky, “Investigation of Rotational Skin Stretch for Proprioceptive Feedback With Application to Myoelectric Systems,” *IEEE Transactions on Neural Systems and Rehabilitation Engineering*, vol. 18, no. 1, pp. 58–66, Feb. 2010, doi: 10.1109/TNSRE.2009.2039602.

[83] A. W. Shehata, L. F. Engels, M. Controzzi, C. Cipriani, E. J. Scheme, and J. W. Sensinger, “Improving internal model strength and performance of prosthetic hands using augmented feedback,” *J NeuroEngineering Rehabil*, vol. 15, no. 1, Art. no. 1, Dec. 2018, doi: 10.1186/s12984-018-0417-4.

[84] A. Gibson and P. Artemiadis, “Object discrimination using optimized multi-frequency auditory cross-modal haptic feedback,” in *2014 36th Annual International Conference of the IEEE Engineering in Medicine and Biology Society*, Aug. 2014, pp. 6505–6508, doi: 10.1109/EMBC.2014.6945118.

[85] K. Bark, J. W. Wheeler, S. Premakumar, and M. R. Cutkosky, “Comparison of Skin Stretch and Vibrotactile Stimulation for Feedback of Proprioceptive Information,” in *2008 Symposium on Haptic Interfaces for Virtual Environment and Teleoperator Systems*, Mar. 2008, pp. 71–78, doi: 10.1109/HAPTICS.2008.4479916.

[86] C. Tejeiro, C. E. Stepp, M. Malhotra, E. Rombokas, and Y. Matsuoka, “Comparison of remote pressure and vibrotactile feedback for prosthetic hand control,” in *2012 4th IEEE RAS EMBS International Conference on Biomedical Robotics and Biomechatronics (BioRob)*, Jun. 2012, pp. 521–525, doi: 10.1109/BioRob.2012.6290268.

[87] N. Thomas, G. Ung, C. McGarvey, and J. D. Brown, “Comparison of vibrotactile and joint-torque feedback in a myoelectric upper-limb prosthesis,” *Journal of NeuroEngineering and Rehabilitation*, vol. 16, no. 1, p. 70, Jun. 2019, doi: 10.1186/s12984-019-0545-5.

[88] I. Saunders and S. Vijayakumar, “The role of feed-forward and feedback processes for closed-loop prosthesis control,” *Journal of NeuroEngineering and Rehabilitation*, vol. 8, no. 1, p. 60, Oct. 2011, doi: 10.1186/1743-0003-8-60.

[89] C. Cipriani, F. Zaccone, S. Micera, and M. C. Carrozza, “On the Shared Control of an EMG-Controlled Prosthetic Hand: Analysis of User–Prosthesis Interaction,” *IEEE Transactions on Robotics*, vol. 24, no. 1, pp. 170–184, Feb. 2008, doi: 10.1109/TRO.2007.910708.

[90] A. Chatterjee, P. Chaubey, J. Martin, and N. Thakor, “Testing a Prosthetic Haptic Feedback Simulator With an Interactive Force Matching Task,” *JPO: Journal of Prosthetics and Orthotics*, vol. 20, no. 2, pp. 27–34, Apr. 2008, doi: 10.1097/01.JPO.0000311041.61628.be.

[91] M. Markovic *et al.*, “The clinical relevance of advanced artificial feedback in the control of a multi-functional myoelectric prosthesis,” *Journal of NeuroEngineering and Rehabilitation*, vol. 15, no. 1, p. 28, Mar. 2018, doi: 10.1186/s12984-018-0371-1.

[92] A. Zimmerman, L. Bai, and D. D. Ginty, “The gentle touch receptors of mammalian skin,” *Science*, vol. 346, no. 6212, pp. 950–954, Nov. 2014, doi: 10.1126/science.1254229.

[93] E. H. Weber, *E.H. Weber on the Tactile Senses*, 2nd ed. Psychology Press, 1996.

[94] S. Weinstein, “Intensive, extensive aspects of tactile sensitivity as a function of body part, sex and laterality,” *The Skin Senses*, pp. 195–222, 1968.

[95] A. Panarese, B. B. Edin, F. Vecchi, M. C. Carrozza, and R. S. Johansson, “Humans Can Integrate Force Feedback to Toes in Their Sensorimotor Control of a Robotic Hand,” *IEEE Transactions on Neural Systems and Rehabilitation Engineering*, vol. 17, no. 6, pp. 560–567, Dec. 2009, doi: 10.1109/TNSRE.2009.2021689.

[96] C. Cipriani, J. L. Segil, F. Clemente, R. F. ff. Weir, and B. Edin, "Humans can integrate feedback of discrete events in their sensorimotor control of a robotic hand," *Exp Brain Res*, vol. 232, no. 11, pp. 3421–3429, Nov. 2014, doi: 10.1007/s00221-014-4024-8.

[97] B. Stephens-Fripp, G. Alici, and R. Mutlu, "A Review of Non-Invasive Sensory Feedback Methods for Transradial Prosthetic Hands," *IEEE Access*, vol. 6, pp. 6878–6899, 2018, doi: 10.1109/ACCESS.2018.2791583.

[98] S. Amsuess *et al.*, "Context-Dependent Upper Limb Prosthesis Control for Natural and Robust Use," *IEEE Transactions on Neural Systems and Rehabilitation Engineering*, vol. 24, no. 7, pp. 744–753, Jul. 2016, doi: 10.1109/TNSRE.2015.2454240.

[99] D. Johansen, C. Cipriani, D. B. Popovic, and L. N. S. A. Struijk, "Control of a Robotic Hand Using a Tongue Control System-A Prosthesis Application," *IEEE Trans Biomed Eng*, vol. 63, no. 7, pp. 1368–1376, 2016, doi: 10.1109/TBME.2016.2517742.

[100] S. Amsuess, P. Goebel, B. Graimann, and D. Farina, "Extending mode switching to multiple degrees of freedom in hand prosthesis control is not efficient," in *2014 36th Annual International Conference of the IEEE Engineering in Medicine and Biology Society*, Aug. 2014, pp. 658–661, doi: 10.1109/EMBC.2014.6943677.

[101] T. R. Farrell and R. F. Weir, "The Optimal Controller Delay for Myoelectric Prostheses," *IEEE Transactions on Neural Systems and Rehabilitation Engineering*, vol. 15, no. 1, pp. 111–118, Mar. 2007, doi: 10.1109/TNSRE.2007.891391.

[102] G. Matrone, C. Cipriani, M. C. Carrozza, and G. Magenes, "Two-channel real-time EMG control of a dexterous hand prosthesis," in *2011 5th International IEEE/EMBS Conference on Neural Engineering*, Apr. 2011, pp. 554–557, doi: 10.1109/NER.2011.5910608.

[103] M. M. White *et al.*, "Usability Comparison of Conventional Direct Control Versus Pattern Recognition Control of Transradial Prostheses," *IEEE Transactions on Human-Machine Systems*, vol. 47, no. 6, pp. 1146–1157, Dec. 2017, doi: 10.1109/THMS.2017.2759762.

[104] H. Bouwsema, C. K. van der Sluis, and R. M. Bongers, “Changes in performance over time while learning to use a myoelectric prosthesis,” *J Neuroeng Rehabil*, vol. 11, p. 16, Feb. 2014, doi: 10.1186/1743-0003-11-16.

[105] H. E. Williams, Q. A. Boser, P. M. Pilarski, C. S. Chapman, A. H. Vette, and J. S. Hebert, “Hand Function Kinematics when using a Simulated Myoelectric Prosthesis,” in *2019 IEEE 16th International Conference on Rehabilitation Robotics (ICORR)*, Jun. 2019, pp. 169–174, doi: 10.1109/ICORR.2019.8779443.

[106] T. G. Kuus, M. R. Dawson, K. Schoepp, and J. P. Carey, “Development Of A Simulated Sensory Motor Prosthesis: A Device To Research Prosthetic Sensory Feedback Using Able-Bodied Individuals,” 2017, pp. 209–212.

[107] J. V. V. Parr, S. J. Vine, N. R. Harrison, and G. Wood, “Examining the Spatiotemporal Disruption to Gaze When Using a Myoelectric Prosthetic Hand,” *Journal of Motor Behavior*, vol. 50, no. 4, pp. 416–425, Jul. 2018, doi: 10.1080/00222895.2017.1363703.

[108] B. W. Hallworth *et al.*, “A Transradial Modular Adaptable Platform For Evaluating Prosthetic Feedback And Control Strategies,” in *Myoelectric Controls and Upper Limb Prosthetics Symposium*, 2020, pp. 203–206.

[109] M. D. Paskett *et al.*, “A Modular Transradial Bypass Socket for Surface Myoelectric Prosthetic Control in Non-Amputees,” *IEEE Transactions on Neural Systems and Rehabilitation Engineering*, vol. 27, no. 10, pp. 2070–2076, Oct. 2019, doi: 10.1109/TNSRE.2019.2941109.

[110] A. W. Wilson, D. H. Blustein, and J. W. Sensinger, “A third arm — Design of a bypass prosthesis enabling incorporation,” in *2017 International Conference on Rehabilitation Robotics (ICORR)*, Jul. 2017, pp. 1381–1386, doi: 10.1109/ICORR.2017.8009441.

[111] P. J. Kyberd, “The influence of control format and hand design in single axis myoelectric hands: assessment of functionality of prosthetic hands using the Southampton Hand Assessment Procedure,” *Prosthet Orthot Int*, vol. 35, no. 3, pp. 285–293, Sep. 2011, doi: 10.1177/0309364611418554.

[112] K. Evans, “Katherine R. Evans,” MSc., University of Alberta, 2016.

[113] J. S. Schofield, K. R. Evans, J. S. Hebert, P. D. Marasco, and J. P. Carey, “The effect of biomechanical variables on force sensitive resistor error: Implications for calibration and improved accuracy,” *J Biomech*, vol. 49, no. 5, pp. 786–792, Mar. 2016, doi: 10.1016/j.jbiomech.2016.01.022.

[114] M. R. Dawson, H. E. Williams, G. S. Murgatroyd, J. S. Hebert, and P. M. Pilarski, “BrachIOPlexus: Myoelectric Training Software for Clinical and Research Applications,” in *Myoelectric Controls and Upper Limb Prosthetics Symposium*, 2020, pp. 90–93.

[115] U. Wijk, P. Svensson, C. Antfolk, I. K. Carlsson, A. Björkman, and B. Rosén, “Touch on predefined areas on the forearm can be associated with specific fingers: Towards a new principle for sensory feedback in hand prostheses,” *J Rehabil Med*, Feb. 2019, doi: 10.2340/16501977-2518.

[116] P. Arias, V. Robles-García, N. Espinosa, Y. Corral, and J. Cudeiro, “Validity of the finger tapping test in Parkinson’s disease, elderly and young healthy subjects: Is there a role for central fatigue?,” *Clinical Neurophysiology*, vol. 123, no. 10, pp. 2034–2041, Oct. 2012, doi: 10.1016/j.clinph.2012.04.001.

[117] C. E. Stepp and Y. Matsuoka, “Object Manipulation Improvements Due to Single Session Training Outweigh the Differences Among Stimulation Sites During Vibrotactile Feedback,” *IEEE Transactions on Neural Systems and Rehabilitation Engineering*, vol. 19, no. 6, pp. 677–685, Dec. 2011, doi: 10.1109/TNSRE.2011.2168981.

[118] M. Štrbac *et al.*, “Short- and Long-Term Learning of Feedforward Control of a Myoelectric Prosthesis with Sensory Feedback by Amputees,” *IEEE Transactions on Neural Systems and Rehabilitation Engineering*, vol. 25, no. 11, pp. 2133–2145, Nov. 2017, doi: 10.1109/TNSRE.2017.2712287.

[119] D. K. Lee, “Alternatives to P value: confidence interval and effect size,” *Korean J Anesthesiol*, vol. 69, no. 6, pp. 555–562, Dec. 2016, doi: 10.4097/kjae.2016.69.6.555.

[120] P. Page, “Beyond Statistical Significance: Clinical Interpretation of Rehabilitation Research Literature,” *Int J Sports Phys Ther*, vol. 9, no. 5, pp. 726–736, Oct. 2014.

[121] G. M. Sullivan and R. Feinn, “Using Effect Size—or Why the P Value Is Not Enough,” *J Grad Med Educ*, vol. 4, no. 3, pp. 279–282, Sep. 2012, doi: 10.4300/JGME-D-12-00156.1.

[122] J. Cohen, *Statistical power analysis for the behavioral sciences*, 2nd ed. Hillsdale, N.J: L. Erlbaum Associates, 1988.

[123] G. Cumming, *Understanding The New Statistics: Effect Sizes, Confidence Intervals, and Meta-Analysis*, 1st ed. Routledge, 2013.

[124] D. Lakens, “Calculating and reporting effect sizes to facilitate cumulative science: a practical primer for t-tests and ANOVAs,” *Front. Psychol.*, vol. 4, 2013, doi: 10.3389/fpsyg.2013.00863.

[125] L. G. Portney, *Foundations of clinical research: applications to evidence-based practice*, Fourth edition. Philadelphia: F.A. Davis, 2020.

[126] “Universität Düsseldorf: gpower,” *G*Power: Statistical Power Analyses for Windows and Mac*, 2020. https://www.psychologie.hhu.de/arbeitsgruppen/allgemeine-psychologie-und-arbeitspsychologie/gpower.html (accessed Jun. 09, 2020).

[127] MATLAB, *Matlab R2018b*. Natick, Massachusetts: The Mathworks, Inc, 2018.

[128] H. C. Kraemer, J. Mintz, A. Noda, J. Tinklenberg, and J. A. Yesavage, “Caution Regarding the Use of Pilot Studies to Guide Power Calculations for Study Proposals,” *Arch Gen Psychiatry*, vol. 63, no. 5, pp. 484–489, May 2006, doi: 10.1001/archpsyc.63.5.484.

[129] P. P. Lele, D. C. Sinclair, and G. Weddell, “The reaction time to touch,” *The Journal of Physiology*, vol. 123, no. 1, pp. 187–203, 1954, doi: 10.1113/jphysiol.1954.sp005042.

[130] M. Wilke, C. Hartmann, F. Schimpf, D. Farina, and S. Dosen, “The interaction between feedback type and learning in routine grasping with myoelectric prostheses,” *IEEE Transactions on Haptics*, pp. 1–1, 2019, doi: 10.1109/TOH.2019.2961652.

[131] Q. Fu and M. Santello, “Learning from the Human Hand: Force Control and Perception Using a Soft-Synergy Prosthetic Hand and Noninvasive Haptic Feedback,” in *Advances in Motor Neuroprostheses*, R. Vinjamuri, Ed. Cham: Springer International Publishing, 2020, pp. 53–69.

[132] D. H. Blustein, N. B. Mesa, E. S. Kuylenstierna, K. E. Parsons, J. S. Hebert, and A. W. Shehata, “Towards Objective Assessment of Ownership Over a Prosthesis,” in *Myoelectric Controls and Upper Limb Prosthetics Symposium*, 2020, pp. 158–161.

6 Appendices

Appendix A : Pilot Study Fragile Object Break Threshold Results Summary

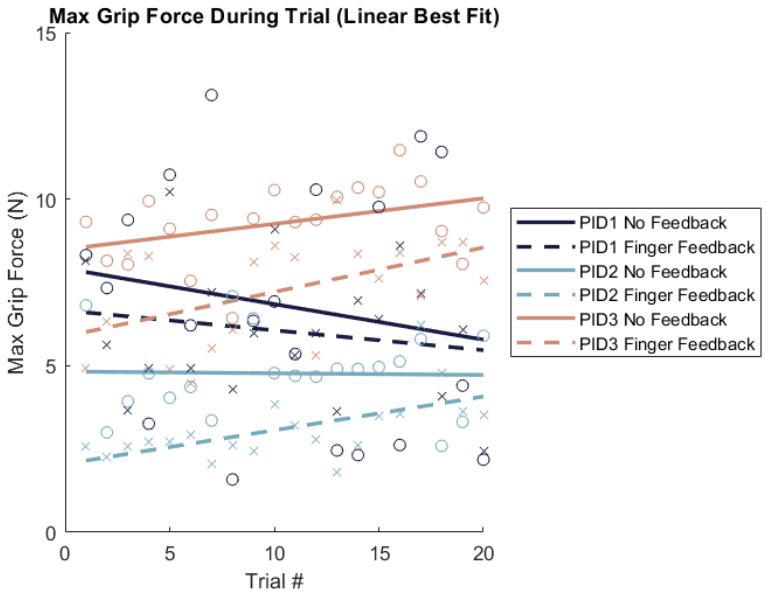

Figure 6.1: Maximum Grasp Threshold Testing Summary

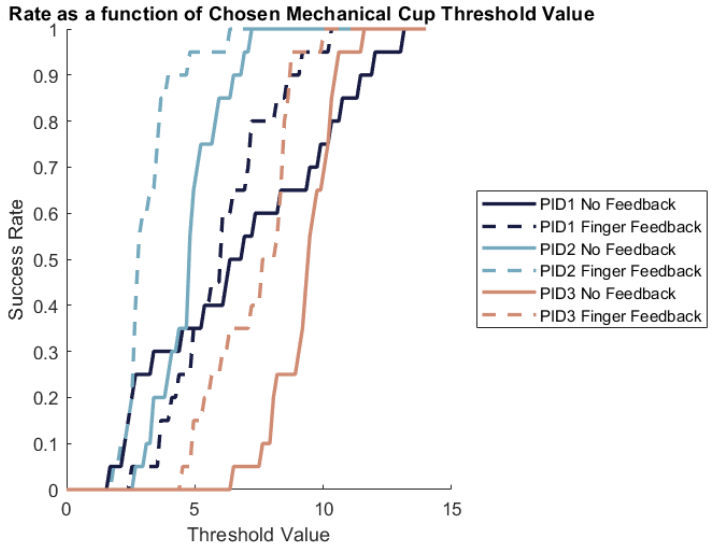

Figure 6.2: Theoretical Success Rate as a Function of Chosen Fragile Object Break Threshold

Table 6.1: Absolute Value Descriptive Statistics Summary

	Success Rate (%)							
	N1		**N2**		**A**		**F**	
	Mean	**STDEV**	**Mean**	**STDEV**	**Mean**	**STDEV**	**Mean**	**STDEV**
PID1	**0.69**	**-**	**0.62**	**-**	**0.79**	**-**	**0.73**	**-**
PID2	**0.50**	**-**	**0.69**	**-**	**0.82**	**-**	**0.63**	**-**
PID3	**0.73**	**-**	**0.87**	**-**	**0.93**	**-**	**0.73**	**-**
	Maximum Grasp (N)							
	N1		**N2**		**A**		**F**	
	Mean	**STDEV**	**Mean**	**STDEV**	**Mean**	**STDEV**	**Mean**	**STDEV**
PID1	**4.98**	**0.88**	**4.23**	**0.98**	**4.70**	**1.29**	**3.73**	**1.49**
PID2	**3.33**	**1.28**	**4.30**	**1.89**	**4.57**	**1.30**	**4.51**	**1.90**
PID3	**3.82**	**1.47**	**3.30**	**1.88**	**4.36**	**2.11**	**3.97**	**1.63**
	Completion Time (s)							
	N1		**N2**		**A**		**F**	
	Mean	**STDEV**	**Mean**	**STDEV**	**Mean**	**STDEV**	**Mean**	**STDEV**
PID1	**5.40**	**0.89**	**6.37**	**2.17**	**5.14**	**0.84**	**5.87**	**1.74**
PID2	**8.72**	**3.97**	**6.38**	**0.71**	**6.11**	**0.48**	**10.13**	**3.79**
PID3	**6.59**	**0.85**	**6.00**	**2.33**	**5.47**	**0.46**	**6.81**	**0.73**
	Grasp Time (s)							
	N1		**N2**		**A**		**F**	
	Mean	**STDEV**	**Mean**	**STDEV**	**Mean**	**STDEV**	**Mean**	**STDEV**
PID1	**1.27**	**0.41**	**1.15**	**0.56**	**1.02**	**0.58**	**1.33**	**0.89**
PID2	**1.36**	**0.44**	**0.97**	**0.42**	**0.81**	**0.33**	**2.05**	**1.35**
PID3	**0.59**	**0.27**	**0.44**	**0.18**	**0.66**	**0.22**	**1.07**	**0.47**
	Adjustments (#)							
	N1		**N2**		**A**		**F**	
	Mean	**STDEV**	**Mean**	**STDEV**	**Mean**	**STDEV**	**Mean**	**STDEV**
PID1	**2.44**	**0.53**	**3.50**	**2.07**	**4.27**	**1.42**	**4.75**	**2.12**
PID2	**5.13**	**1.81**	**4.11**	**1.17**	**3.86**	**1.35**	**7.60**	**4.33**
PID3	**3.55**	**1.21**	**3.62**	**1.45**	**2.93**	**0.62**	**4.09**	**1.30**

Table 6.2: Within-Participant Descriptive Statistics Summary

	Success Rate (%)					
	A-N		F-N		F-A	
	Mean	STDEV	Mean	STDEV	Mean	STDEV
PID1	0.13	-	0.07	-	-0.06	-
PID2	0.23	-	0.03	-	-0.20	-
PID3	0.13	-	-0.07	-	-0.20	-
	Maximum Grasp (N)					
PID1	0.09	1.08	-0.87	1.13	-0.97	1.38
PID2	0.76	1.50	0.69	1.73	-0.06	1.57
PID3	0.80	1.86	0.41	1.68	-0.39	1.92
	Completion Time (s)					
PID1	-0.74	1.37	-0.01	1.65	0.74	1.28
PID2	-1.44	2.08	2.58	3.17	4.01	2.45
PID3	-0.82	1.48	0.51	1.57	1.33	0.60
	Grasp Time (s)					
PID1	-0.19	0.52	0.12	0.64	0.31	0.72
PID2	-0.36	0.39	0.89	0.88	1.25	0.90
PID3	0.14	0.22	0.56	0.32	0.42	0.35
	Adjustments (#)					
PID1	1.30	1.45	1.78	1.69	0.48	1.74
PID2	-0.76	1.44	2.98	2.86	3.74	2.96
PID3	-0.65	1.14	0.51	1.33	1.16	0.97

Table 6.3: Between Participant Descriptive Statistics Summary

	A-N		F-N		F-A	
	Mean	STDEV	Mean	STDEV	Mean	STDEV
Success Rate (%)	0.16	0.04	0.01	0.06	-0.15	0.07
Maximum Grasp (N)	0.04	0.32	0.06	0.68	0.07	0.37
Completion Time (s)	-1.00	0.31	1.03	1.12	2.03	1.42
Grasp Time (s)	-0.14	0.21	0.52	0.31	0.66	0.42
Adjustments (#)	-0.04	0.95	1.76	1.01	1.79	1.41

*Table 6.4: Linear Regression Summary for Maximum Grasp Force of Testing Set, M=slope, R=R-Squared Value, p=p-value, * indicates a significant correlation*

	Block 1	Block 2	Block 3	Block 4
PID 1	M=0.008 R=-0.141 p=0.927	M=0.156 R=0.086 p=0.197	M=-0.054 R=-0.093 p=0.549	M=0.002 R=-0.167 p=0.993
PID 2	**M=-0.194** **R=0.641** **p=0.010***	M=0.034 R=-0.120 p=0.853	M=-0.160 R=-0.035 p=0.420	M=-0.064 R=-0.031 p=0.450
PID 3	M=-0.076 R=-0.062 p=0.535	M=0.206 R=0.226 p=0.079	M=-0.004 R=-0.091 p=0.974	M=0.014 R=-0.082 p=0.917

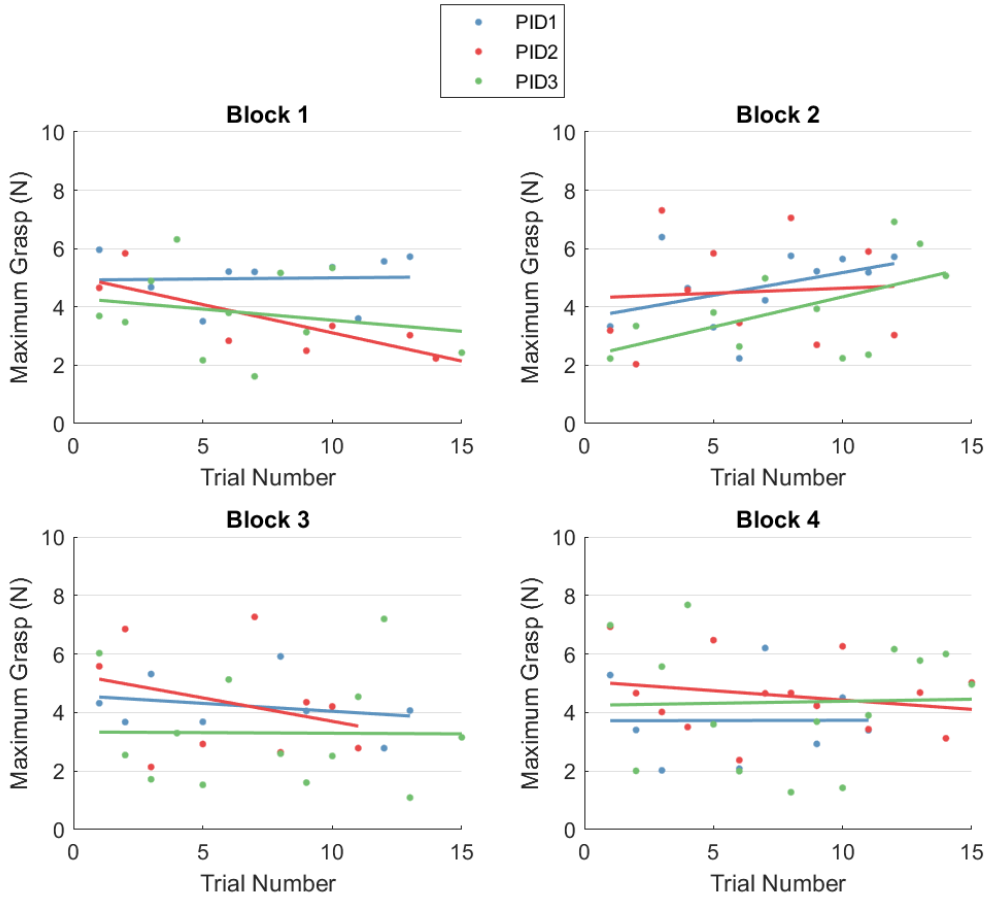

Figure 6.3: Linear Regression Models for Maximum Grasp Metrics Over Testing Set

*Table 6.5: Linear Regression Summary for Completion Time of Testing Set, M=slope, R=R-Squared Value, p=p-value, * indicates a significant correlation*

	Block 1	Block 2	Block 3	Block 4
PID 1	M=0.160 R=0.511 p=0.018*	M=-0.033 R=-0.090 p=0.687	M=0.333 R=0.407 p=0.053	M=-0.287 R=0.295 p=0.095
PID 2	**M=0.065** **R=-0.157** **p=0.832**	M=-0.261 R=-0.049 p=0.467	M=-0.058 R=-0.042 p=0.438	M=-0.053 R=0.180 p=0.073
PID 3	M=-0.021 R=-0.100 p=0.770	M=-0.080 R=0.141 p=0.139	M=-0.022 R=-0.089 p=0.891	M=-0.004 R=-0.082 p=0.895

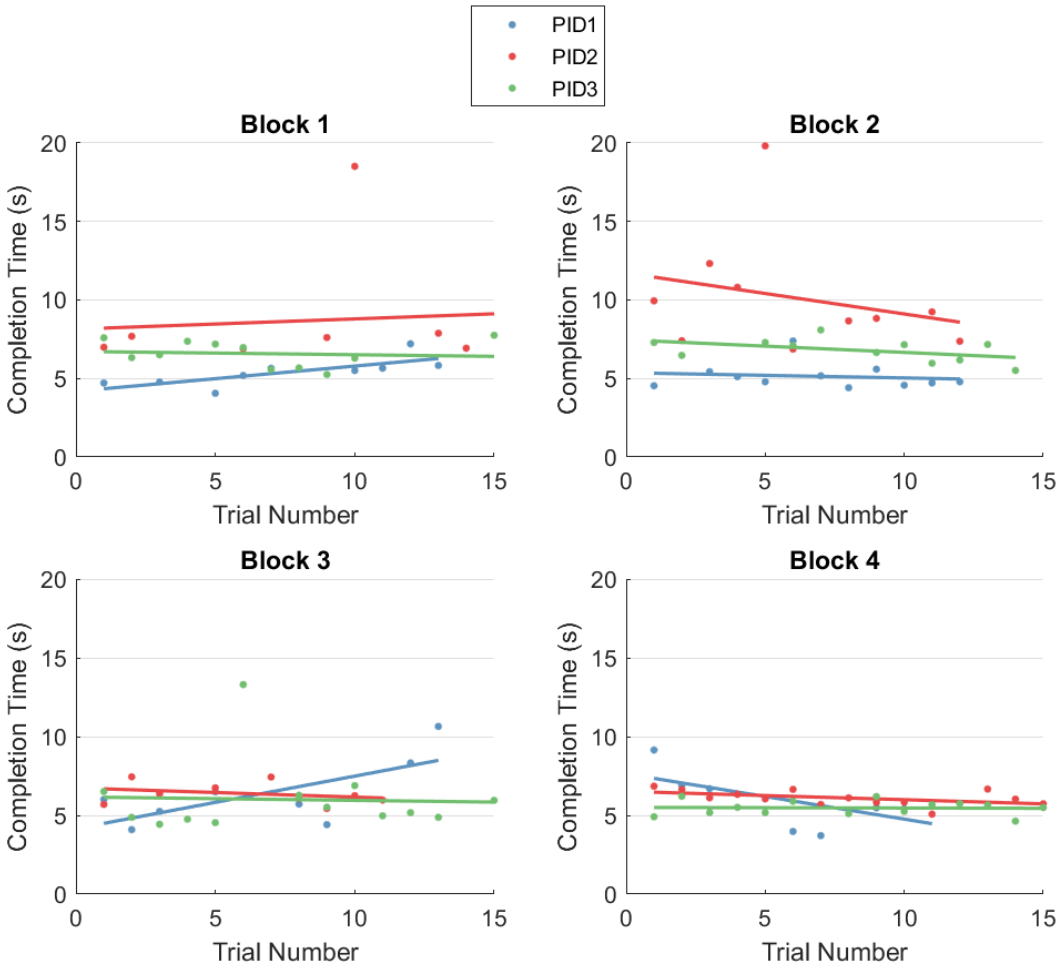

Figure 6.4: Linear Regression Models for Completion Time Metrics Over Testing Set

*Table 6.6: Linear Regression Summary for Grasp Time of Testing Set, M=slope, R=R-Squared Value, p=p-value, * indicates a significant correlation*

	Block 1	Block 2	Block 3	Block 4
PID 1	M=0.028 R=-0.048 p=0.451	M=0.006 R=-0.109 p=0.910	M=0.046 R=-0.001 p=0.358	M=-0.159 R=0.365 p=0.066
PID 2	**M=0.023** **R=-0.065** **p=0.479**	M=-0.011 R=-0.124 p=0.932	M=-0.015 R=-0.125 p=0.749	M=-0.040 R=0.251 p=0.039*
PID 3	M=0.033 R=0.164 p=0.119	M=-0.033 R=-0.011 p=0.369	M=-0.002 R=-0.089 p=0.885	M=0.005 R=-0.073 p=0.742

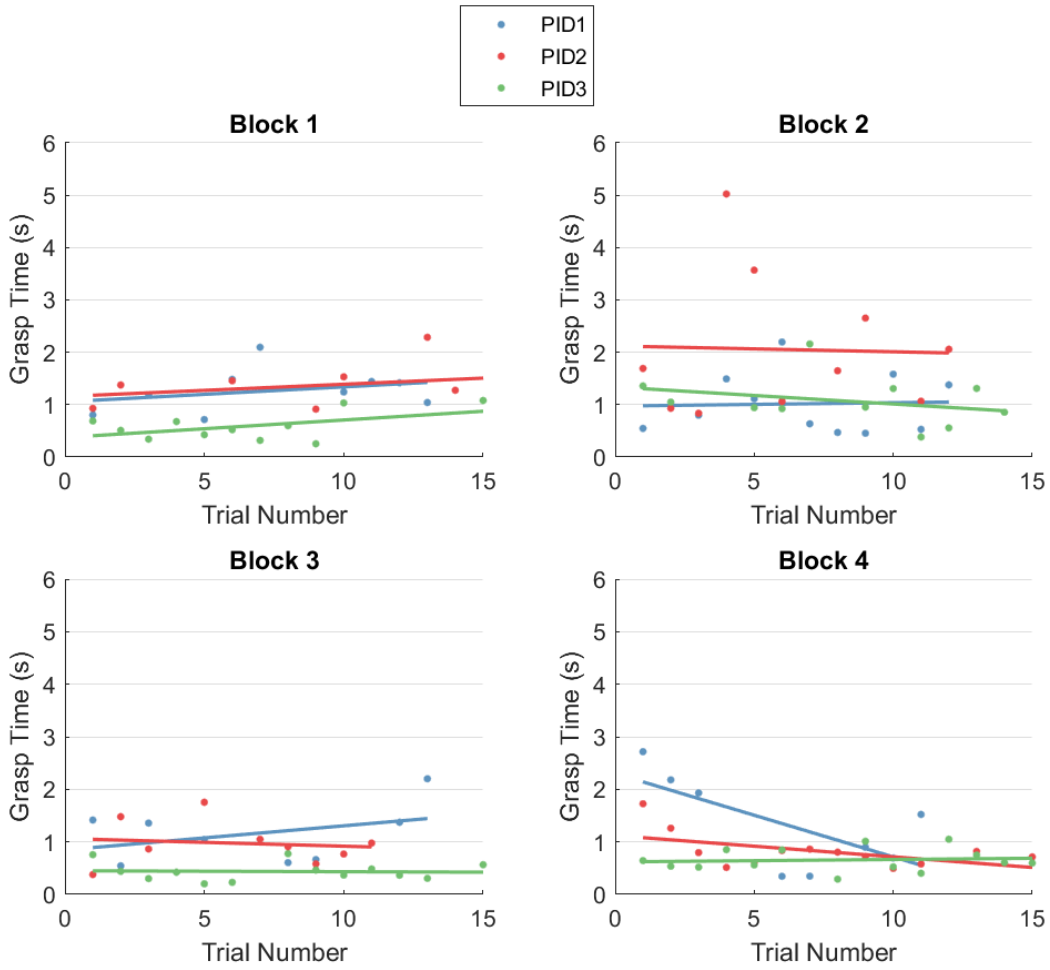

Figure 6.5: Linear Regression Models for Grasp Time Metrics Over Testing Set